uOttawa

L'Université canadienne
Canada's university

FACULTÉ DES ÉTUDES SUPÉRIEURES ET POSTOCTORALES

u Ottawa

L'Université canadienne
Canada's university

FACULTY OF GRADUATE AND POSDOCTORAL STUDIES

Xudong Li

AUTEUR DE LA THÈSE / AUTHOR OF THESIS

M.A.Sc. (Civil Engineering)

GRADE / DEGREE

Department of Civil Engineering

FACULTÉ, ÉCOLE, DÉPARTEMENT / FACULTY, SCHOOL, DEPARTMENT

Laboratory Studies on the Bearing Capacity of Unsaturated Sands

TITRE DE LA THÈSE / TITLE OF THESIS

Dr. Sai Vanapalli

DIRECTEUR (DIRECTRICE) DE LA THÈSE / THESIS SUPERVISOR

CO-DIRECTEUR (CO-DIRECTRICE) DE LA THÈSE / THESIS CO-SUPERVISOR

EXAMINATEURS (EXAMINATRICES) DE LA THÈSE / THESIS EXAMINERS

Dr. S. Sivathayalan

Dr. M. Fall

Gary W. Slater

Le Doyen de la Faculté des études supérieures et postdoctorales / Dean of the Faculty of Graduate and Postdoctoral Studies

LABORATORY STUDIES ON THE BEARING CAPACITY OF UNSATURATED SANDS

by

Xudong Li

A Thesis

Submitted under the Supervision of

Dr. Sai K. Vanapalli, P.Eng.

In partial fulfillment of the requirements for

the degree of Master of Applied Science

in Civil Engineering

Department of Civil Engineering

University of Ottawa

Ottawa, Canada K1N 6N5

August 2008

Your file Votre référence
ISBN: 978-0-494-48475-3
Our file Notre référence
ISBN: 978-0-494-48475-3

ABSTRACT

In this thesis, extensive experimental studies were undertaken by conducting more than 250 bearing capacity tests on model footings to investigate the bearing capacity of three compacted (coarse-grained, sub-coarse-grained, and fine-grained) sands under both saturated and unsaturated conditions. These tests were conducted in specially designed equipment which includes two test systems for conducting bearing capacity tests using model footings. The designed equipment system had provisions for soil drainage, soil suction profile set for measuring the variation of matric suction with depth of water table, tensiometer holders, vacuum water pumps and other accessories. Two different soil containers (short container with 300 mm in diameter and 300 mm in height and the tall container with 300 mm in diameter and 700 mm in height) were used in the study. The bearing capacity was determined using four different sizes of square model footings (i.e. 20 mm × 20 mm, 25 mm × 25 mm, 37.5 mm × 37.5 mm, and 50 mm × 50 mm). All the equipment was designed by the author and fabricated in the student workshop at University of Ottawa.

The experimental results demonstrated that the bearing capacity of unsaturated fine-grained sand increases as the matric suction increases. However, experimental studies on coarse-grained sand show that bearing capacity appears to decrease as the matric suction increases. Some practical reasons for such a behavior are explained in the thesis.

Experimental studies have also demonstrated that footing sizes in the range of 20 mm × 20 mm to 150 mm × 150 mm had no significant influence on the bearing capacity of sandy soils. The boundary conditions (i.e., ratio of soil container size to footing size) have some effect on the bearing capacity of sands.

A separate experimental program Saturated compacted silt after settlement offers significant resistance to the applied static loads without undergoing creep, however; bearing capacity reduces significantly when it is subjected to dynamic or cyclic loading conditions.

ACKNOWLEDGEMENTS

I am very grateful to my supervisor Dr. Sai K. Vanapalli for his guidance, encouragement, valuable advice and suggestions throughout this research program.

I would like to thank Geotechnical Lab technician Kulan Ambalavanar for helping me purchase and set up various facilities and equipment required for the research program. I appreciate the help received from John Perrins in the student workshop who trained and helped me to design and fabricate the test equipments used in the present research program.

Thanks go to my colleagues Won Taek Oh, Lu Lu, Rui Sun, and the other graduate students in geotechnical engineering program at the University of Ottawa for their assistance, especially for helping me to move the 100 kg-soil container on and off the loading machine for more than 300 times.

Finally, I thank the faculty and staff in Civil Engineering Department for providing support to my graduate study and thesis experiment.

Table of Contents

Table of Figures

Table of Tables

CHAPTER 1

INTRODUCTION

1.1 Statement of the Problem

Soil mechanics involves a combination of applying the principles of mechanics and hydraulics to engineering problems dealing with soil as an engineering material. Terzaghi (1943) developed a framework to interpret the mechanical behavior of saturated soils using the effective stress principle as a key tool. The principles of soil mechanics are commonly used in engineering practice for several soils such as saturated sands, silts and clays, and dry sands. However, soils could either be saturated with water or have other fluids in the voids (e.g., air) along with water. There are numerous soils; for example, expansive, compacted or collapsible soils that are commonly encountered in engineering practice are typically in a state of unsaturated condition. About 33% of the earth's surface is considered either arid or semi-arid and the soils in these regions are unsaturated soils. A reasonable interpretation of the soil behavior in these regions is not possible using the mechanics of saturated soils.

In many regions; including arid and semi-arid regions, shallow foundations are usually located above the ground water table where the soil is typically in a state of unsaturated condition. Bearing capacity is one of the key parameters required in the design of shallow foundations. Terzaghi (1943) and Meyerhof (1951) approaches are commonly used in engineering practice for the determination of the bearing capacity of both saturated and unsaturated soils. The contribution of capillary stresses or the matric suction towards the bearing capacity of unsaturated soils is conventionally ignored. Estimation of the bearing capacity of shallow foundations using the conventional approaches may lead to uneconomical designs (Steensen Bach et al. 1987, Vanapalli and Mohamed 2007).

1.2 Background

Research during the last 50 years has demonstrated that engineering behavior of unsaturated soils can be interpreted in terms of two independent stress state variables, namely; net normal stress, $(\sigma_n - u_a)$ and matric suction, $(u_a - u_w)$ (Bishop and Blight 1963, Fredlund and Morgenstern 1977, Alonso et al. 1990). The matric suction is defined as the difference between the pore air pressure, u_a and pore water pressure, u_w. Several studies have shown that the engineering behavior of unsaturated soils including the bearing capacity is significantly influenced by matric suction (Broms 1964, Steensen-Bach et al. 1987, Fredlund and Rahardjo 1993, Schnaid et al. 1995, Miller and Muraleetharan 1998, Oloo et al. 1997, Costa et al. 2003, Yongfu 2004, Mohamed and Vanapalli 2006, and Vanapalli et al. 2007). However, no practical applications are reported in the literature with respect to the bearing capacity of unsaturated soils (Fredlund and Rahardjo 1993, Oloo et al. 1997). Such a scenario may be attributed to lack of a theoretical framework to interpret the bearing capacity of unsaturated soils.

More recently, Vanapalli and Mohamed (2007) have provided a relationship to predict the variation of bearing capacity of unsaturated soils with respect to matric suction using the saturated shear strength parameters (c', ϕ') and the Soil-Water Characteristic Curve (SWCC). This relationship was developed conducting bearing capacity tests using two different sizes of square model footings (100 mm × 100 mm and 150 mm × 150 mm) in a relatively large size soil tank (900mm × 900 mm × 750 mm) on a compacted sand (fine-grained sand). There was a good comparison between the measured and predicted bearing capacity values. This relationship was also used for interpreting the bearing capacity results published in the literature and found to be reasonably encouraging towards predicting the bearing capacity of unsaturated soils under drained loading conditions. The proposed relationship shows a smooth transition between the bearing capacity of unsaturated soils and the conventional Terzaghi's (1943) bearing capacity equation for saturated soils. In other words, Vanapalli and Mohamed (2007) equation will be equal to Terzaghi's bearing capacity equation when the matric suction value is set equal to zero.

Oh and Vanapalli (2008) proposed a methodology to estimate the bearing capacity and settlement characteristics in unsaturated sandy soils by predicting the stress versus settlement behaviour. The proposed method needs only parameters under saturated conditions (effective

cohesion, c', effective internal friction angle, $\phi'$and the modulus of elasticity, E_{sat}) along with the Soil-Water Characteristic Curve (SWCC). The proposed method and finite element analysis were performed using an elastic - perfectly plastic model. The predicted bearing capacities and settlements from the proposed method and finite element analysis were compared with the model footing test results of sands. There was good agreement between the measured bearing capacity and settlement values and the predicted results. The method proposed in this paper is promising and can be applied to unsaturated soils in engineering practice. Computer modeling studies from this study also show that the soil stresses due to foundation loading are with in a radius of 5 to 6 times the width of foundation. The studies demonstrated bearing capacity can be determined using relatively smaller tanks using different sizes of model footings to understand the bearing capacity behavior of different soils under unsaturated conditions avoiding laborious large tank studies.

1.3 Objectives of the Proposed Research

The focus of the present research program was directed towards determination of the bearing capacity of saturated and unsaturated sands under a controlled laboratory environment using three different compacted (coarse-grained, sub-coarse-grained, and fine-grained) sands and four different sizes of square model footings. The research tests were conducted in specially designed equipment which includes two test systems that contain alumina soil containers for conducting bearing capacity tests using model footings, soil drainage system, soil suction profile set for measuring the variation of matric suction with depth of water table, tensiometer holders, vacuum water pumps and other accessories. Two soil containers (short container with 300 mm in diameter and 300 mm in height and the tall container with 300 mm in diameter and 700 mm in height) were used in the study. All the equipment was designed by the author and fabricated in the student workshop at University of Ottawa.

The main objectives of this research are summarized as follows:

i. To design and construct two bearing capacity test systems for the determination of the bearing capacity using model footings in a laboratory environment under both saturated and unsaturated conditions.

ii. To test and determine the best compaction method for each soils.

iii. To determine the bearing capacity of three different sands using different size model footings.

iv. To evaluate the bearing capacity of unsaturated compacted soils (coarse grained sand and fine-grained sand) by undertaking a comprehensive experimental investigation.

v. To study the relationship between bearing capacity and different matric suction of unsaturated compacted soils.

1.4 Scope of the Thesis

A comprehensive experimental program was undertaken to determine the bearing capacity of three compacted sands both in saturated and unsaturated conditions.

The four different soils used in the present research program are: (i) compacted coarse-grained sand – Unimin 2075, (ii) compacted sub-coarse-grained sand – Ottawa sand, (iii) compacted fine-grained sand – Unimin 7030, and (iv) silica silt – Sil-co-sil 106. All four soils have no plasticity, and plastic index value was equal to zero. Four square shaped model footings were used in the experimental program (i.e., 20mm × 20mm, 25mm × 25mm, 37.5mm × 37.5mm, and 50mm × 50mm).

The matric suction was controlled and the bearing capacity of the surface model footings were determined for the different soils studied is listed in Table 1- 1.

Table 1- 1 Values of matric suction were used in the test

Soil	I_p	Matric suction, $(u_a - u_w)$ (kPa)									
Unimin 2075	0	0	2	4	6						
Ottawa Sand	0	0	1	2	3	4	5	6	7	8	Dry
Unimin 7030	0	0	2	4	6	8	10	12	14	18	
Sil-co-sil 106	0	0									

Several series of tests were conducted to determine the bearing capacity of each soil in both saturated and unsaturated conditions (Table 1- 1). The saturated condition was achieved by maintaining the water table at the surface of the soil in the soil container while conducting

bearing capacity tests. Unsaturated conditions with different values of matric suction in the soil were achieved by lowering water table to different depths below the soil surface. The matric suction values in stress bulb zone under the footing were measured using commercial Tensiometers. A special unit of suction profile set was designed to obtain the relationship of matric suction and depth of water table. This unit was useful to estimate the depth of water table below the footing such that a known matric suction value can be applied. In other words, a pre-calibrated relationship was developed and used as a guide to help to achieve expected matric suction in stress bulb zone by lowering the water table to some depth below the soil surface.

The shear strength parameters, namely; the effective cohesion, c' and the angle of internal friction ϕ' of the tested soil were determined using the direct shear test apparatus. Other soil properties such as the grain size distribution, compaction curve were also determined in the laboratory.

1.5 Outline of the Thesis

This thesis consists of six main chapters. This is chapter 1, "Introduction". The other chapters are organized as follows:

The second chapter, "Review of Literature", provides a brief review on the mechanics of saturated and unsaturated soils and bearing capacity of saturated and unsaturated soils. Limitations of the presently used equations in interpreting the bearing capacity of soils are also detailed.

The third chapter, "Equipments and Methodology", presents detailed information of all the equipments used in the tests, including the design details of the equipments specially fabricated for conducting the proposed research program.

The fourth chapter, "Soil Properties", summarizes the properties of all four soils and details of the various laboratory tests conducted such as the grain size distribution, suction profile, Soil Water Characteristic Curve (SWCC), and the shear strength characteristics.

The fifth chapter, "Silica Silt Compaction and Strength Characteristics", provides details of Sil-co-sil 106's compaction, settlement (collapse), suction sensitivity to vibration, and shear strength and stress-displacement characteristics under static and dynamic loading conditions.

The sixth chapter, "Bearing Capacities Tests", provides analyses of all the test results. The relationship of bearing capacity with respect to matric suction is discussed for the different sands studies. Comparisons between the variation of bearing capacity with respect to matric suction and Soil Water Characteristic Curve (SWCC) are also summarized.

The seventh chapter, "Conclusions", presents the summary and conclusions of this research program and also provides several recommendations for future research work.

CHAPTER 2

REVIEW OF LITERATURE

This chapter provides a brief review about the mechanics of saturated and unsaturated soils along with the bearing capacity of saturated soils and unsaturated soils. Limitation of the presently used bearing capacity equations towards interpreting the bearing capacity of soils is highlighted. In the summary section, justification is provided with respect to the need for undertaking a research program using specially designed equipment to determine the bearing capacity of compacted unsaturated sands.

2.1 General

Soil mechanics is a discipline that applies principles of several fields that include kinematics, dynamics, fluid mechanics, and mechanics of materials to explain the engineering behavior of saturated soils. Together with Rock mechanics, it forms the basis for solving several practical geotechnical engineering problems in civil engineering, geophysical engineering and engineering geology.

The ability of a soil to support a load from a structural foundation without failing in shear is known as its bearing capacity. Bearing capacity is one of the key properties required in the design of foundations, dams, retaining walls, bridge abutments, and temporary support structures. It is commonly defined as the largest intensity of pressure which may be applied by a structure to the soil without causing failure of soil in shear or excessive settlement.

2.2 Basic Characteristics of Soils

Soil is usually composed of three phases: solid, liquid, and gas. The mechanical properties of soils depend directly on the interactions of these phases with each other and with applied potentials (e.g., stress, hydraulic head, electrical potential, and temperature difference).

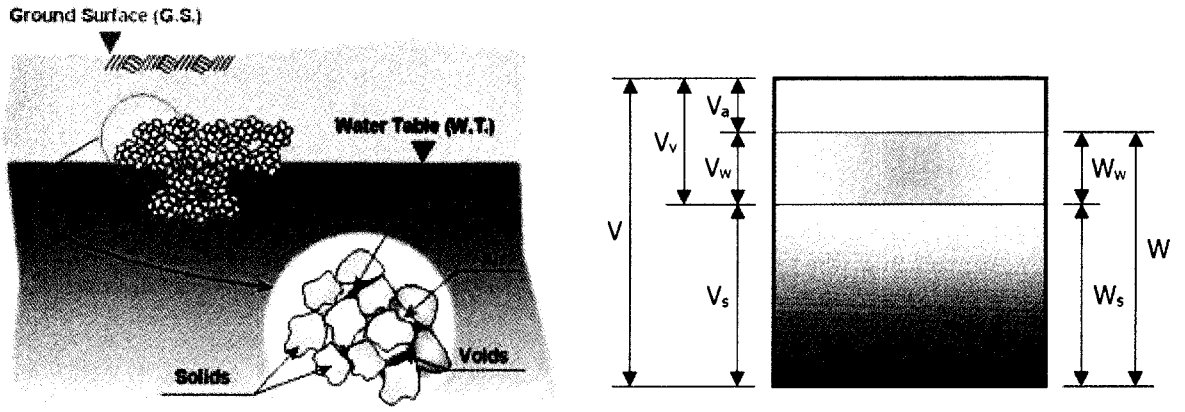

Figure 2- 1 A phase diagram of soil indicating the weights and volumes of air, soil, water, and voids (from http://en.wikipedia.org/wiki/Soil_mechanics).

The solid phase of soils contains various amounts of crystalline clay and non-clay minerals, non-crystalline clay material, organic mater, and precipitated salts. The minerals are commonly formed by atoms of elements such as oxygen, silicon, hydrogen, and aluminum, organized in various crystalline forms. These elements along with other elements such as calcium, sodium, potassium, magnesium, and carbon comprise over 99% of the solid mass of soils (Spangler & Haandy 1982).

Solid particles of soil are classified by particle size as clay, silt, sand, gravel, cobbles, or boulders (ASTM, 1997). Particles of sand and gravel typically consist of silica. They can be rounded due to abrasion while being transported by wind or water, or sharp-cornered, or anything in between, and are roughly equal-dimensional. Soil mineralogy has a significant influence on the size, shape, and physical and chemical properties of soil particles and thus its load-carrying ability and compressibility.

The structure of a soil is the combined effects of fabric (particle association, geometrical arrangement of particles, particle groups, and pore spaces in a soil), composition, and interparticle forces. The structure of soils is also used to account for differences between the properties of natural (structured) and remolded soils (destructured). The structure of a soil reflects all facets of the soil composition, history, present state, and environment. Initial conditions dominate the structure of young deposits at high porosity or freshly compacted soils;

whereas older soils at lower porosity reflect the post-depositional changes (Spangler & Haandy 1982).

The liquid phase in soils is commonly composed of water containing various types and amounts of dissolved electrolytes. However, the gas phase in unsaturated soils is usually air. Organic gases may be present in zones of high biological activity or in chemically contaminated soils.

2.3 Unsaturated Soil Mechanics

2.3.1. Introduction

Unsaturated soils contain both air and liquid phases in the soil pores. They can be either naturally occurring soils, such as those found in arid and tropical zones, or artificially created (man-made) soils such as those that are formed by compaction.

Fundamental principles pivotal to understanding the engineering behavior of saturated soils emerged with the concept of effective stress in the 1930s (Terzaghi 1943). However, there was considerable interest in understanding the behavior of unsaturated soils along with saturated soils. This is documented through the research papers published in the First International Conference on Soil Mechanics and Foundation Engineering in 1936.

Theoretically based framework of stress state variables for interpreting the engineering behavior of an unsaturated soil was proposed 40 years later within the context of multiphase continuum mechanics (Fredlund and Morgenstern 1977). Two stress state variables, namely; net normal stress, $(\sigma_n - u_a)$ and matric suction, $(u_a - u_w)$ which is the difference between the pore-air pressure, u_a and pore-water pressure u_w are used for explaining the behavior of unsaturated soils. The behavior of unsaturated soils could be viewed as a natural extension of saturated soil behavior (Fredlund and Morgenstern 1976). More details of the stress state variables are presented in later sections of this chapter.

The 1980s was a period when boundary-value problems were solved using numerical, finite element, and finite difference modeling methods with the aid of computers. The 1990s and beyond have become a period where there has been an emphasis on the implementation of

unsaturated soil mechanics into routine geotechnical engineering practice. The challenge was to find techniques that would ensure convergence of highly nonlinear partial differential equations on a routine basis (Thieu et al. 2001; Fredlund et al. 2002a, b). Seepage modeling of saturated–unsaturated soils problems received more attention and applied in conventional engineering practice (Fredlund and Rahardjo 1993). Concern for stewardship toward the environment further promoted interest in seepage and geoenvironmental, advection-dispersion modeling. The study of contaminant transport and thermal soil properties for unsaturated soils also took on the form of nonlinear soil property functions (Newman 1996; Lim et al. 1998; Pentland et al. 2001).

The four international conferences held in Paris, France (1995), Beijing, China (1998), Recife, Brazil (2002) and Carefree, U.S.A (2006) have been fruitful to exchange information on the engineering behavior of unsaturated soils. In recent years, there is an increased interest in the application of the mechanics of unsaturated soil into engineering practice. The research presented in this thesis is also a step in that direction; the focus being towards understanding the bearing capacity of unsaturated sands.

2.3.2. Various Phases in Unsaturated Soils

Unsaturated soils contain both air and fluid phases in their pores. Soil in a state of saturated condition is commonly referred to as a two-phase mixture (i.e., solids and water), but an unsaturated soil includes two other independent phases (i.e., air and the contractile skin or the air–water interface) (Fredlund and Rahardjo, 1993). The contractile skin acts like a thin membrane interwoven throughout the voids of the soil, acting as a partition between the air and water phases. It is the interaction of the contractile skin with the soil structure that causes an unsaturated soil to have a significant influence on its mechanical behavior (i.e., volume change and shear strength properties). The unsaturated soil properties change in response to the position of the contractile skin. It is important to view an unsaturated soil as a four-phase mixture for purposes of stress analysis, within the context of multiphase continuum mechanics (Fredlund and Morgenstern, 1976).

The contractile skin can be considered as part of the water phase with regard to changes in volume–mass soil properties but must be considered as an independent phase when describing

the stress state and phenomenological behavior of an unsaturated soil (Fredlund and Rahardjo 1993). Numerous research studies on the nature of the contractile skin point toward its independent role in the mechanics of unsaturated soils. A surface tension of approximately 75 MN/m translates into a unit stress in the order of 140,000 kPa. Lyklema (2000) showed that the distribution of water molecules across the contractile skin takes the form of a hyperbolic tangent function as shown in Figure 2- 2. Properties of the contractile skin are different from that of ordinary water and have a water molecular structure similar to that of ice (Derjaguin and Churaev 1981; Matsumoto and Kataoka 1988).

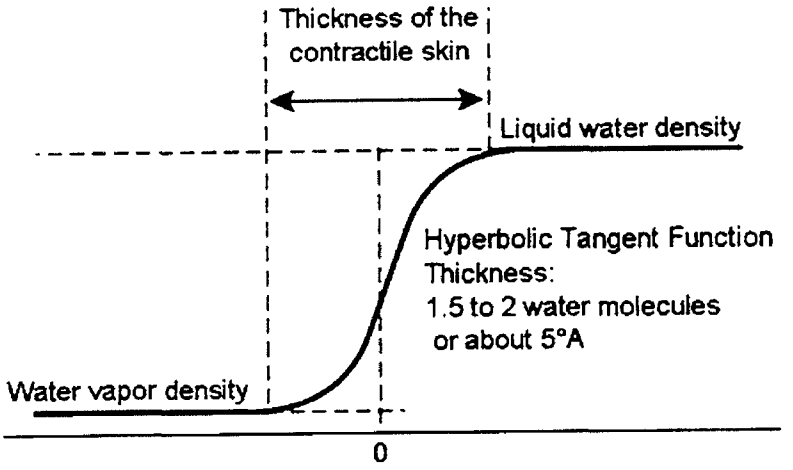

Figure 2- 2 Density distribution across the contractile skin (from Lyklema 2000)

The details of the laws describing the behavior of the contractile skin are not fully understood by researchers but the contractile skin is known to play a dominant role in unsaturated soil behavior from many decades. Terzaghi (1943) stated that "*surface tension is valid regardless of the physical causes. ... The views concerning the molecular mechanism which produces the surface tension are still controversial. Yet the existence of the surface film was established during the last century beyond any doubt.*"

The suction in the unsaturated soils can range from zero at the water table to a maximum tension of approximately 1,000,000 kPa under dry soil conditions (Croney et al. 1958). For the same range of suction, degree of saturation of the soil various from 100% to zero. The suction in soils varies from zero to 1,000,000 kPa irrespective of the type of soil. The changes in soil suction result in distinct zones of saturation. The zones of saturation can be been defined in situ as well

as in the laboratory through the use of soil–water characteristic curve (Figure 2- 3) (Vanapalli et al. 1999).

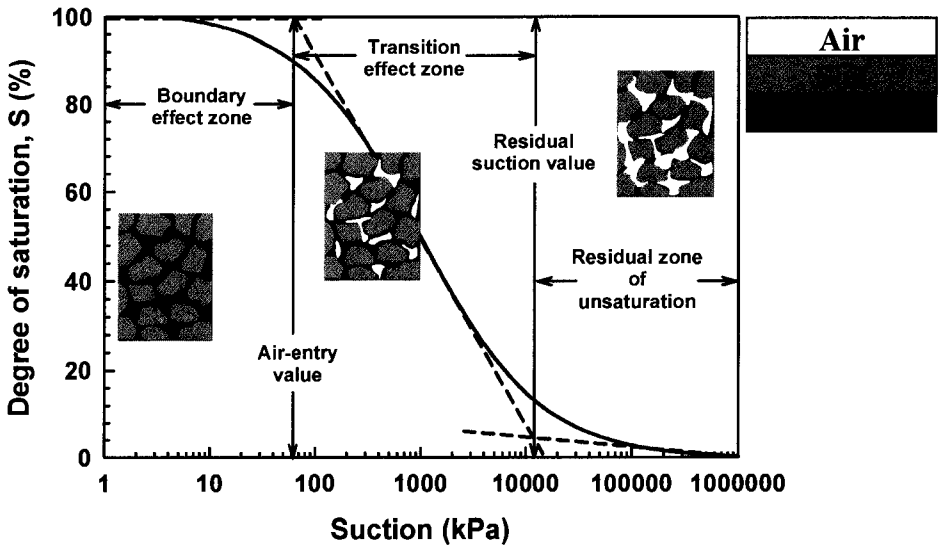

Figure 2- 3 Soil–water characteristic curve and its various zones (modified after Vanapalli et al. 1999)

2.3.3. Soil Water Characteristic Curve

The Soil Water Characteristic Curve (SWCC) defines the amount of water in a soil versus soil suction (Figure 2- 3). The amount of water in the soil is commonly defined in more than one way. Three common variables used to define the amount of water in the soil are: gravimetric water content, w, volumetric water content, θ, and degree of saturation, S. This relationship is also referred in the literature using different terms such as Soil Water Retention Curve (SWRC) or Soil Moisture Curve (SMC) along with Soil-Water Characteristic Curve (SWCC) as used in this thesis.

There is no unique SWCC but rather, there is an infinite number of scanning curves contained within a drying (desorption) boundary curve and an adsorption (wetting) boundary curve (Figure 2- 4). It is the primary drying and wetting curves that are of greatest relevance to unsaturated soil mechanics. The drying curve is easier to measure and is therefore it is this curve that is generally measured in the laboratory. Most of the research studies published in the literature use the drying SWCC (Fredlund & Rahardjo 1993). The scanning curves define the pathways between the boundary curves. However, for many geotechnical practical applications, a drying

SWCC may be sufficient. Several models are available in the literature that takes into account of hysterisis. Gallipoli et al. (2003) recently has proposed a simplified hysteresis model for the water content versus soil suction relationship that can be used in geotechnical engineering practice

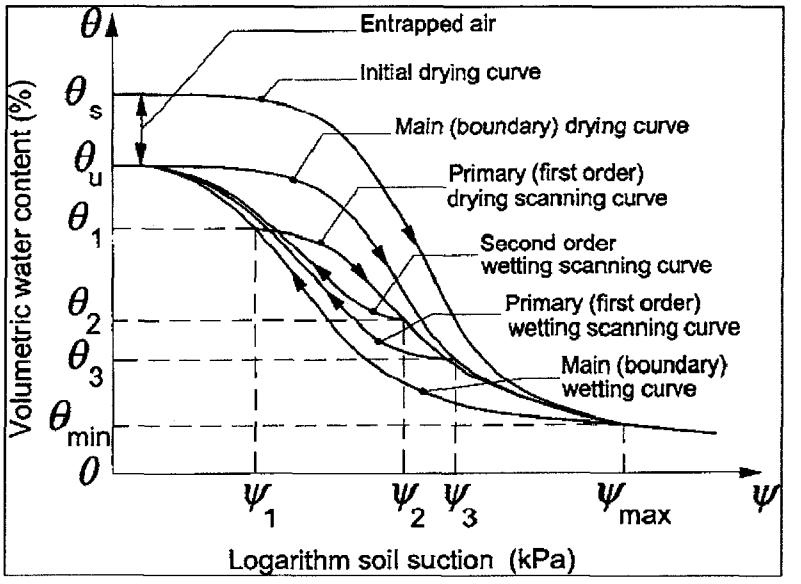

Figure 2- 4 Bounding and scanning curves that comprise the drying and wetting behavior of an unsaturated soil (from Pham et al. 2003a, b)

Several investigators have used SWCC as a tool in the prediction of engineering properties of unsaturated soils such as the coefficient of permeability and the shear strength during the last 15 years (Fredlund et al. 1994, Aubertin et al. 1995, Vanapalli et al. 1996, Leong & Rahardjo 1997, Bao et al. 1998). These studies are simple and encouraging to engineers to implement the mechanics of unsaturated soils into practice.

2.3.4. Stress State

The stress state for an unsaturated soil can be defined in the form of two independent stress tensors (Fredlund and Morgenstern 1977). There are three sets of possible stress tensors, of which only two are independent. The stress state variables most often used in the formulation of unsaturated soil problems form the following two tensors:

$$\begin{bmatrix} (\sigma_x - u_a) & \tau_{yx} & \tau_{zx} \\ \tau_{xy} & (\sigma_y - u_a) & \tau_{zy} \\ \tau_{xz} & \tau_{yz} & (\sigma_z - u_a) \end{bmatrix} \quad \text{Eq.2- 1}$$

$$\begin{bmatrix} (u_a - u_w) & 0 & 0 \\ 0 & (u_a - u_w) & 0 \\ 0 & 0 & (u_a - u_w) \end{bmatrix} \quad \text{Eq.2- 2}$$

where σ_x, σ_y, and σ_z = total stresses in the x, y, and z directions, respectively; u_w = pore–water pressure; and u_a = pore–air pressure.

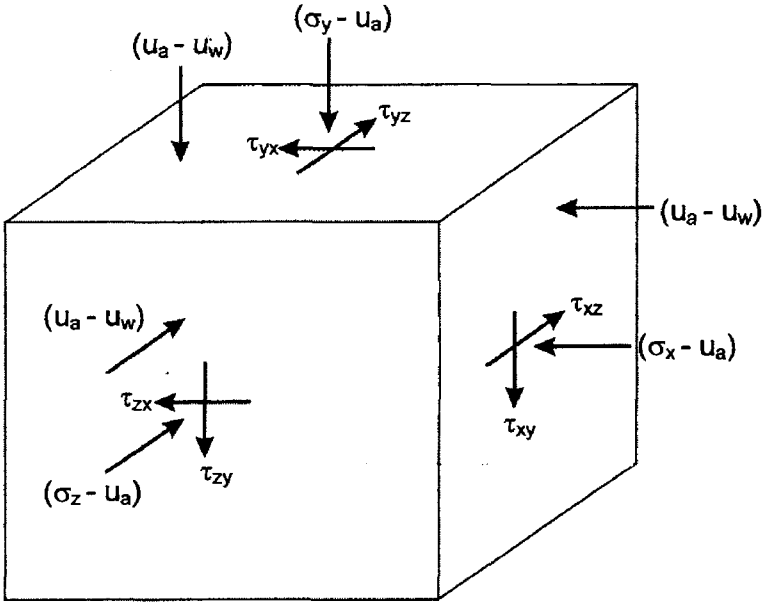

Figure 2- 5 Definition of stress state at a point in an unsaturated soil (Fredlund and Morgenstern 1977)

The stress tensors contain surface tractions that can be placed on a cube to represent the stress state at a point (Figure 2- 5). The stress tensors provide a fundamental description of the stress state for an unsaturated soil. It has also been shown that osmotic suction forms another independent stress tensor when there are changes in salt content of either a saturated or an unsaturated soil (Barbour and Fredlund 1989). All the stress state variables are independent of soil properties and become the "key tools" towards describing phenomenological behavior as well as defining functional relationships for unsaturated soil properties.

As a soil approaches saturation, the pore–air pressure, u_a, becomes equal to the pore–water pressure, u_w. At this point, the two independent stress tensors revert to a single stress tensor that can be used to describe the behavior of saturated soils:

$$\begin{bmatrix} (\sigma_x - u_w) & \tau_{yx} & \tau_{zx} \\ \tau_{xy} & (\sigma_y - u_w) & \tau_{zy} \\ \tau_{xz} & \tau_{yz} & (\sigma_z - u_w) \end{bmatrix} \qquad \textbf{Eq.2- 3}$$

Stress tensors containing stress state variables form the basis for developing a behavioral science for particulate materials. The stress tensors make it possible to write first, second, and third stress invariants for each stress tensor. The stress invariants associated with the first and second stress tensors are shown in Fredlund and Rahardjo (1993).

Several investigators made an attempt to explain the unsaturated soils behavior using a single stress state variable. These equations proposed in the literature relate different stress state variables to a single stress variable through the inclusion of soil properties. The best known single-valued relationship to describe effective stress in unsaturated soils is Bishop's equation (Bishop 1959):

$$\sigma' = (\sigma - u_a) + \chi(u_a - u_w) \qquad \textbf{Eq.2- 4}$$

where σ' = effective stress and χ = soil parameter related to degree of saturation, S which ranges from 0 to 1.

Another form of Bishop's equation has been used by several researchers in the development of elasto-plastic models (Jommi 2000; Wheeler et al. 2003; Gallipoli et al. 2003).

$$\sigma^*_{ij} = \sigma_{ij} - \left[S u_w + (1-S) u_a \right] \delta_{ij} \qquad \textbf{Eq.2- 5}$$

where σ_{ij} = total stress tensor; δ_{ij} = Kroneker delta or substitution tensor; σ^*_{ij} = Bishop's average soil skeleton stress.

In this case, the degree of saturation has been substituted for the χ soil parameter.

2.3.5. Shear Strength

The shear strength constitutive relationship provides a mathematical equation relating the normal and shear components of the stress tensor. Any one of several shear strength failure criteria could be extended from saturated to unsaturated soil conditions. The Mohr–Coulomb failure criterion was extended to embrace unsaturated soils by Fredlund et al. (1978). In a general form, the shear strength equation can be written as follows:

$$\tau = c' + (\sigma_n - u_a)\tan\phi' + (u_a - u_w)f_1 \qquad \textbf{Eq.2- 6}$$

where τ=shear strength;

c' = effective cohesion intercept;

σ_n = total normal stress on the failure plane at failure;

ϕ' = effective angle of internal friction;

f_1 = soil property function defining the relationship between shear strength and soil suction; the derivative of which [i.e., $df_1 / d(u_a - u_w)$], gives the instantaneous rate of change in shear strength.

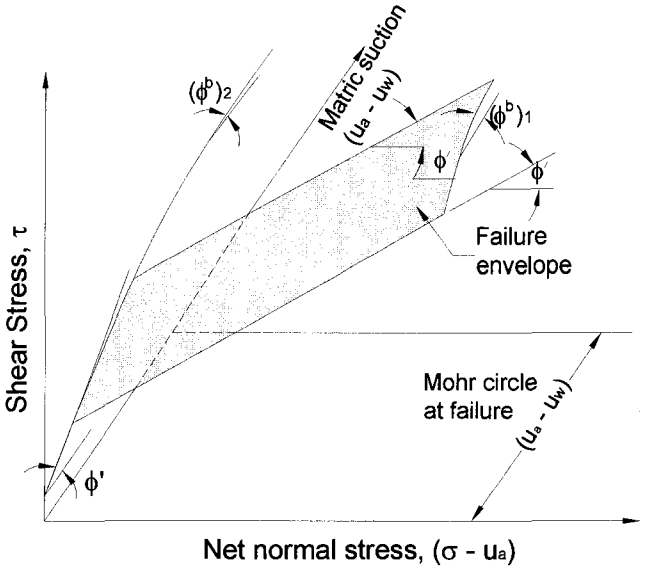

Figure 2- 6 Extended Mohr-Coulomb failure surface as a function of the stress state using Fredlund et al. 1978 equation (from Oh et al. 2008).

Figure 2- 6 shows a three-dimensional constitutive surface with matric suction plotted perpendicular to the conventional two-dimensional Mohr–Coulomb plot. The shear strength parameters c', and ϕ' are presented as saturated soil constants; however, the soil property function, f_1, is a function of matric suction (Gan et al. 1988). More recently studies show that there is a relationship between the SWCC and the the shear strength (Vanapalli et al. 1996) (Figure 2- 7).

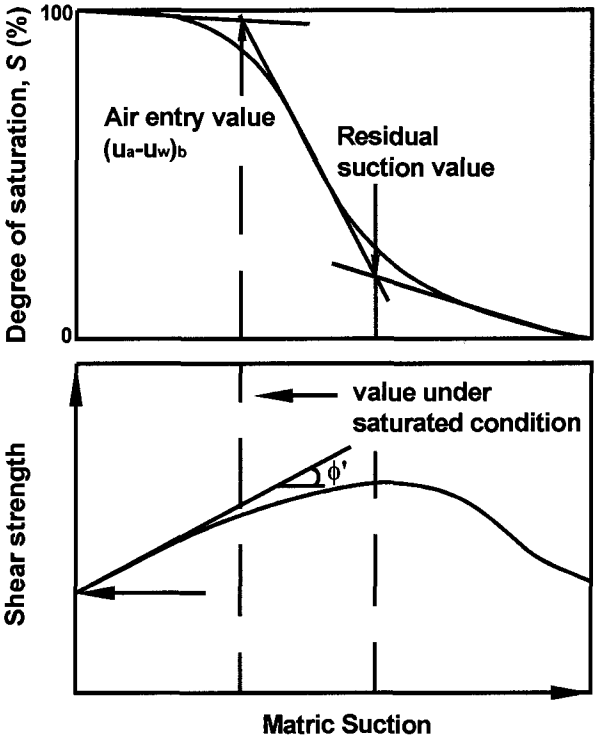

Figure 2- 7 Curvature to the shear strength envelope with respect to matric suction (modified after Vanapalli et al. 1996)

The shear strength of an unsaturated soil bears a relationship to key points along the SWCC. Under low suction conditions (i.e., less than the air entry value of the soil), the derivative of f_1, tends to equal the tangent of the effective angle of internal friction of the saturated soil (i.e., tan ϕ') (Vanapalli et al. 1996). At high suction conditions (i.e., greater than residual soil suction), the derivative of f_1, has been shown to tend toward zero for several soils with varying silt and clay contents (Nishimura and Fredlund 2001). Sandy soils have shown that the slope may even

become negative at suctions greater than the residual value (Donald 1956; Gan and Fredlund 1996).

A linear form of the general shear strength equation (i.e., Eq.2-7) was published by Fredlund et al. (1978):

$$\tau = c' + (\sigma_n - u_a)\tan\phi' + (u_a - u_w)\tan\phi^b \qquad \textbf{Eq.2- 7}$$

The linear form is more appropriate for limited ranges of matric suction, particularly for fine-grained soils. Some of the earlier unsaturated soils shear strength data sets (e.g., Bishop et al. 1960) show a close fit to the linear equation (Fredlund and Rahardjo 1993). The linear form is also more convenient to use for shear strength solutions.

Vanapalli et al. (1996a) proposed a semi-empirical procedure based on the equation proposed by Fredlund et al. (1978) to predict the variation of shear strength with respect to matric suction using the saturated shear strength parameters and the SWCC as given below.

$$\tau = c' + (\sigma_n - u_a)\tan\phi' + (u_a - u_w)(S^{\kappa})(\tan\phi') \qquad \textbf{Eq.2- 8}$$

where S is the degree of saturation and κ a is fitting parameter.

Several other empirical or semi-empirical procedures are available in the literature to predict or estimate the shear strength of unsaturated soils (Garven & Vanapalli 2006).

Most of data on shear strength of unsaturated soils appear to have been undertaken on compacted soils with initial water content and density and then wetted such that the initial suction was allowed to come toward a zero value (Gan and Fredlund 1996, Vanapalli et al. 1996). The soil specimens are then subjected to a series of increasing matric suctions along the desorption branch of the SWCC. Since there is hysteresis between the drying and wetting curve it would be anticipated that soils may exhibit a different shear strength envelope if first subjected to high matric suction conditions and then reduced to a series of suction values along the wetting curve.

Melinda et al. (2004) reported the shear strength results on a residual soil from Singapore tested along both the drying curve and the wetting curve. The results showed that the measured shear strengths along the drying curve are higher than those measured along the wetting curve. These results can be explained on the basis of the hysteresis of the SWCC that shows the matric suction having a greater cross-sectional area over which to act along the drying curve, for a specific suction. The difference in shear strength between drying and wetting conditions appears to be related to the magnitude of the drying and wetting hysteresis loop.

2.4 Bearing Capacity of Unsaturated Soils

The measured bearing capacity from field tests is typically higher than the estimated or computed bearing capacity values using analytical and empirical methods (Terzaghi 1943, Meyerhof 1951 and 1956, Vesic 1973). This behavior may be attributed to neglecting the contribution suction towards the bearing capacity of soils (Steensen-Bach et al. 1987, Fredlund and Rahardjo 1993). There has been considerable interest during the last twenty years towards understanding the engineering behavior of unsaturated soils; however, there are limited studies with respect to the bearing capacity of unsaturated soils.

2.4.1. Broms (1964)

Broms (1964) developed a method to evaluate the bearing capacity of flexible pavement in unsaturated soils. This method assumed that the failure takes place in fully saturated subgrade soil. The bearing capacity was found is a function of the degree of saturation, S, the apparent cohesion, c and internal friction angle, ϕ. From this study, it was found that the degree of saturation has a significant effect on the bearing capacity of the pavement. A decrease in the degree of saturation from 100 to 90% increased the bearing capacity of two fine-grained soils (i.e., silt and clay) by approximately 2 and 8% respectively. Such a behavior suggests that bearing capacity of the fine-grained soils reduces due to an increase in the degree of saturation, S. Figure 2- 8 shows the relationship between the tire pressure and the ultimate wheel load with respect to degree of saturation, S.

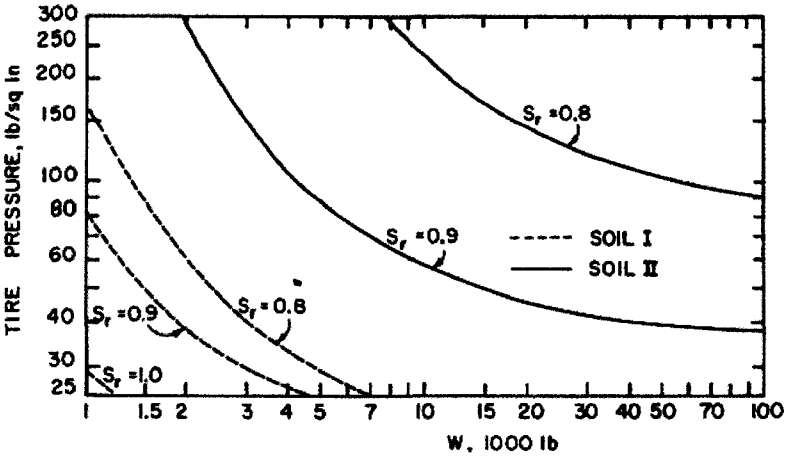

Figure 2- 8 The tire pressure versus wheel load of flexible pavement (Broms 1964)

2.4.2. Steensen-Bach et al. (1987)

The bearing capacity of two different sands under a surface footing in saturated and unsaturated conditions was studied. The capillary pressure below the footings was determined by in-situ measurements using Tensiometers and by laboratory determination of the capillary curves. It was found that the measured bearing capacity of unsaturated sand is typically 4 to 6 times higher than the saturated bearing capacity of the same soils. Based on experimental studies on model tests on two sands, Steensen-Bach (1987) concluded that the presence of capillary pressures is certainly fact, not fiction, and its effect should be carefully considered.

2.4.3. Fredlund and Rahardjo (1993)

Fredlund and Rahardjo (1993) proposed bearing capacity equations for unsaturated soils by extending conventional bearing capacity equations including the influence of matric suction in the term apparent cohesion extending total stress approach. The apparent cohesion consists of two components. The first component is the effective cohesion, c' and the other component is the contribution due to matric suction, $(u_a - u_w)$. The contribution of matric suction, $(u_a - u_w)$ can be considered as an additional cohesion component in total stress approach. In the other words, the conventional bearing capacity theory can be extended to unsaturated soils by adding the component of suction to effective cohesion, c'. The increase of the cohesion is due to matric suction is illustrated in Figure 2- 9 for various ϕ^b values.

$$c_{unsat} = c' + (u_a - u_w)\tan\phi^b \qquad \text{Eq.2- 9}$$

where: c_{unsat} = total cohesion, kPa

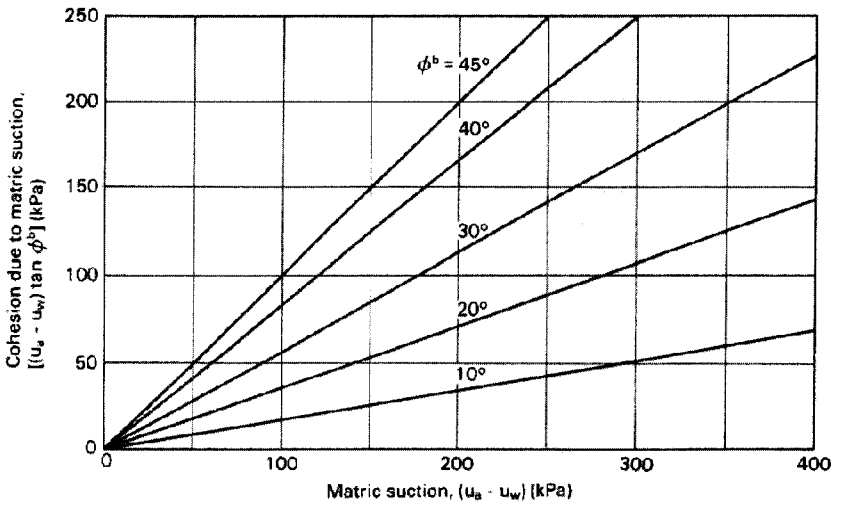

Figure 2- 9 The component of cohesion due to matric suction for angles (Fredlund and Rahardjo 1993)

A theoretical study was undertaken to evaluate the effect of soil matric suction on the ultimate bearing capacity using a square footing embedded in clay type of soil. Based on this study, it was reported an increase in the bearing capacity by 27% when the suction increased by an amount equal to the undrained shear strength of the fine-grained soil. Figure 2- 10 shows the relationship between the bearing capacity of a strip footing for various matric suction values, obtained by Fredlund and Rahardjo (1993).

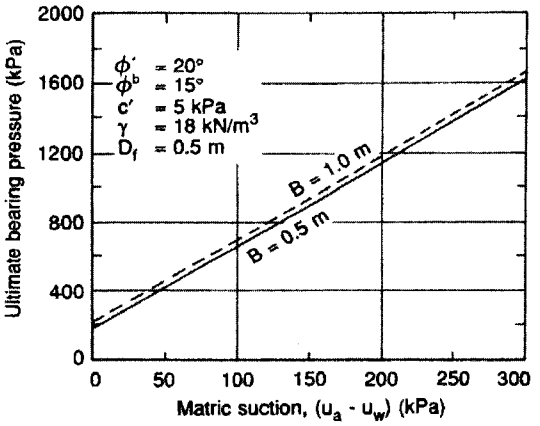

Figure 2- 10 Bearing capacity versus matric suction for a strip footing (Fredlund and Rahardjo 1993)

Figure 2- 11, Profile 1 shows the variation of matric suction above the ground water table again Profile 2, which is conventional analyses ignoring the influence of matric suction. The use of Profile 2 should be encouraged in engineering practice as it is more rational. Conventional analyses for saturated soils ignore the influence of contribution of suction towards bearing capacity.

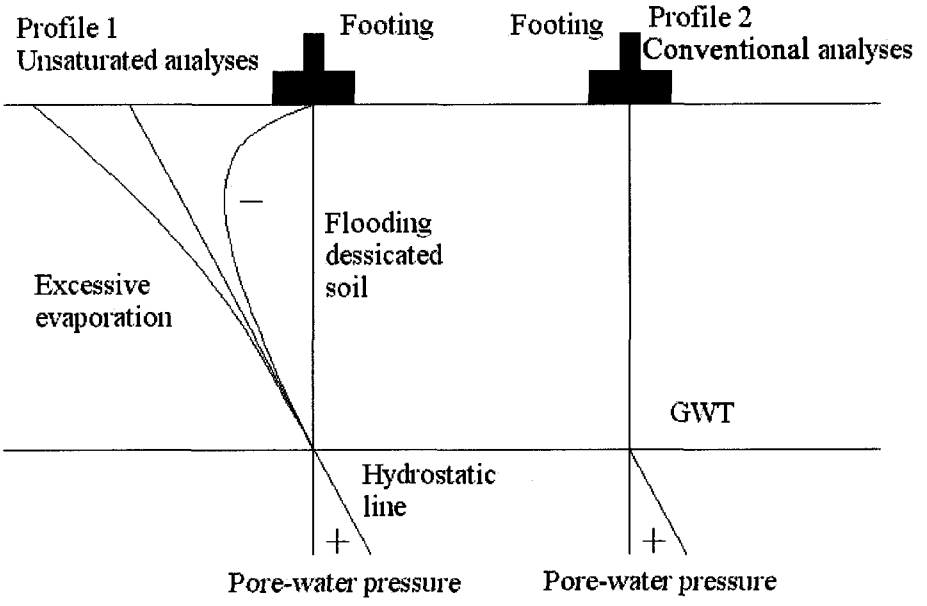

Figure 2- 11 Typical schematic pore-water profiles below a spread footing (Fredlund and Rahardjo, 1993)

2.4.4. Oloo (1994)

Oloo (1994) proposed a method for designing unpaved roads consisting of a base layer overlying a subgrade using bearing capacity design approach highlights the significant role played by matric suction on the bearing capacity of pavement structures. In addition, experimental studies of model footings on silt and till specimens show that the bearing capacity increased non-linearly with an increase in the matric suction. A relationship was proposed to predict the bearing capacity assuming a constant value of ϕ^b (internal friction angle with respect to matric suction).

2.4.5. Costa et al. (2003)

Costa et al. (2003) carried out a study to investigate the effects of matric suction on the results of plate load tests performed on Lateritic soil deposit, which was in a state of unsaturated condition. The soil suctions were measured by Tensiometers located at different depths as shown in Figure 2- 12.

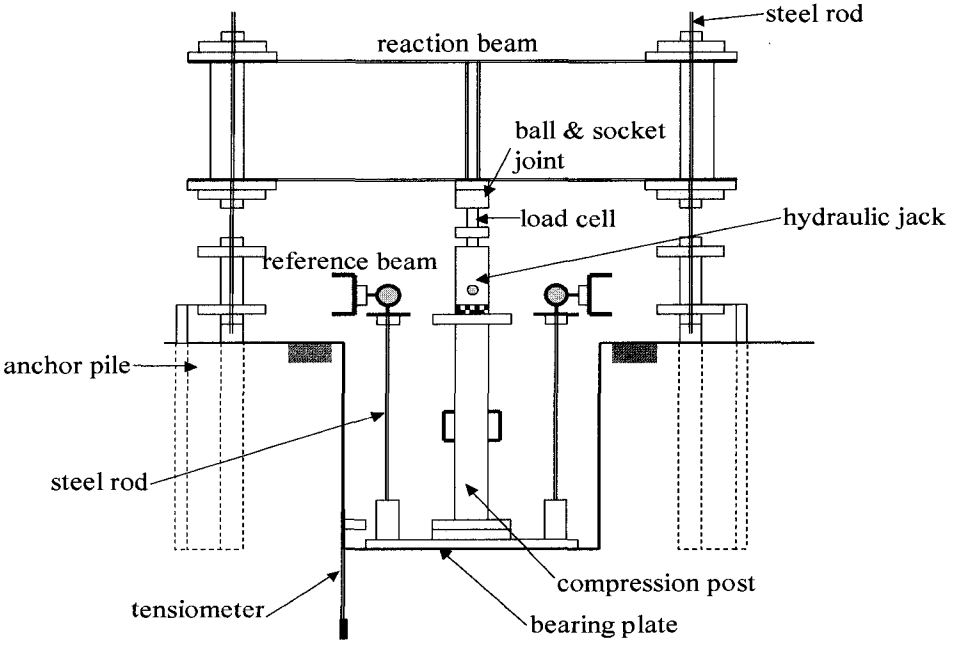

Figure 2- 12 General schematic of the testing assembly and used apparatus (Costa et al. 2003)

In-situ results suggest that the contribution of matric suction was substantial and the increase of matric suction lead to a nonlinear decrease of settlement.

2.4.6. Procedure for Predicting the Bearing Capacity of Unsaturated Soils under Drained Loading Conditions

Mohamed and Vanapalli (2006) carried out model footing tests in a specially designed bearing capacity tank (University of Ottawa Bearing Capacity Equipment, UOBCE, 900×900×750 mm), which has provisions to simulate both saturated and unsaturated conditions in the tank (Fig. 2-13). The variation of bearing capacity with respect to matric suction of compacted coarse-grained sand was determined in this study using two different sizes of model footings (i.e., 100

mm x 100 and 150 mm x 150 mm).

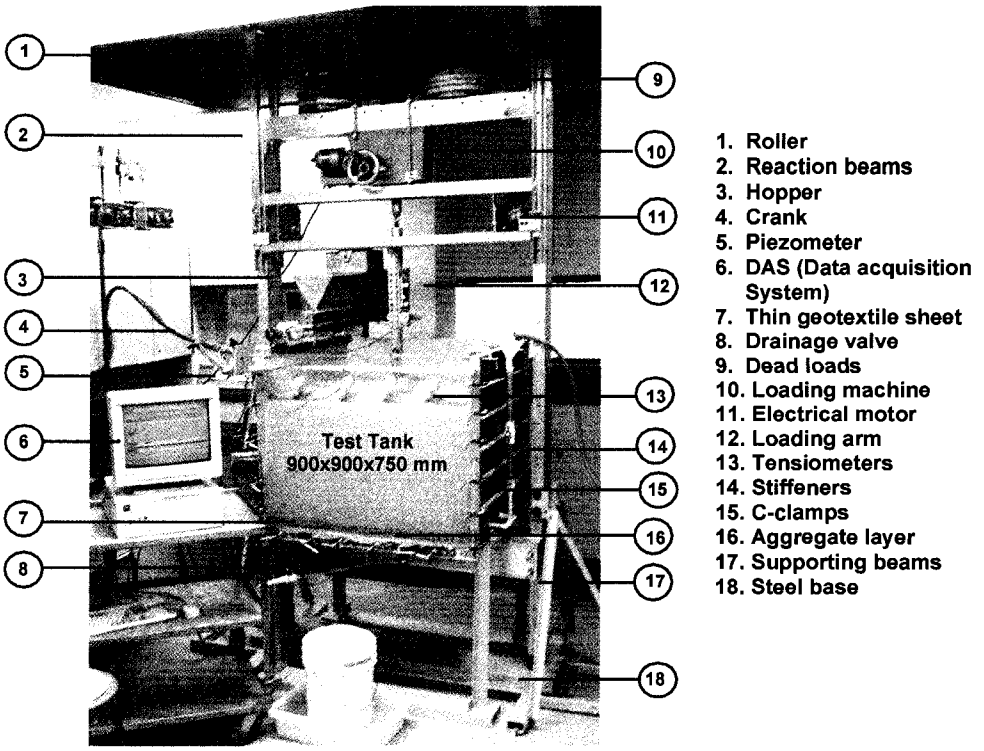

Figure 2- 13 University of Ottawa Bearing Capacity Equipment (UOBCE) (from Mohamed and Vanapalli, 2007)

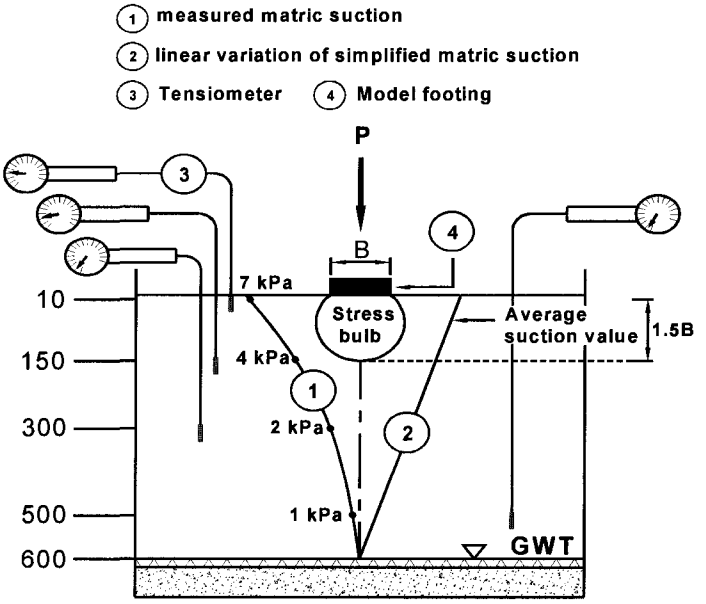

Figure 2- 14 Variation of measured matric suction values in the UOBCE with depth along with hydrostatic matric suction distribution. (after Oh and Vanapalli, 2008)

The variation of matric suction values with depth in the UOBCE was measured using several tensiometers (Figure 2- 14). The matric suction value at the center of gravity of the matric suction distribution diagram from 0 to 1.5B depth region was considered as the average value of matric suction for the analysis of the experimental results. This is the zone of depth in which the stresses due to loading are predominant (Poulos and Davis, 1974).

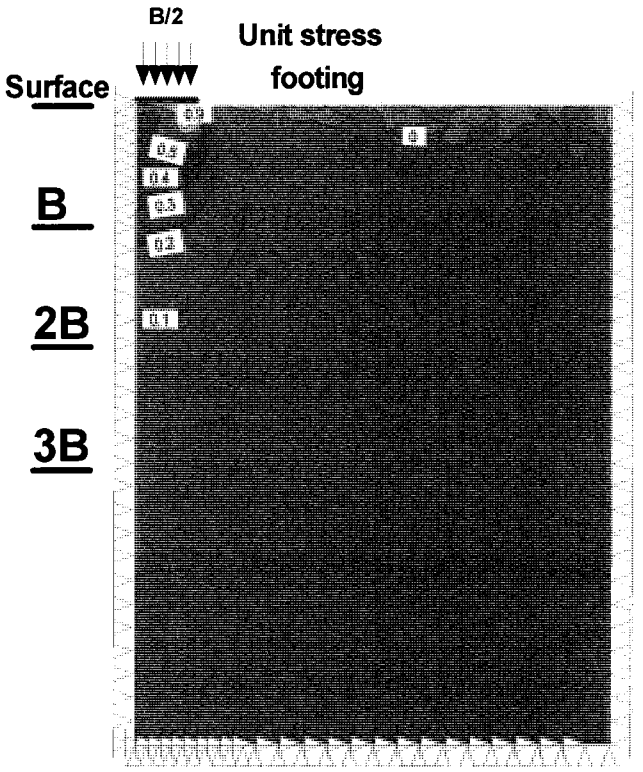

Figure 2- 15 Vertical stress distribution contours obtained from SIGMA/W due to an applied unit stress on a rigid footing in UOBCE (after Oh and Vanapalli, 2008)

More recently, Oh and Vanapalli (2008) have undertaken computer modelling studies using the results of Vanapalli and Mohamed (2007) (Figure 2- 15). The vertical stress distribution contours due to an applied unit stress on rigid footing using axisymmetric analysis (Dia. = 112.8 mm, which represents an equivalent diameter for 100 x 100 mm square footing) in the UOBCE were modelled. The results shown in Figure 2- 15 were obtained from the finite element analysis (SIGMA/W of GEO-SLOPE) using linear elastic model. It can be seen that the stress intensity under the center of a footing at a depth lower than 1.5B is less than 0.15 in comparison to the applied unit stress at the surface. These results are consistent with the conventional stress distribution theory concepts based on elastic analysis and support the assumption that the

average matric suction value can be estimated from 0 to 1.5B depth region. These results are interesting and demonstrate that bearing capacity model studies can be undertaken using relatively smaller size tanks such as 300 mm diameter yielding similar results.

Vanapalli and Mohamed (2007) proposed an equation to predict the variation of bearing capacity with respect to matric suction for surface model footings on unsaturated soils using the saturated shear strength parameters (i.e. c' and ϕ') and the SWCC as below:

$$q_{ult} = [c' + (u_a - u_w)_b (1 - S^{\psi}) \tan\phi' + (u_a - u_w)_{AVR} S^{\psi} \tan\phi'] \times N_c \xi_c + 0.5 B \gamma N_\gamma \xi_\gamma \qquad \textbf{Eq.2- 10}$$

where:
q_{ult} is the ultimate bearing capacity

ψ is a fitting parameter, $(u_a - u_w)_{AVR}$ is average (representative) suction value, B is the width of footing

L is the length of footing

γ is soil unit weight

N_c and N_q are bearing capacity factors from Terzaghi (1943)

N_γ is bearing capacity factor from Kumbhokjar (1993)

$\xi_c \left\{ = \left[1.0 + \left(\frac{Nq}{Nc} \right) \left(\frac{B}{L} \right) \right] \right\}$ and $\xi_\gamma \left\{ = \left[1.0 - 0.4 \left(\frac{B}{L} \right) \right] \right\}$ are shape factors from Vesić (1973)

The procedure for predicting the bearing capacity of unsaturated soils under drained loading conditions using Eq.2-10 is similar to predicting the shear strength of unsaturated soils proposed by Vanapalli et al. (1996) using Eq.2-8.

Using some of their own results and others from the literature, Vanapalli and Mohamed (2007) provided comparisons between the measured bearing capacities and predicted bearing capacity values (using Eq.2-10) of unsaturated soils for both coarse and fine-grained soils. There was a reasonable good comparison. Figure 2- 16 shows some typical results of their studies on a mediate coarse-grained sand.

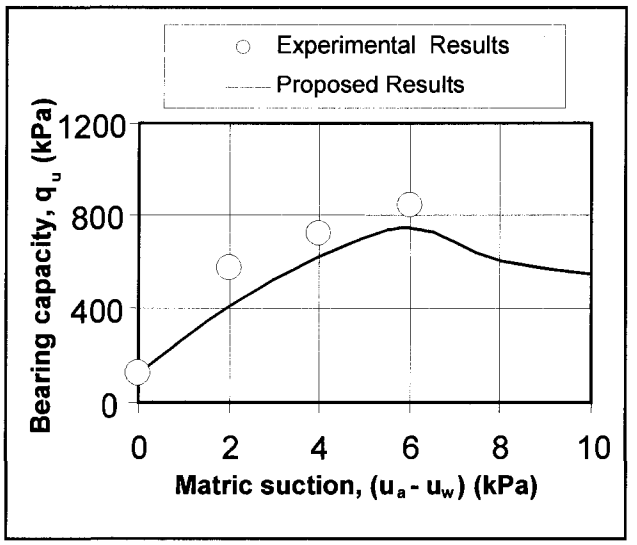

Figure 2- 16 Comparison between measured and predicted bearing capacity of a compacted unsaturated sand (from Vanapalli and Mohamed 2007)

In addition, Vanapalli and Mohamed (2007) also provided a relationship (Figure 2- 17) between the fitting parameter, ψ and I_p that can be used for predicting the bearing capacity of unsaturated soils as given below:

$$\psi = -0.0031(I_p^2) + 0.3988(I_p) + 1 \qquad \textbf{Eq.2- 11}$$

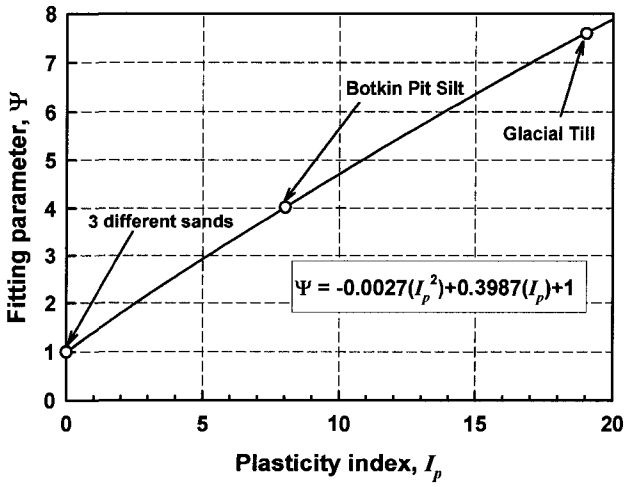

Figure 2- 17 Relationship between the bearing capacity fitting parameter, ψ and the plasticity index, I_p

2.4.7. Procedure for Predicting the Bearing Capacity of Unsaturated Soils under Undrained Loading Conditions

Vanapalli et al. (2007) have conducted a series of model footing tests on statically compacted unsaturated Indian Head till soil samples at different matric suction values to determinate the contribution of matric suction towards bearing capacity of unsaturated soils under undrained loading conditions in specially designed equipment (Figure 2- 18). The soil was compacted in the plastic mould and saturated using a downwards flow of water simulating natural flow behavior in field conditions. This flow was achieved through compaction plate (with drainage holes) placed on the surface of the compacted soil. During this process, the compactor plate was securely placed on the surface of compacted soil and fixed to the cross bar of the loading machine to prevent any possible volume change of soils due to swelling. Once the compacted soil in the plastic container was fully saturated, it was subjected to natural air drying for several days. The changes in the suction values with respect to depth in the soil sample due to air drying were monitored using tensiometers.

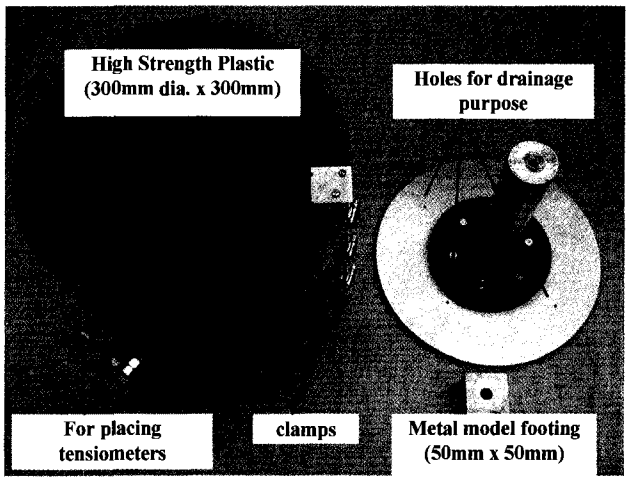

Figure 2- 18 Equipment used for determining the bearing capacity of unsaturated soils under undrained loading conditions (from Vanapalli et al. 2007)

The bearing capacity of a 50 mm x 50 mm footing was determined by loading it in a conventional loading frame. After the tests, three specimens were collected from the compacted soils using 50mm diameter stainless steel thin-wall tubes. Two of the specimens were used for measuring the undrained strength by conducting unconfined compression tests (1.14 mm/min).

The remainder specimen was used for measuring matric suction following axis translation technique to verify the accuracy of the suction measurements using tensiometers. In addition, the water content variation with respect to depth was also investigated.

Using the results of these studies, Vanapalli et al. (2007) have proposed a relationship for estimating the bearing capacity of unsaturated soils under undrained loading conditions from unconfined compression test results.

The bearing capacity can be predicted with the equation:

$$q_{ult} = [q_{u(unsat)} / 2][1 + (B / L)(N_q / N_c)]N_{cs} \qquad \textbf{Eq.2- 12}$$

where, q_{ult} =ultimate bearing capacity, kPa

$q_{u(unsat)}$ =unconfined compression shear strength for an unsaturated, kPa

N_c, N_q =cohesion and surcharge factors

N_{cs} =factor associated with cohesion under undrained condition

B, L=footing width and length, m

Eq.2-12 is similar in form as Skempton (1948) equation for estimating the bearing capacity of saturated soils from conventional unconfined compression tests results. The results of this study suggest that there is a good comparison between the measured bearing capacity values from model footing tests and estimated bearing capacity values from unconfined compression tests (Figure 2- 11).

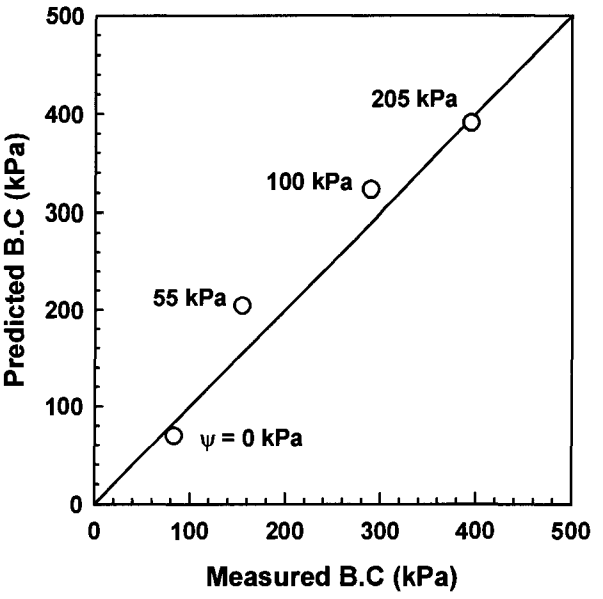

Figure 2- 19 Comparison between the measured and predicted bearing capacity under undrained loading conditions of compacted Indian Head till specimens (from Vanapalli et al. 2007)

2.5 Summary

This chapter provides a brief background related to the bearing capacity of unsaturated soils both under drained and undrained loading conditions. Most of the studies summarized in this chapter are undertaken at the University of Ottawa geotechnical laboratory based on limited number of experimental studies. There is a need for more laboratory studies to better understand the bearing capacity of unsaturated soils using model footings. Based on the present understanding, two new units of equipment have been designed and fabricated to facilitate conducting bearing capacity tests using model footings at a relatively faster rate. The remainder of the chapters in this thesis provides details of equipment design and present the results and analysis of more than 250 tests undertaken to study the bearing capacity of different compacted sands.

CHAPTER 3

EQUIPMENTS AND METHODOLOGY

3.1 Introduction

This chapter provides details of two bearing capacity test systems designed and fabricated by the author at the University of Ottawa student workshop. Information related to other equipment used in this research program such as the suction profile apparatus for determination of the variation of suction with respect to ground water table and the Tempe cell with its accessories for measuring the Soil Water Characteristic Curve (SWCC) are also detailed. In addition, key details with respect to other minor accessories are also highlighted. The methodologies associated with conducting the various laboratory tests using the various equipments are also summarized.

3.2 Bearing Capacity Test Systems

Two different bearing capacity test systems are used in the present research program. In the first bearing capacity test system a short soil container is used. The model footing will be placed on the surface of the compacted soil specimen in the short soil container under both saturated and unsaturated conditions and loaded to failure using a conventional loading frame (Figure 3- 1). Such loading frames are commonly used in geotechnical laboratories for determining the shear strength parameters using a triaxial cell. Figure 3- 1 also shows other accessories used along with the test system for the determination of bearing capacity of model footings.

Figure 3- 2 shows the second bearing capacity test system with a tall soil container and other accessories. An electrically operated and mechanically controlled loading mechanism with a robust loading frame is used.

More details related to both the systems and the other elements are discussed in greater detail in later sections of the chapter.

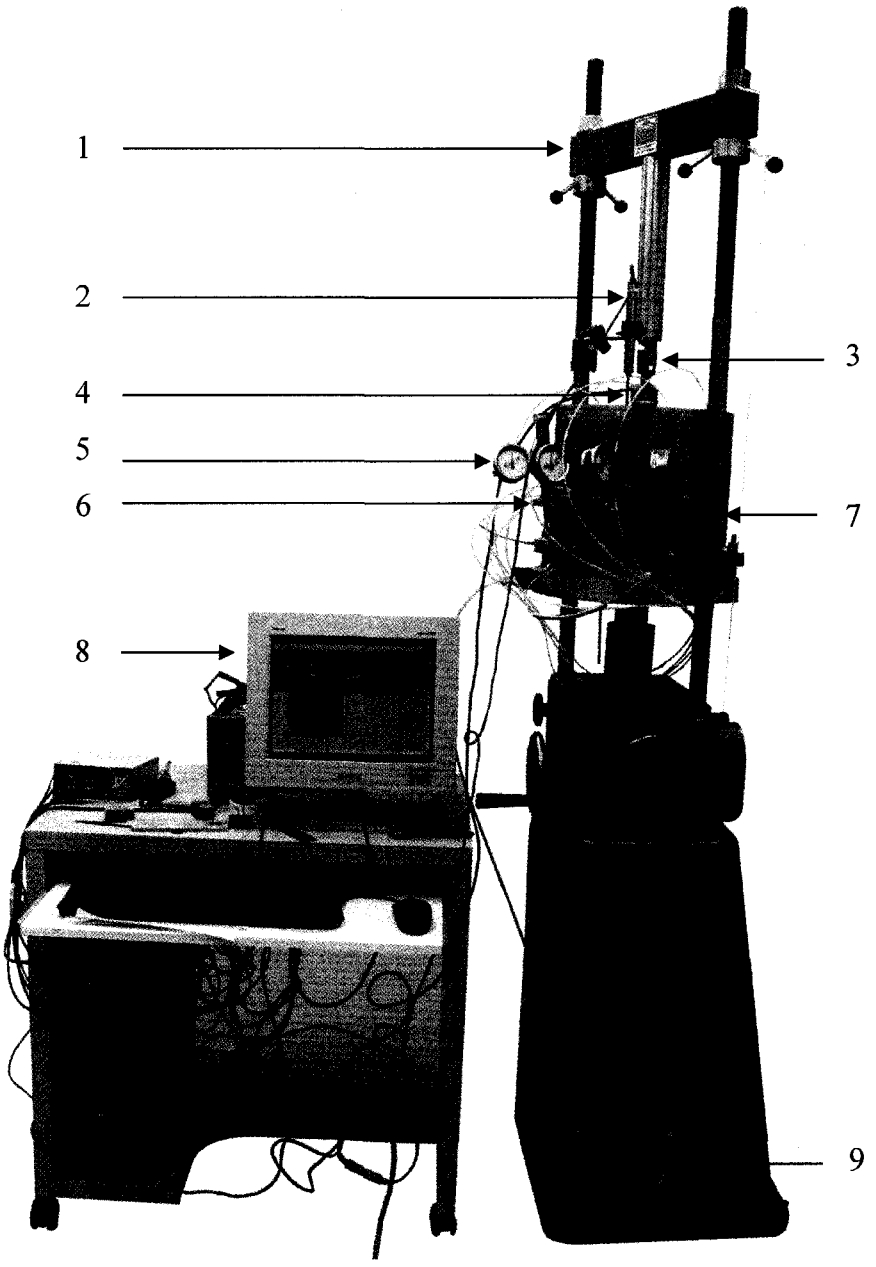

1. Loading Machine
2. Settlement transducer
3. Load cell
4. Footing
5. Tensiometer
6. Tensiometer holders
7. Soil container
8. Data acquisition system
9. Water container

Figure 3- 1 Bearing capacity test system I with short soil container

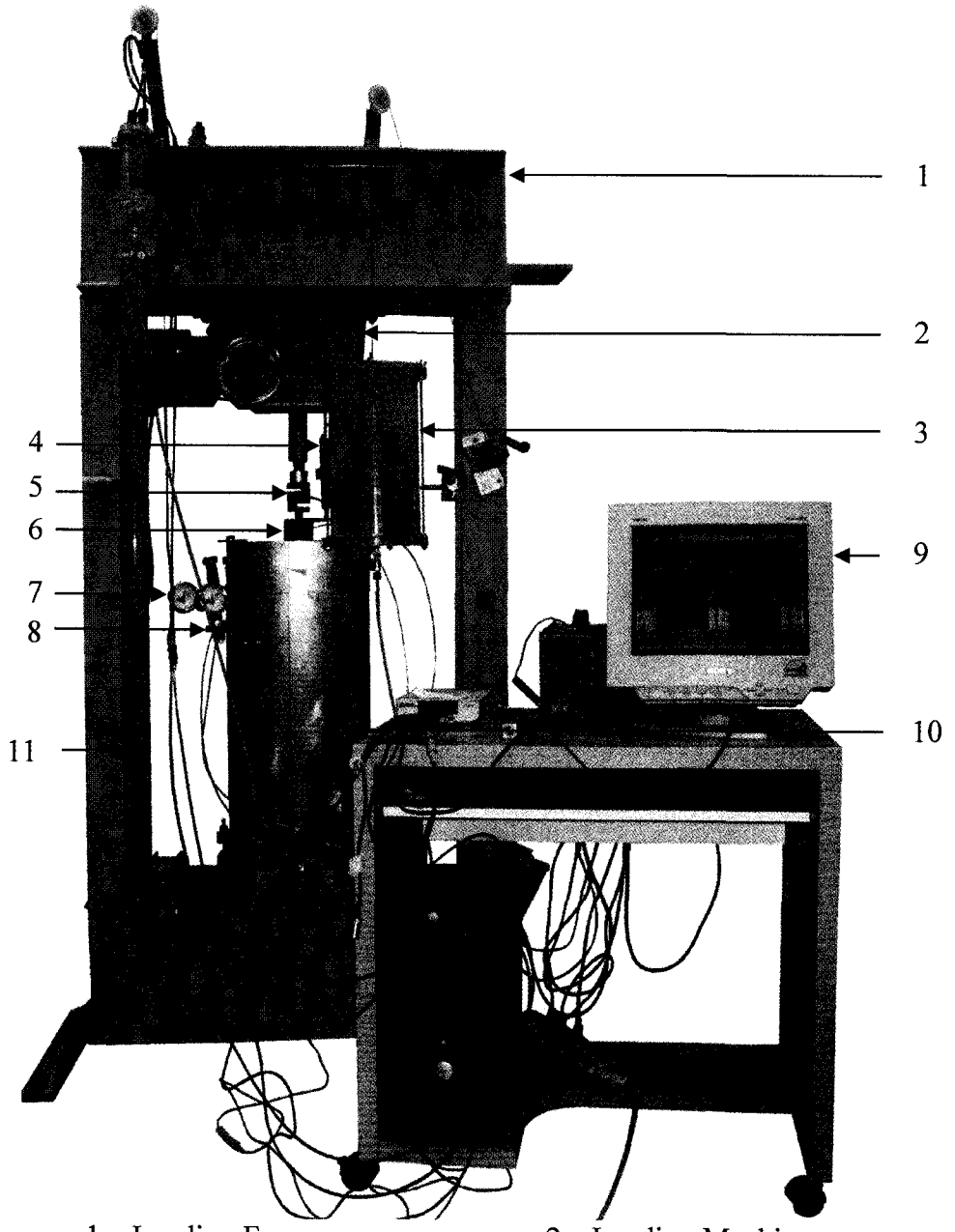

1. Loading Frame
2. Loading Machine
3. Water container
4. Settlement transducer
5. Load cell
6. Footing
7. Tensiometer
8. Tensiometer holders
9. Data acquisition system
10. Soil container
11. Suction profile set

Figure 3- 2 Bearing capacity test system II with tall soil container

3.3 Model Surface Footings

A series of aluminum square footings with dimensions of 20 mm × 20 mm, 25 mm × 25 mm, 37.5 mm × 37.5 mm and 50 mm × 50 mm were used in the present study. The objective of using different size footings in the study is to understand the influence of footing size on the bearing capacity of unsaturated soils (Figure 3- 3).

All the model footings are relatively smaller in size in comparison to the diameter of the soil containers (both short and tall). The ratio of soil container size to footing size is greater than 6. As the soil container size is considerably large in comparison to footing size there will be no stresses arising due to the loading of the footing on the boundaries of the soil container. In other words soil container size has no influence of measured bearing capacity values. Earlier studies by Poulos and Davis (1974) and modeling studies by Oh and Vanapalli (2008) support these observations.

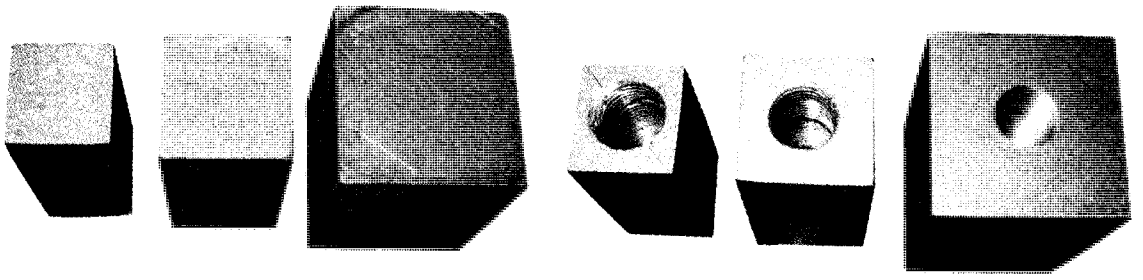

Figure 3- 3 Different square footings used in the test program

3.4 Soil Containers

Two soil containers; namely, tall and short soil containers were used in the research program. Both these containers had other assemblies and elements to facilitate saturation and desaturation of the soil sample in the container. Figure 3- 4 shows the schematic of the container with all the various elements.

The tall soil container facilitates in varying the ground water table below the footing to a greater depth in comparison to the short cylinder. More details with respect to the different bearing

capacity tests conducted using short and tall cylinders are discussed in later sections of the chapter.

Figure 3- 5 shows the different elements of both the short and tall cylinders. Figure 3- 5a is assembled tall soil container which is fabricated from cylindrical tube of 300 mm in diameter, 700 mm in height and 8mm in thickness. Figure 3- 5b is the short soil container of 300mm in diameter, 300mm in height and 8mm in thickness. The base Figure 3- 5c shows the base plate with circular grooves to facilitate drainage of water both into and out of the container. The circular grooves of the bottom plate are in turn covered using a stainless steel lid (Figure 3- 5d) of 260mm in diameter and 1.25mm in thickness with small holes (2mm in diameter). This plate facilitates gradual and even movement of water into and out of the soil container. On the lid a geotextile and filter paper are provided (Figure 3- 5e) to prevent the soil particles from getting into the circular grooves of the base plate and valves. Several trial studies were undertaken to develop this system which facilitates uniform movement of water.

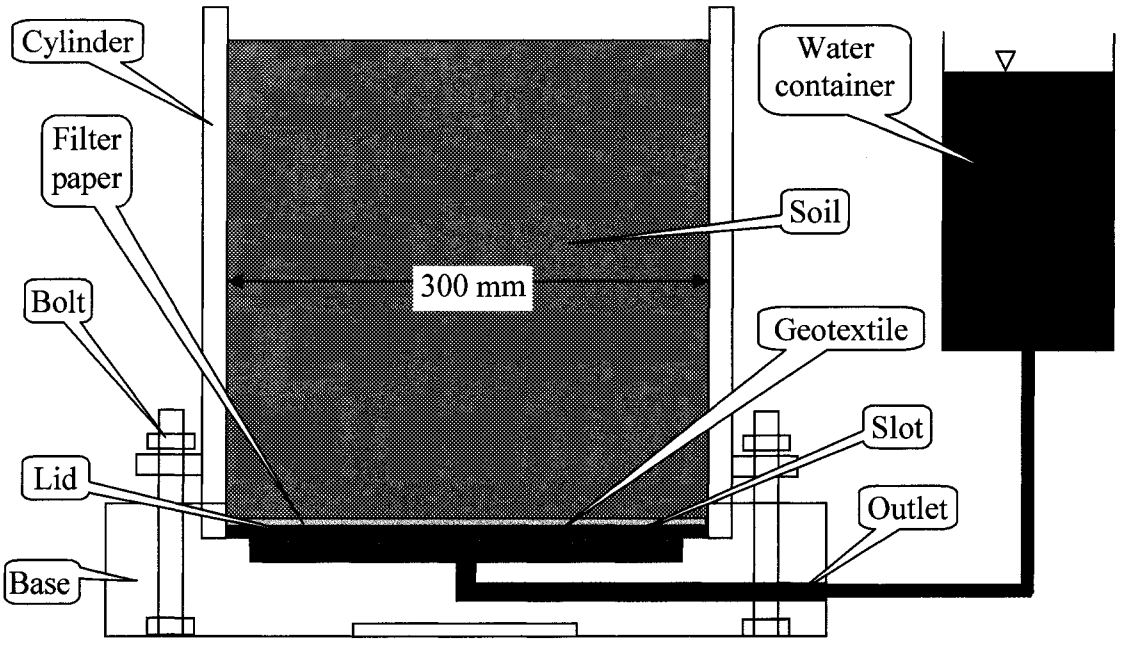

Figure 3- 4 Schematic of the soil container with various elements

The two soil containers of different lengths are used to achieve different suction values or vary the ground water table below the footings for conducting the bearing capacity tests. The tall soil

container (length in 700 mm) is used to achieve relatively high matric suction values or low ground water table, because tall soil container allows to lower the water table to the depth of 700 mm below soil surface; however, the short soil container only allows to lower the water table to a depth of 300 mm.

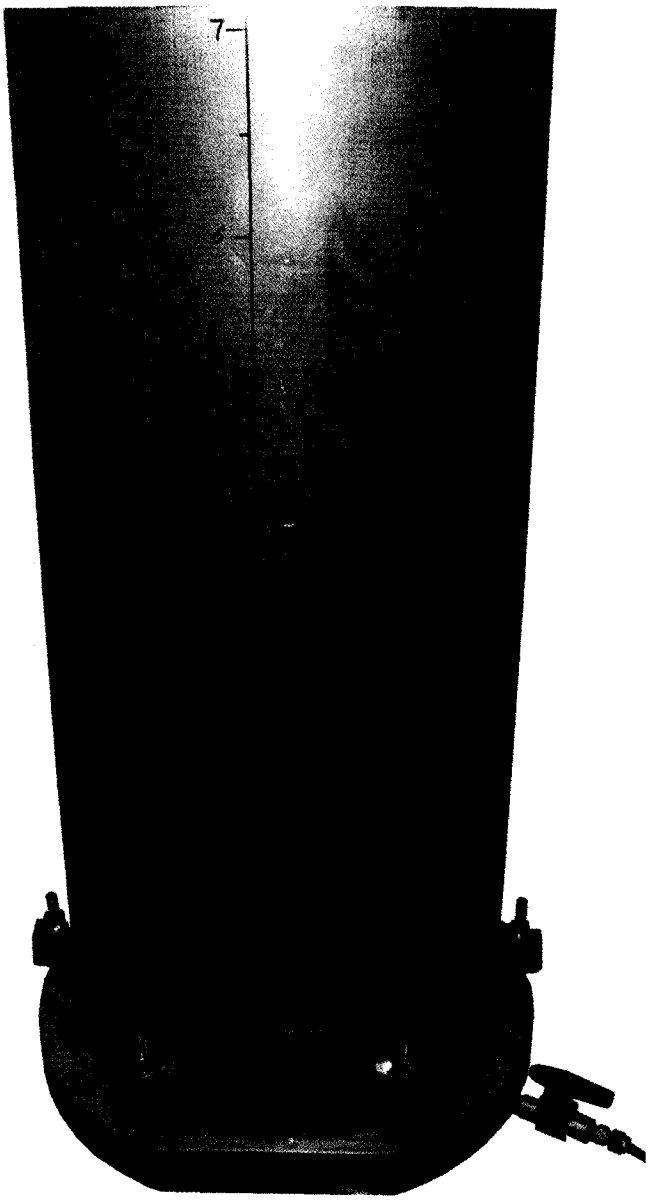

(a) Fully assembled tall soil container

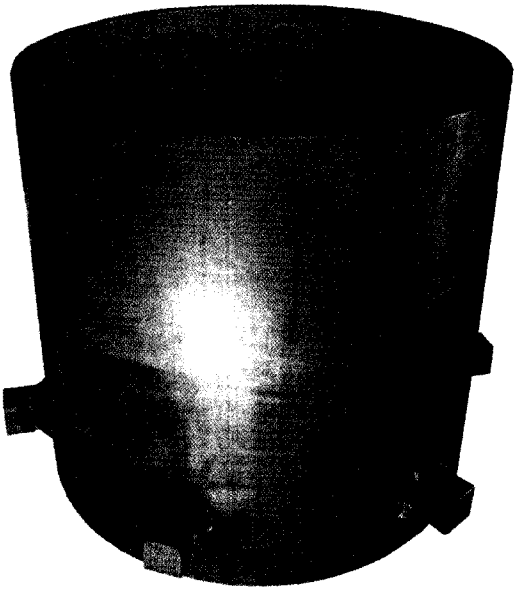

(b) Short soil container

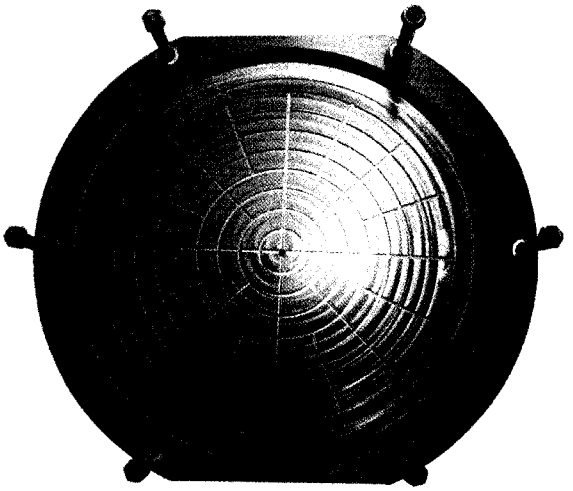

(c) Base plate (for both the short and tall soil containers)

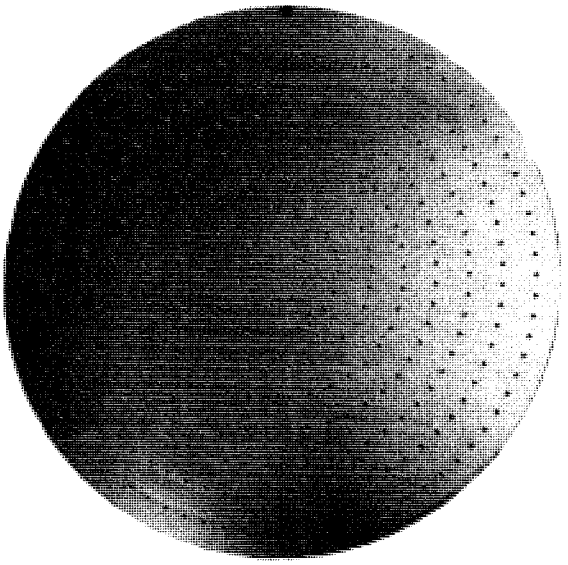

(d) Lid

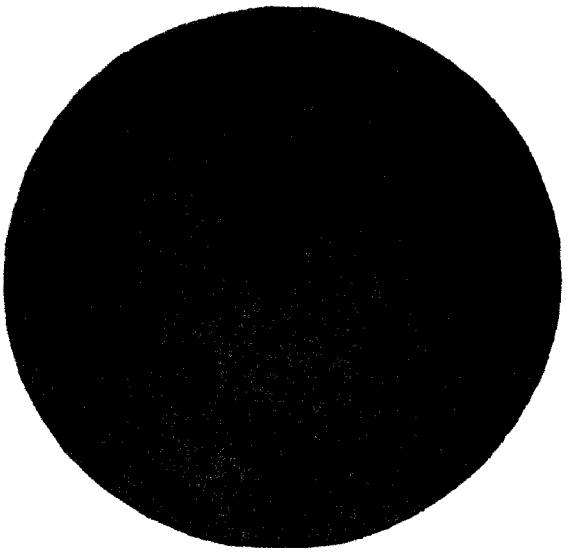

(e) Geotextile

Figure 3- 5 Various components of the soil containers

From a practical perspective of conducting the tests in a laboratory environment, the tall soil container is to heavy for moving (with weight of greater 100 kg when it is filled up with the compacted soil). The short soil container (length in 300 mm) is not too heavy and can be easily maneuvered in the laboratory. Bearing capacity tests were conducted using samples that were prepared by static compaction and vibratory compaction methods. Short soil containers were used for conducting the bearing capacity after subjecting the soil samples to vibration for compacting them using a vibration machine.

3.5 Wykeham Farrance Loading Frame

The two soil containers with soils are loaded using different loading frames. The short soil container (300 mm in height) is loaded using TX57 loading machine in this test. TX57 (Figure 3- 6) is a Wykeham Farrance Eng. Ltd. product and facilitates loading the model footing in soil containers using six different strain rates. The maximum load capacity using this machine is 14 kN.

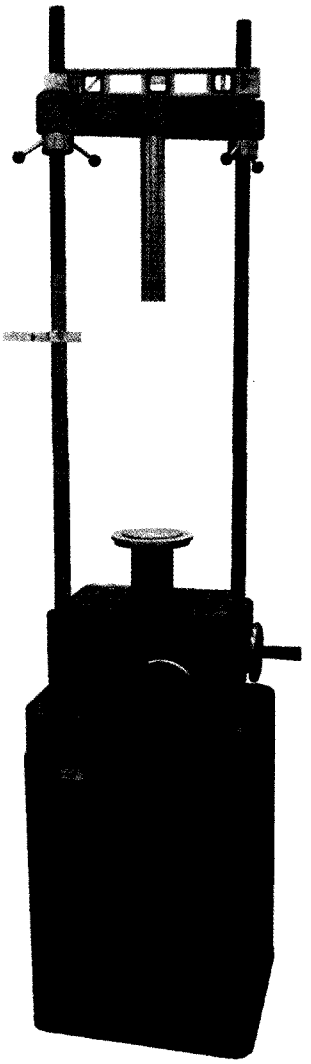

Figure 3- 6 Wykeham Farrance TX57 loading machine

3.6 ENERPAC Loading Frame

ENERPAC loading frame was used for loading the tall soil container (700mm in height). (Figure 3- 7). The frame is a part of H-Frame Presses made by Enerpac Hydraulic Technology. It is made of steel and its height is 1930 mm (76") and 1030 mm (i.e., 40.50") and wide. It has press capacity of 50 tons.

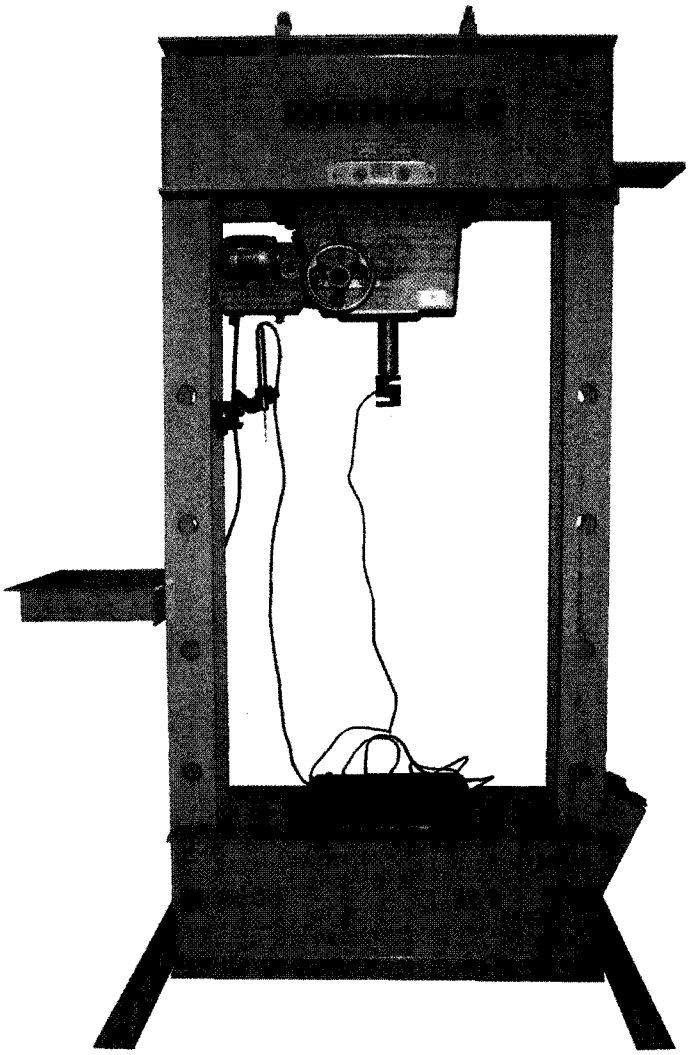

Figure 3- 7 ENERPAC loading frame

Engineering Laboratory Equipment Ltd loading machine is attached on the top of this frame. It is an electrically operated and mechanically controlled loading system for loading the model footings. The engine is mounted on and fixed to the frame by a piece of specially designed steel (250 mm× 400 mm× 8 mm) and bolts which were designed and manufactured at the University of Ottawa student workshop.

3.7 Tensiometers

Tensiometer (Figure 3- 8) is conventionally used for the direct measurement of matric suction in unsaturated soils in a range of 1 to 100 kPa.

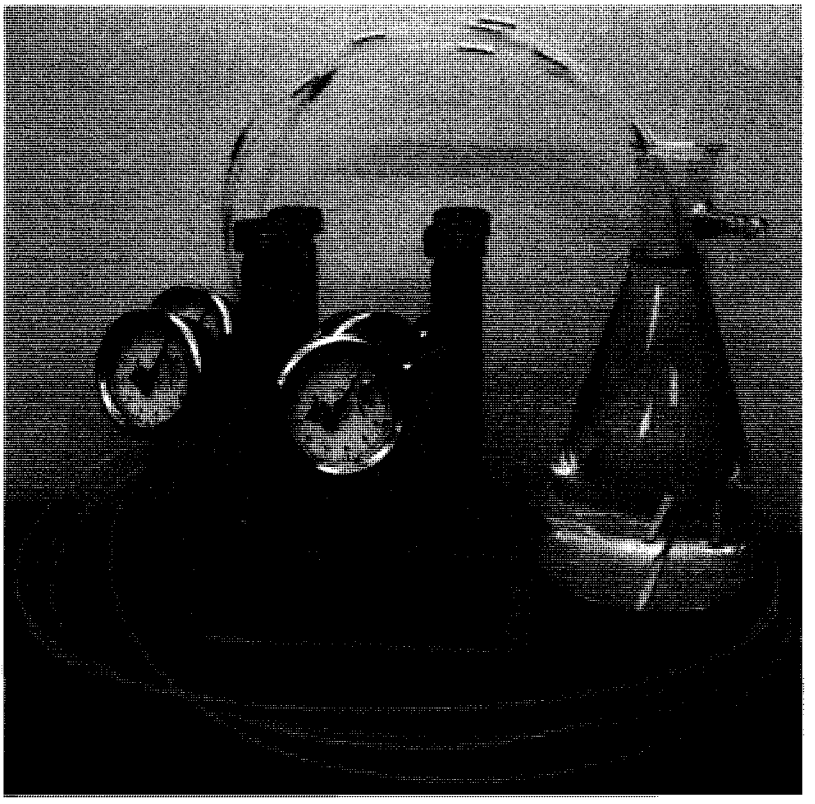

Figure 3- 8 Tensiometers Model 2100 with the plastic stand

3.7.1. Tensiometer Structure

The tensiometers used in the test are made by Soilmoisture Equipment Corp. in California, USA. The unit used for the present research is model 2100 and consists of a plastic body tube, a porous ceramic cup sensor with a 1 bar (100 kPa) air-entry value, and a vacuum dial gauge. A thin neoprene tube is also used to connect body tube and ceramic cup to transfer suction from sensor to gauge.

Ceramic cup is typically an inverted cup or small probe that can be filled with water. This tip is used to create a saturated hydraulic connection between the unsaturated soil and the water in the

Tensiometer body through the use of a pressure sensor. A typical setup of laboratory commercial Tensiometer is shown in Figure 3- 9.

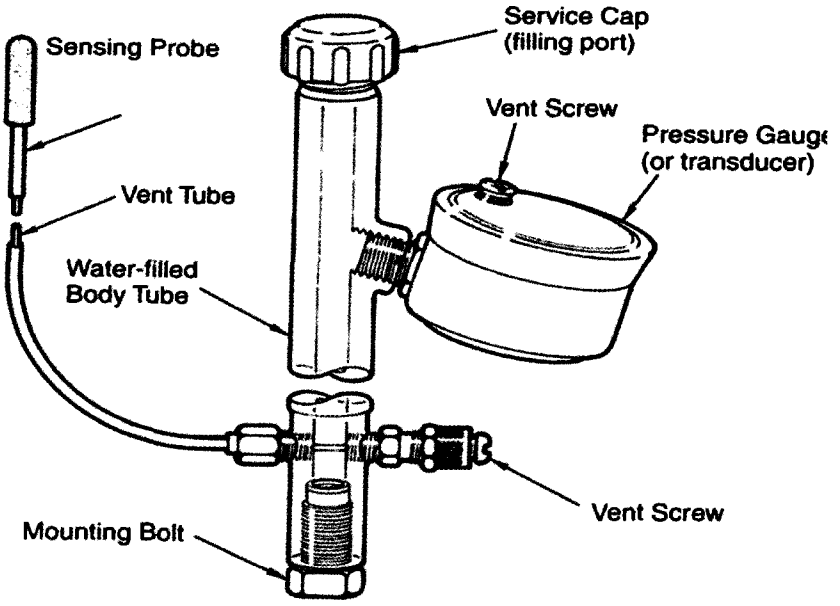

Figure 3- 9 Schematic of the small-tip laboratory Tensiometer (from Fredlund and Rahardjo 1993)

3.7.2. Principle and Methodology

The technique for measuring the matric suction in soils using the Tensiometer relies on the properties of the high-air entry (HAE) materials typically prepared using ceramic materials such as kaolinite. The HAE materials are characterized by microscopic pores of relatively uniform size and size distribution. The surface tension forces maintain the gas-liquid interfaces formed in the material's pores of the saturated HAE material (ceramic disk). Physically, surface tension acts as a membrane for separating the air and water phases.

The maximum sustainable difference between the air pressure, u_a, above the disk and the water pressure, u_w, within and below the disk is inversely proportional to the maximum pore size of the material and mathematically expressed using Young-Laplace Eq.3-1. Figure 3- 10 shows schematically explains the operating principle of HAE ceramic cup (Lu and Likos, 2004).

$$(u_a - u_w)_b = \frac{2T_s}{R_S} \qquad \text{Eq.3- 1}$$

where, $(u_a - u_w)_b$ = the air-entry value, kPa

T_s = the surface tension of the air water interface, kPa

R_s = the effective radius of the maximum pore size of the HAE material

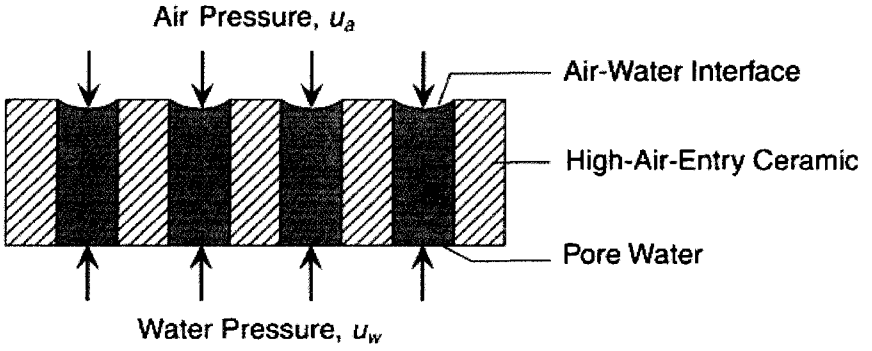

Figure 3- 10 Operating principle of HAE ceramic cup (from Lu and Likos 2004)

3.7.3. Measurement of Matric Suction

Figure 3- 11 shows the details with respect the measurement of the matric suction in unsaturated soils. The matric suction is negative pore water pressure with respect to atmospheric pressure and is transmitted via saturated ceramic disk and facilitates the flow of water (i.e., drying process) to the soil from the Tensiometer. The sensor will read the matric suction at the equilibrium condition when water no longer moves out. If the soil is being saturated (i.e., wetting process) water will flow in the ceramic disk from the soil. It should be noted that there is no effect of osmotic suction on the pressure measurements since the ceramic tip is permeable to dissolved solutes. The matric suction measurements should be corrected for the difference in elevation between the sensor and the pressure gauge. In practice, reliable Tensiometer measurements using standard testing equipment are limited to 70 to 80 kPa approximately (Fredlund and Rahardjo, 1993). Impurities, dissolved gasses and air bubbles may concentrate in tiny crevices on the walls of the sensor body and that may cause some cavitations to occur and as a result reduce suction values.

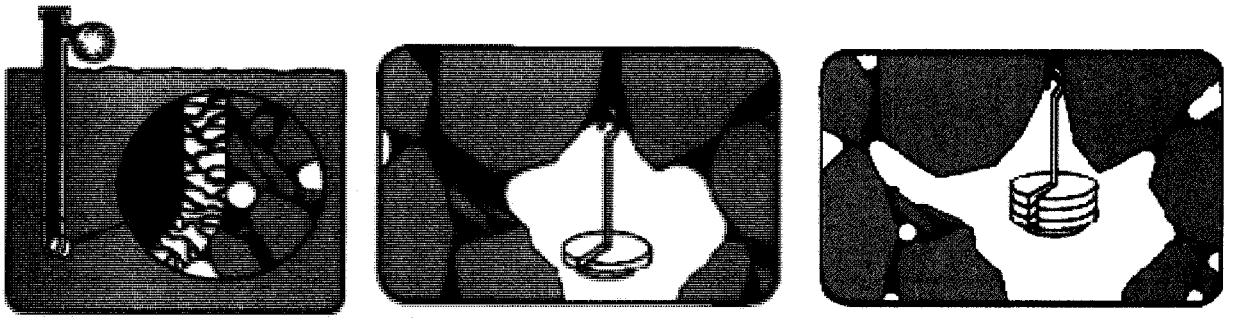

Figure 3- 11 Schematic of the cross-section of a typical saturated ceramic disk (from Lu and Likos 2004)

3.7.4. Calibration of Tensiometer

The following steps should be followed for proper calibration and setting up the Tensiometers:

i. The ceramic cup should be immersed in water for at least an one hour or more to fill the pores with water.
ii. Fill the Tensiometer system with de-aired water. A small suction value has to be applied at the filler end to remove air from the bourdon tube in the vacuum dial gauge.
iii. The plastic tube has to be air-free and the tube can be tapped to release the air bubbles then open the service cap.
iv. The system should be fully saturated with de-aired water. Small vacuum pressure may be applied to remove air bubbles if any from the system.
v. The air-free water should be flushed again through the system to remove the air.
vi. Replace and tighten the service cap and the water vent screw. After performing the above steps, Tensiometer is ready for laboratory or field installation.
vii. Long-term evaporation from the ceramic cup should be avoided, since it results in evaporation deportation deposits on the surface of the cup, which reduces the sensitivity.

Some of above details are summarized using the information from the Soilmoisture corporation manual.

3.7.5. Tensiometer Installation

In order to install the Tensiometer in the soil, a good contact is required between the ceramic cup and the soil to maintain continues link between the pore water and the measurement system. A thin wall 6 mm tube can be used to core a hole in the soil to place the ceramic cup. The plastic tube should be handled carefully and not to be bent. The ceramic cup must be mounted in the region where soil suction values are required (Fredlund and Rahardjo 1993).

After installation is completed, the unit will come to equilibrium with the soil and the soil suction will be read directly on the dial gauge in kPa as shown in Figure 3- 12.

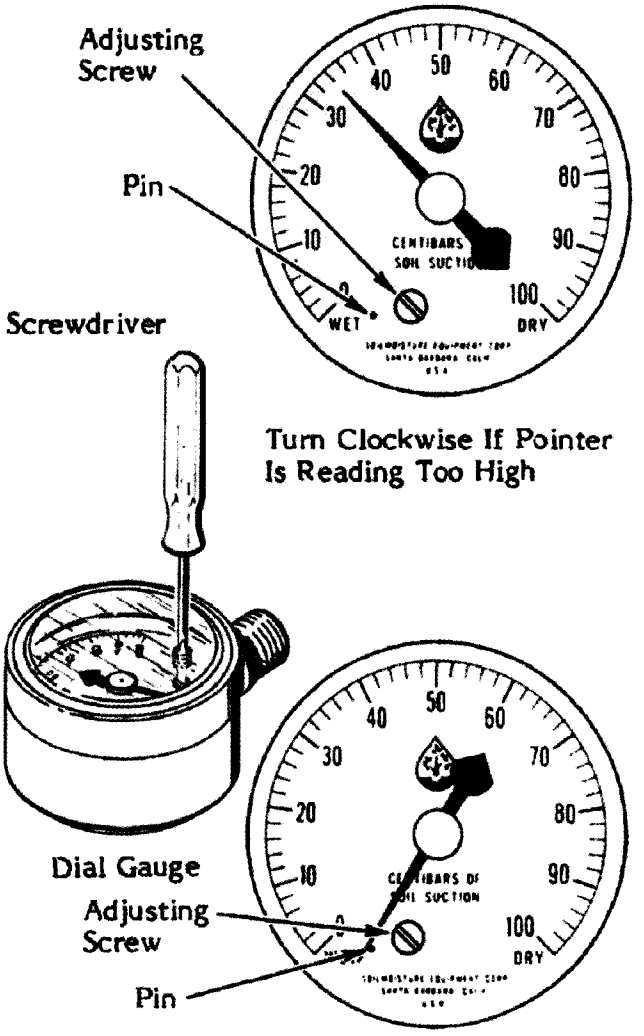

Figure 3- 12 Schematic showing adjustment process of the gauge (from Soil-Moisture manual - 2006)

3.8 Tensiometer Holders

Two different types of tensiometer holders were specially designed to support the Tensiometers. The first type of holder is used to calibrate the Tensiometer (see Figure 3- 8 and Figure 3- 13). The ceramic cup should be immersed into the water at the same elevation with the dial gauge of tensiometer before suction values are measured after adjusting the reading of gauge reading to zero to calibrate Tensiometer. The ceramic cup should be inserted into water again to make sure the reading of Tensiometer back to zero after each suction measurement to ensure the reliability of the measurements of suction.

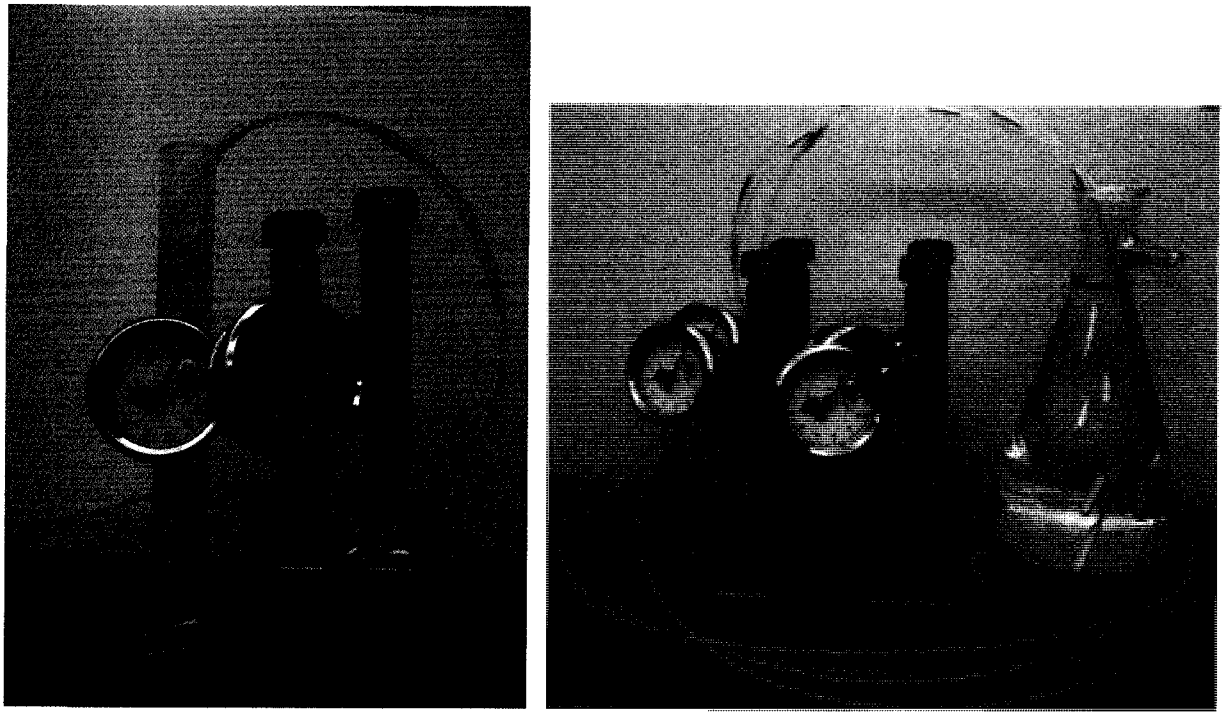

Figure 3- 13 Tensiometer supporting stands

The second type of holder (Figure 3- 14) is designed to adjust elevation levels so that the Tensiometer can be mounted on to soil container and adjust the dial gauge of the Tensiometer at the same elevation with the ceramic cup to eliminate elevation effects of the measured readings.

The suction range that can be studied for coarse-grained soils is typically in the range of 0 to 10 kPa and hence all precautions should be taken to measure the readings with greater reliability.

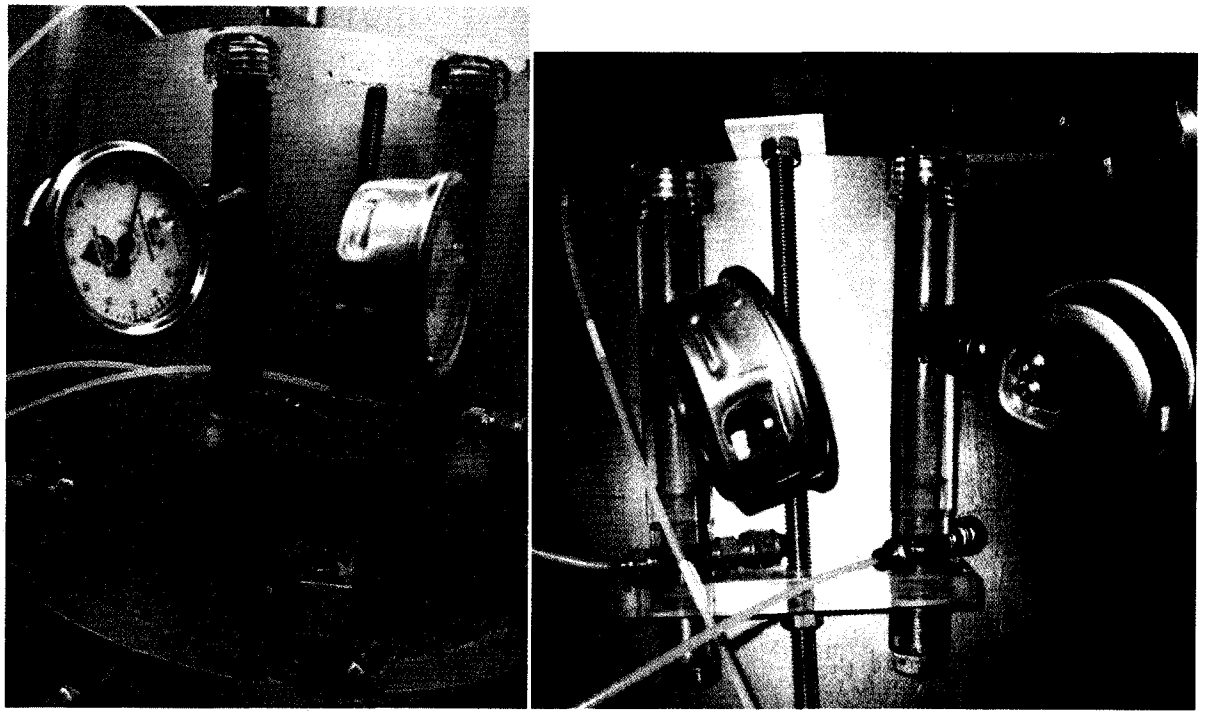

Figure 3- 14 Tensiometer holders

3.9 Load Cell

A "S"-Beam load cell 20210 (Figure 3- 15) was used to measure the load. The unit can function both in tension or compression and is lightweight. The output can be received and recorded with Data Acquisition System (DAQ).

The key features of load cell are:

i. 25 to 40,000 pounds capacities
ii. Nickel/Chrome Plated Alloy Steel
iii. Complete environmental protection
iv. NTEP Certified versions available for Class III 5,000 divisions and Class III L 10,000 divisions
v. Factory Mutual (F.M.) Approved

In this research program, two load cells with capacities of 500lb and 1000lb were used. The specifications of load cell S20210 are summarized in Table 3- 1.

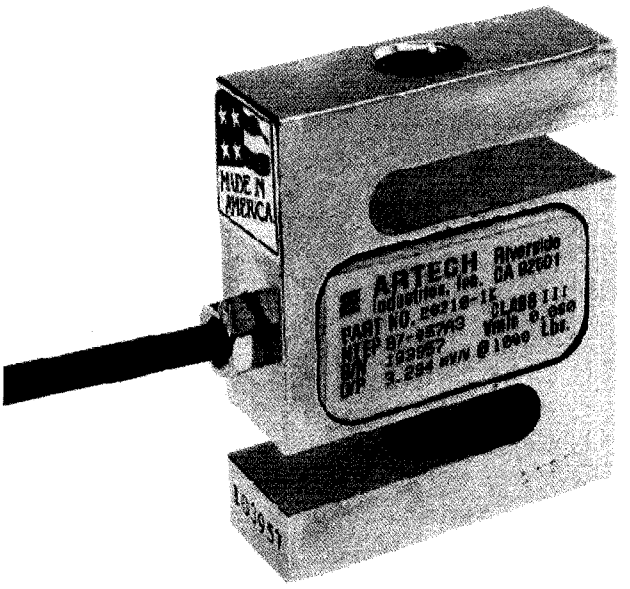

Figure 3- 15 "S"-Beam load cell 20210

Table 3- 1 Specification "S"-Beam load cell 20210

Standard Capacities : (lbs.)	25, 50, 75, 100, 150, 200, 250, 300, 500, 750, 1K, 1.5K, 2K, 2.5K, 3K, 5K, 10K, 15K, 20K 30K, 40K
Excitation Voltage :	10VDC - Maximum 15VDC
Rated Output :	3.0 mv/v Minimum
Non-Linearity :	< 0.03% FSO (Full Scale Output)
Hysteresis :	< 0.02% FSO
Non-Repeatability :	< 0.01% FSO
Zero Balance :	± 1.0% FSO
Bridge Resistance :	350 Ohms nominal
Safe Overload :	150% of rated capacity
Temperature : Compensated Range : Effect of Output : Effect on Zero :	 0 - 150 deg. F < 0.0008% FSO/deg. F < 0.0011% FSO/deg. F
Finish :	Nickel/Chrome plated

Above features and specification comes from the Artech Industries Inc web site

3.10 Displacement Transducer

The displacements were measured using Linear Strain Transducer (LSCT), HM-2310 and HS25/5115 (Figure 3- 16). The key features of the transducers used in the research program are:

i. Less than 250g spring force on spindle.
ii. Non-linearity better than ± 0.1% of full scale deflection.
iii. Hysterisis-compensated with linearity better than ± 0.1% of full scale in both directions.
iv. Stainless steel casing.
v. Requires input of 10V DC with an output up to 6.5mV per volt.

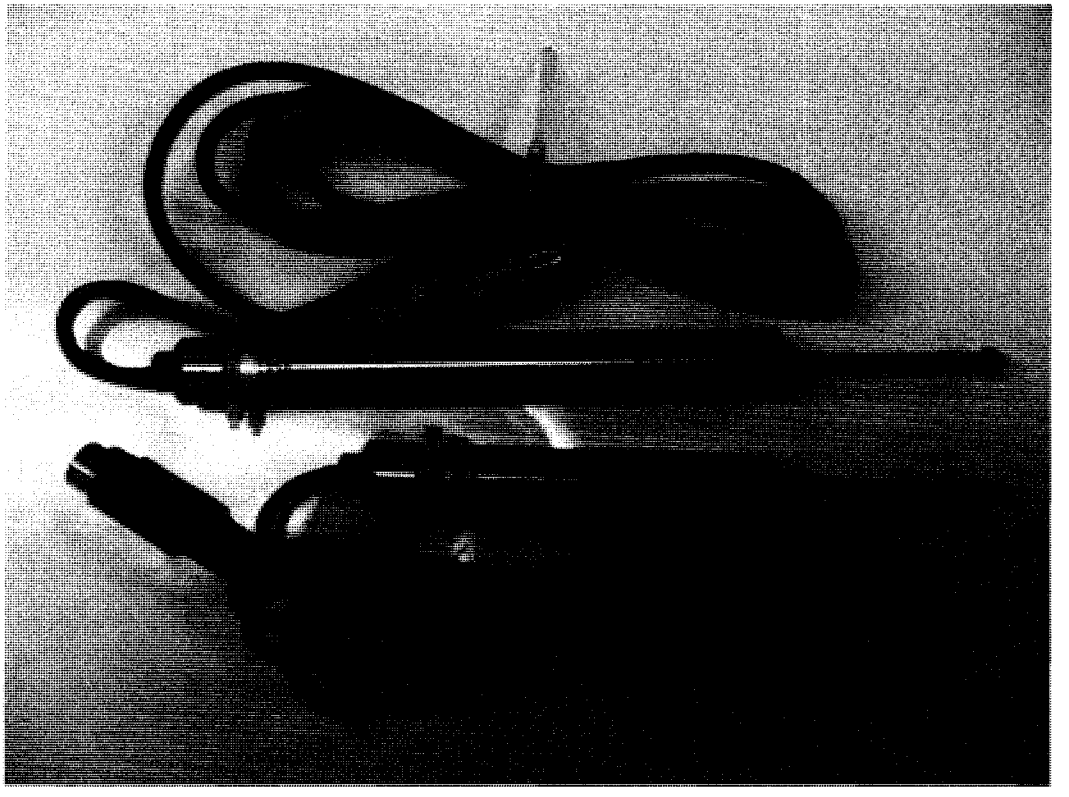

Figure 3- 16 Linear strain transducer (LSCT)

3.11 Suction Profile Set

Suction profile set was designed by author to measure the relationship between matric suction and depth of ground water table. The set consist of a long transparent acrylic soil column, a water container, thin plastic drain tube, valves and a pulley block. Suction profile set is fixed on the left post of bearing capacity frame (See Figure 3-2 and Figure 3- 21). The relationship between matric suction and depth of ground water table measured using this unit can be used to achieve expected matric suction in the soil container of bearing capacity test system faster by simply adjusting the water table. In other words, Tensiometers were not placed into the soil containers while loading the model footing. There were three reasons or advantages of using this methodology. The first reason is to expedite or achieve the expected matric suction value in the tested sands by controlling the depth of water table below model footings. The second reason is to avoid the influence of Tensiometers on the soil structure of the compacted soil in the soil containers while determining the bearing capacity of model footings. The third reason can be attributed to the difficulties in inserting the Tensiometer ceramic tip into the compacted soil. It should be noted that similar compaction procedures were used for compacting both the soil in the soil column in the profile set and the soil containers to achieve "identical" testing conditions.

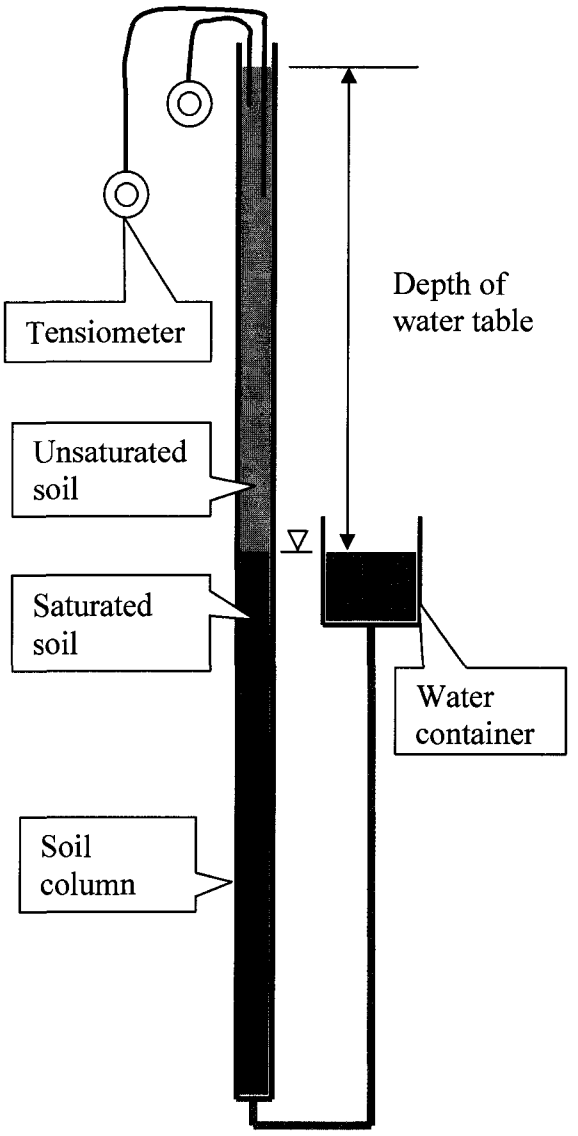

Figure 3- 17 Schematic diagram of suction profile set

The soil column was connected to water container using a thin plastic drain tube and to the valves such that the depth of ground water table in sand can be controlled by adjusting the

elevation of water container. The provision of pulley block was useful in controlling the elevation of the water container. Typically two or more Tensiometers were installed in the sand in soil column at different depths below the soil surface to measure the suction in the sand. Equilibrium conditions with respect to suction values were typically achieved in a period of 12 to 24 hours.

3.12 Data Acquisition System

A data acquisition system (DAQ) was designed to collect data of measured parameters. The DAQ system constitutes of hardware and software. The hardware part includes sensors, cables and electronics components. The software part includes the data acquisition logic and the analysis software (and some other utilities that can be used to configure the logic or to move data from data acquisition memory to a laptop or to a desktop computer).

Data acquisition system used in present research program consists of SCB-68 68-Pin Shielded Connector Block and personal computer as well as data processing software, such as MS Excel.

The SCB-68 is a shielded I/O (Input and Output) connector block with 68 screw terminals for easy signal connection to a National Instruments 68- or 100-pin DAQ device. The SCB-68 features a general breadboard area for custom circuitry and sockets for interchanging electrical components. These sockets or component pads allow RC (resistor-capacitor) filtering, 4 to 20 mA current sensing, open thermocouple detection, and voltage attenuation. The open component pads allow signal conditioning to be easily added to

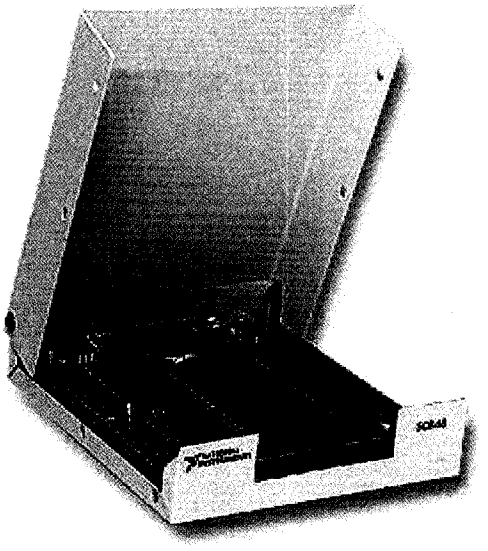

Figure 3- 18 SCB-68 68-pin shielded connector block

the analog input (AI) signals and to the DAC0OUT, DAC1OUT, and PFI0/TRIG1 signals of a 68-pin or 100-pin DAQ device.

3.13 Tempe Cell

The Tempe cell apparatus is commonly used for measuring the Soil-Water Characteristic Curve (SWCC) extending the axis-translation technique (see 4.3.4 for more details). Tempe cell apparatus is similar to the pressure plate apparatus which is commonly used for measuring the SWCC for a larger suction range (i.e., 0 to 1500 kPa). Several specimens can be used for measuring the SWCC simultaneously using the pressure plate apparatus (Vanapalli et al. 1999). The Tempe cell is smaller in comparison to the pressure plate apparatus and facilitates the measurement of SWCC of an individual specimen typically for the low matric suction range typically in the range of 0 to 500 kPa. The Tempe cell consists of a saturated high air entry disk (HAED) which facilitates in separating air and water phases in a closed vessel. The difference between the applied air pressure, u_a and the pore water pressure, u_w at equilibrium conditions is the matric suction, $(u_a - u_w)$. The pore water pressure, u_w connection is typically open to atmosphere; hence the applied air pressure, u_a is the matric suction, $(u_a - u_w)$ in the soil specimen.

The setup details used in present research program for measuring the SWCC in the laboratory using Tempe cell apparatus is shown in Figure 3- 19. A pressure gauge with a sensitivity of measuring suction values of 0.2 kPa is connected to a pressure regulator

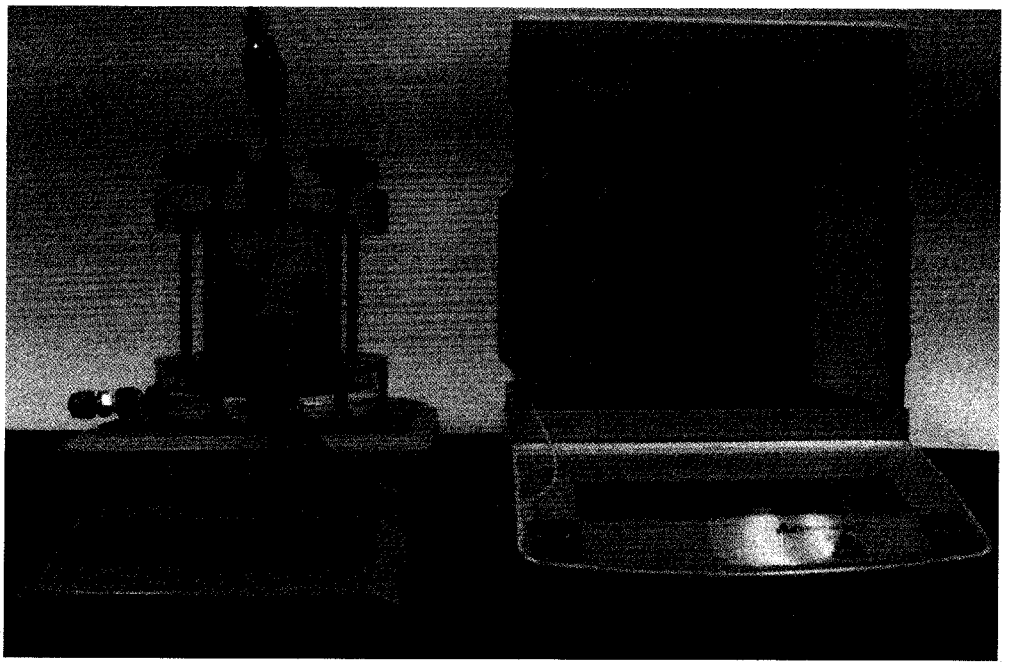

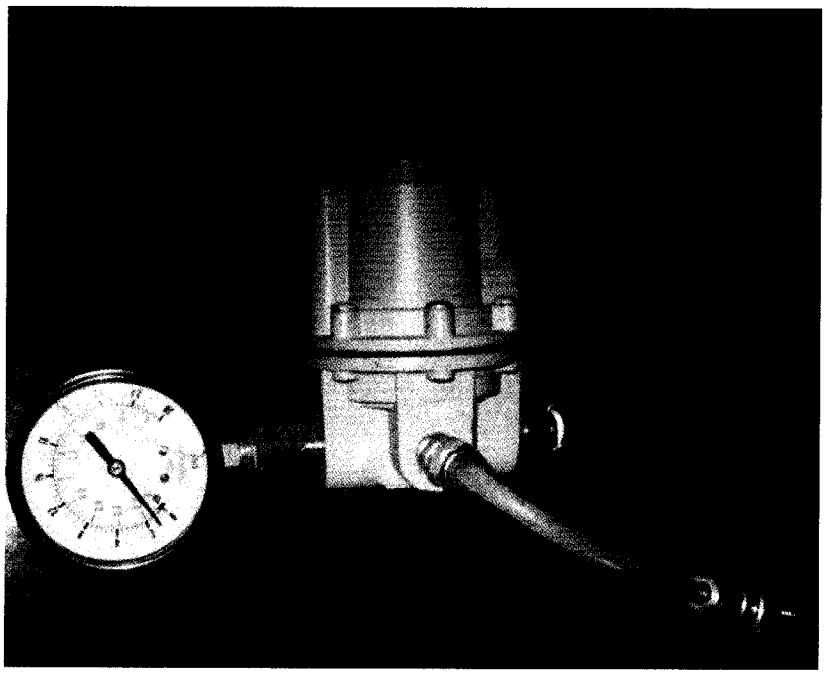

Figure 3- 19 Tempe cell and pressure gauge

3.14 Direct Shear Apparatus

Direct Shear Apparatus used in the experiment is EL 26-2112 is manufactured by ELE International.

The ELE Direct/Residual Shear Apparatus uses a microprocessor controlled, menu-driven drive system with keyboard entry for precise shear speed setting and control. The use of a microprocessor controlled drive system and keyboard entry provides the unit with a wide range of features which include pause and speed reset during testing, RS232C interface for computer control, operator programming of speed and control functions, self-test diagnostics and many other features. A return to start datum provides a positive means of reversing the shear box when either preparing for a new test or continuing with residual testing procedures.

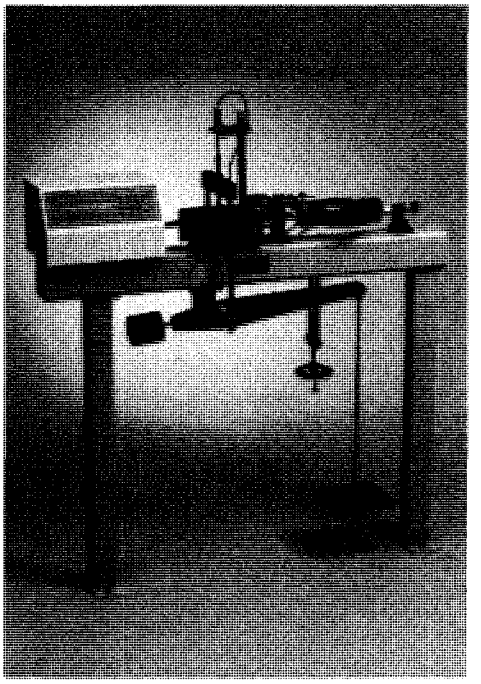

Figure 3- 20 EL 26-2112

Safety forward/reverse travel limit switches are incorporated into the system as standard and are monitored through the electronics. The electronics are housed in a modern styled shroud, which is adjustable for optimum viewing. The specification of EL26-2112 is as Table 3- 2:

Table 3- 2 Specification of EL26-2112

Speed Range	0.00001 to 9.99999mm/minute
Max Specimen Size	100mm.
Max Design Shear Force	5 kN
Max Design Normal Load	1,000 kg
Max stress for Specimen 60mmX60mm	2800kPa (100kg in 10:1 ratio)

Most of the above information about Direct Shear Apparatus EL26-2112 is derived from user manual of EL26-2112.

3.15 Other Equipment Accessories

Several special accessories were designed and developed to assist in the experimental program.

Figure 3- 21 is suction profile set fixing stand. This device was designed and used to fix and hold suction profile set on to vibratory machine while compacting sand in the soil container in the suction profile set during the compaction of sand using vibration method.

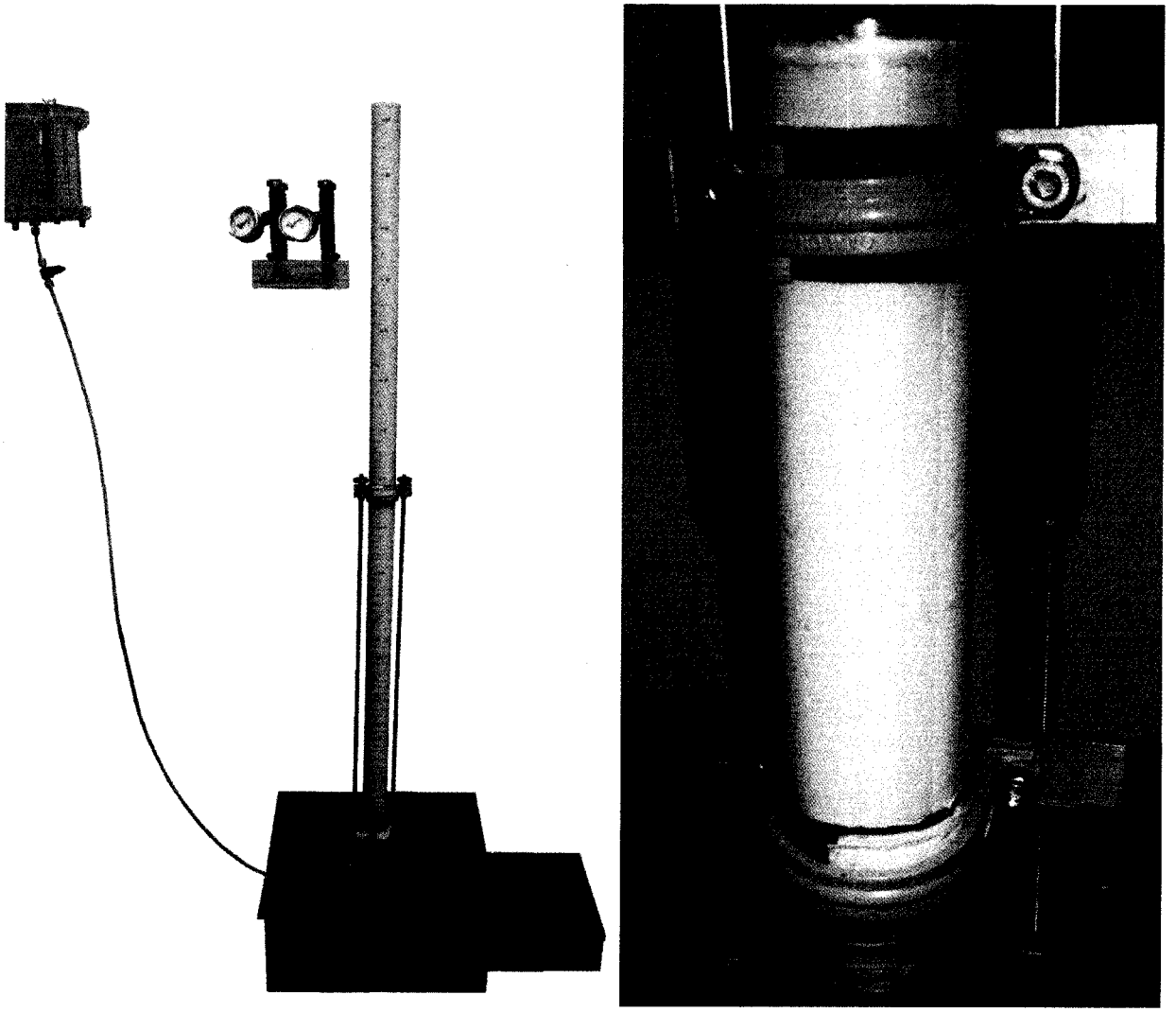

Figure 3- 21 Suction profile set fixing stand

Figure 3- 22 are two Vacuum pumps; one is hand pump, and the other pump is driven with vacuum machine. The vacuum pumps are used to connect to soil container and to remove water from soils using vacuum or negative air-pressure.

When pumping air out of the plastic cylinders, there is negative pressure in the plastic cylinders. The negative pressure in the plastic cylinder draws the water into the plastic cylinder from soil

in the soil container. This technique decreases the degree of saturation of the soil to achieve expected soil suction when water table is lower than the soil container.

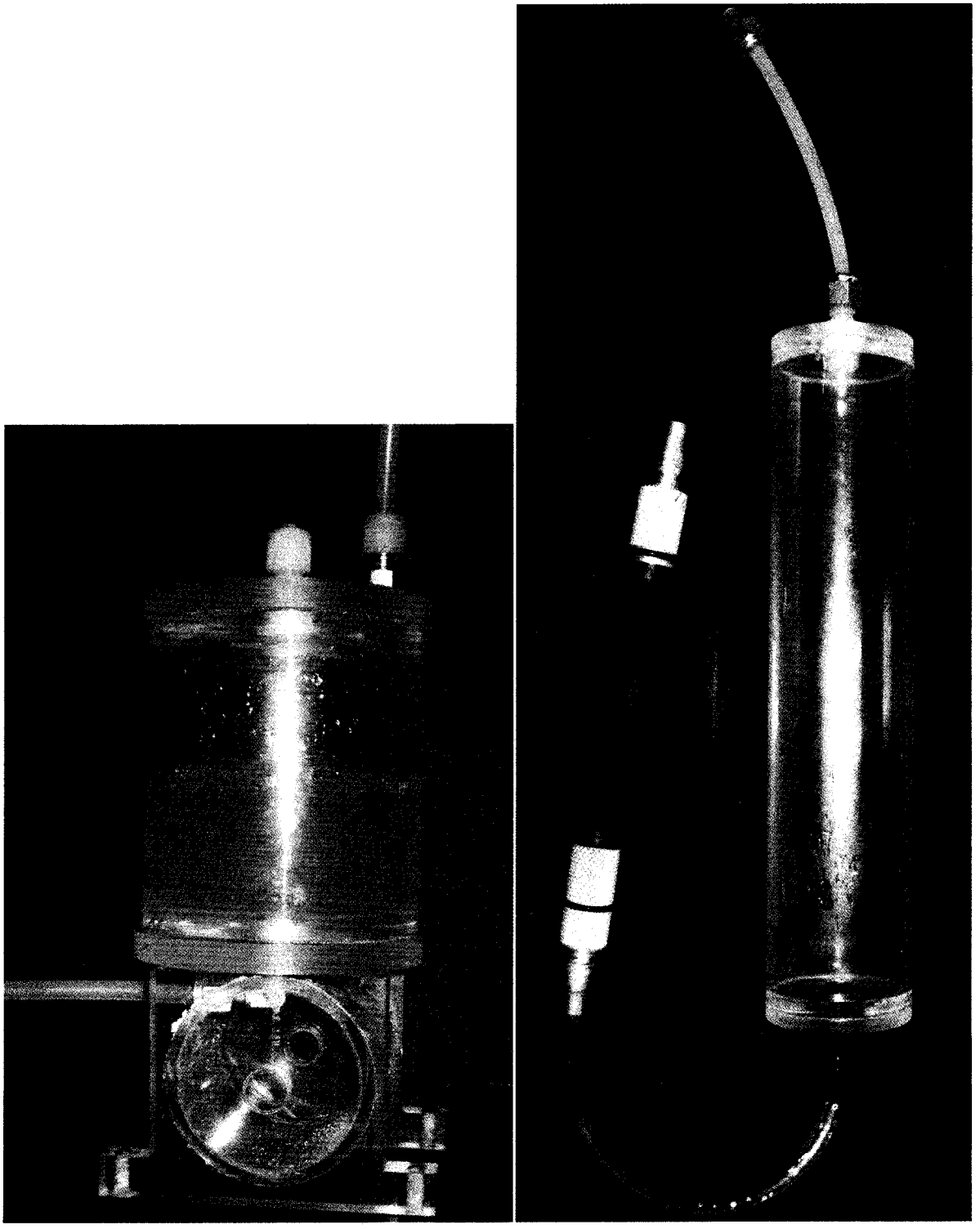

Figure 3- 22 Vacuum cylinder unit and vacuum hand pump

CHAPTER 4

SOIL PROPERTIES

4.1. Introduction

This chapter summarizes the properties of four soils studied in this research program; namely, Unimin 2075 sand, Ottawa sand, Unimin 7030 sand and Sil-co-sil 106. The soil properties of Unimin 7030 sand were determined by Mohamed (2006) who worked on a different topic in the Geotechnical laboratory of University of Ottawa. Some properties of Ottawa sand are summarized from published literature. The Soil Water Characteristic Curve (SWCC) and shear strength parameters of three sands (i.e., Unimin sand 2075 and Unimin sand 7030 and Ottawa sand) were determined using direct shear apparatus. The results of these studies were used in the analysis of the bearing capacity tests results which are described in the latter chapters. The SWCC and shear strength parameters of Sil-co-sil were not determined because the objectives of the study using this soil were different. More details about the research program related to Sil-co-sil are discussed in a later chapter.

4.2. Unimin 2075 Sand

Unimin No. 2075 sand is commercial sand and is a product of Unimin Canada Inc. This sand is composed of 99.71% quartz (SiO_2). This sand is named No. 2075, meaning 75% retained on mesh 20 (0.841 mm). The data of chemical composition supplied by manufacture is listed in the Table 4-1.

4.2.1. Chemical Composition

Table 4- 1Chemical composition of Unimin sand 2075

Chemical compound	Mean % by weight
Silicon dioxide (SiO_2)	99.71
Iron oxide (Fe_2O_3)	0.050
Aluminum oxide (Al_2O_3)	0.072
Calcium oxide (C_aO)	0.010
Titanium oxide (T_iO_2)	0.006
Magnesium oxide (M_gO)	0.019
Potassium oxide (K_2O)	0.030
Sodium oxide (Na_2O)	0.006
Loss on ignition	0.096

4.2.2. Grain Size Distribution

Table 4- 2 and Figure 4-1 summarize the laboratory results of sieve analysis conducted using 1000g sand.

Table 4- 2 Grain size distribution of Unimin sand 2075

USA Std Sieve	Typical Values			
	Retained	% Retained		% Passing
Mesh	(gms)	Individual	Cumulative	Cumulative
8	0	0	0.00	100.00
10	0.8	0.08	0.08	99.92
12	20	2.0	2.09	97.91
16	757.9	75.8	78.13	21.87
20	164.37	16.44	94.62	5.38
30	43.26	4.33	98.96	1.04
Pan	10.37	1.04	100.00	0.00

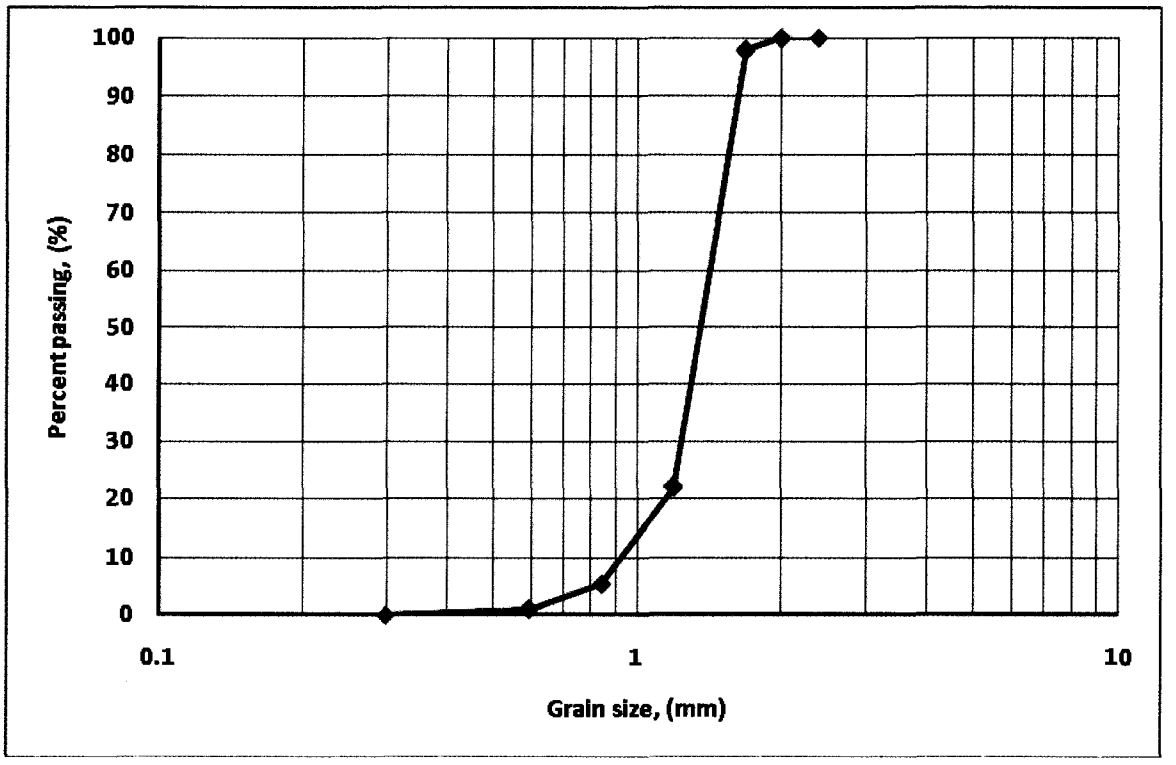

Figure 4- 1 Grain size distribution of Unimin sand 2075

4.2.3. Suction Profile

Suction profile of Unimin 2075 was measured using the suction profile set described in Chapter 3. The results from suction profile set (i.e., variation of suction above the water table measured) were used in the estimation of suction below the footings while interpreting bearing capacity results conducted in the two different soil containers (i.e., tall and short). The suction values in the sand column of the suction profile set were determined using two or more Tensiometers. Typically, the first Tensiometer was installed 50 mm below the soil (sand) surface, and the second one was installed 100 mm below the soil surface. The Unimin 2075 sand was initially saturated in suction profile set by raising the water level using water column tank from bottom of the sand column. A period of 24 hrs was found to be sufficient to saturate the sand. The water table was then lowered to 50 mm below the soil surface for a period of 24 h for capillary suctions to reach equilibrium conditions. The matric suction values above the water table was then measured using Tensiometers following the procedures described in Chapter 3.

The water table for other tests was varied to different levels (i.e., 150 mm, 250 mm, 350 mm, 450 mm, and 550 mm) and suction values were measured after achieving equilibrium conditions. Figure 4- 2 summarizes the measured suction values above the water table for Unimin 2075 sand.

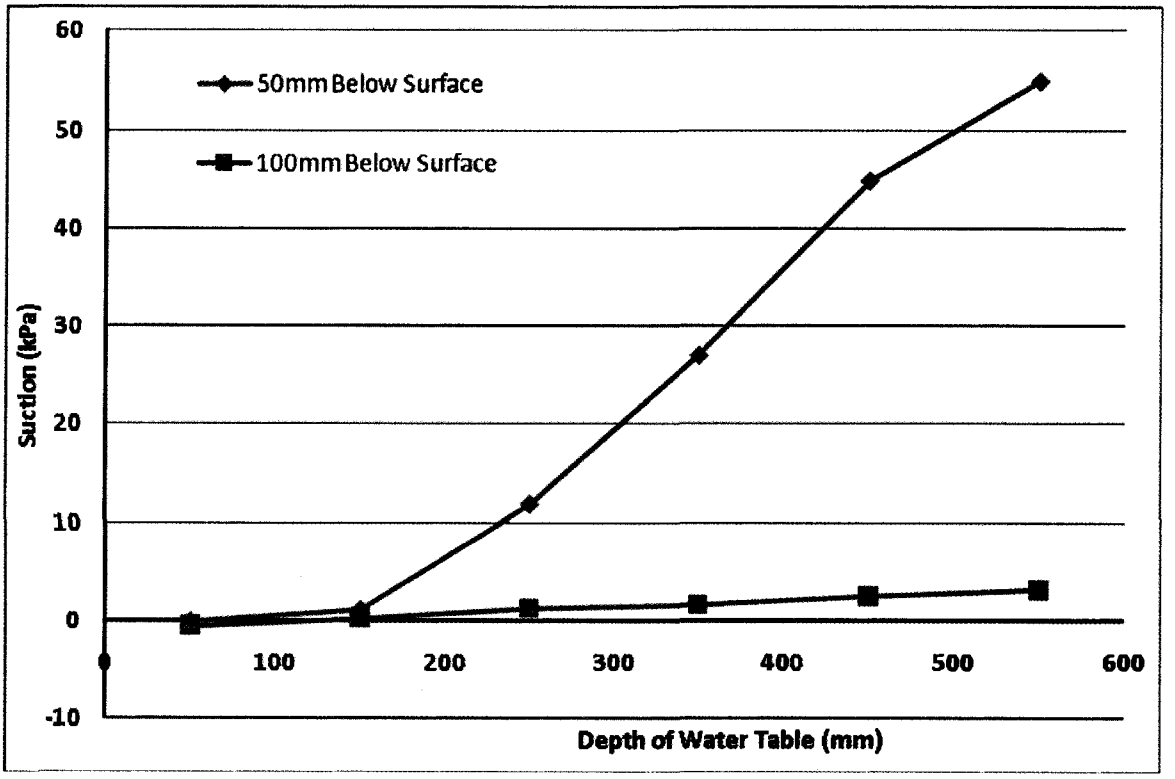

Figure 4- 2 Suction profile of Unimin 2075

Suction profile of Unimin 2075 shows that the matric suction near soil surface (50 mm below the soil surface) increases steeply as the depth of water table increases. The depth of water table 100 mm below the soil surface however has little effect on suction values. The rapid increase of matric suction values at the soil surface of Unimin 2075 sand may be attributed to evaporation.

4.2.4. Shear Strength

The effective shear strength parameters (i.e., c' and ϕ') of Unimin 2075 sand were measured using direct shear apparatus. Figure 4- 2 summarizes the results of the direct shear tests conducted using different normal stress. The effective cohesion, c' was equal to zero and angle of internal friction $\phi' = 43°$.

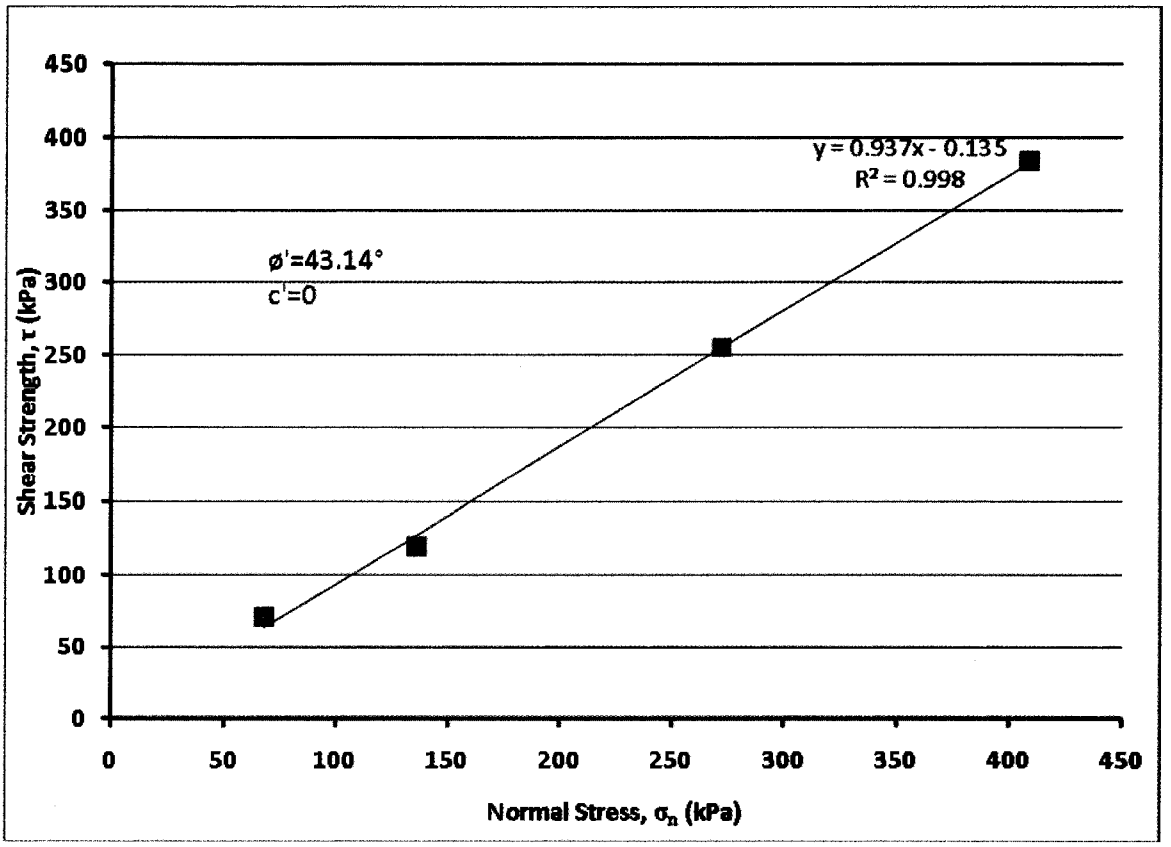

Figure 4- 3 Direct shear test results of Unimin 2075

4.3. Ottawa Sand

Ottawa sand, mined in Ottawa, Illinois, was used in this research program is coarse silica sand. This sand has been studied extensively studied in the literature. The individual particles of this sand are uniform in size and spherically shaped. Consequently, the behavior of this material may be modeled as a group of uniformly sized spheres from a theoretical stand point.

4.3.1. Grain Size Distribution

Table 4- 3 and Figure 4- 4 summarize the laboratory results of sieve analysis conducted using 1000g sand

Table 4- 3 Grain size distribution of Ottawa sand

USA Std Sieve	Typical Values			
	Retained	% Retained		% Passing
Mesh	g	Individual	Cumulative	Cumulative
12	0	0.00	0.00	100.00
16	0.97	0.10	0.10	99.90
20	137.76	13.90	14.00	86.00
30	798.24	80.57	94.57	5.43
40	42.99	4.34	98.91	1.09
60	9.72	0.98	99.89	0.11
pan	1.11	0.11	100.00	0.00

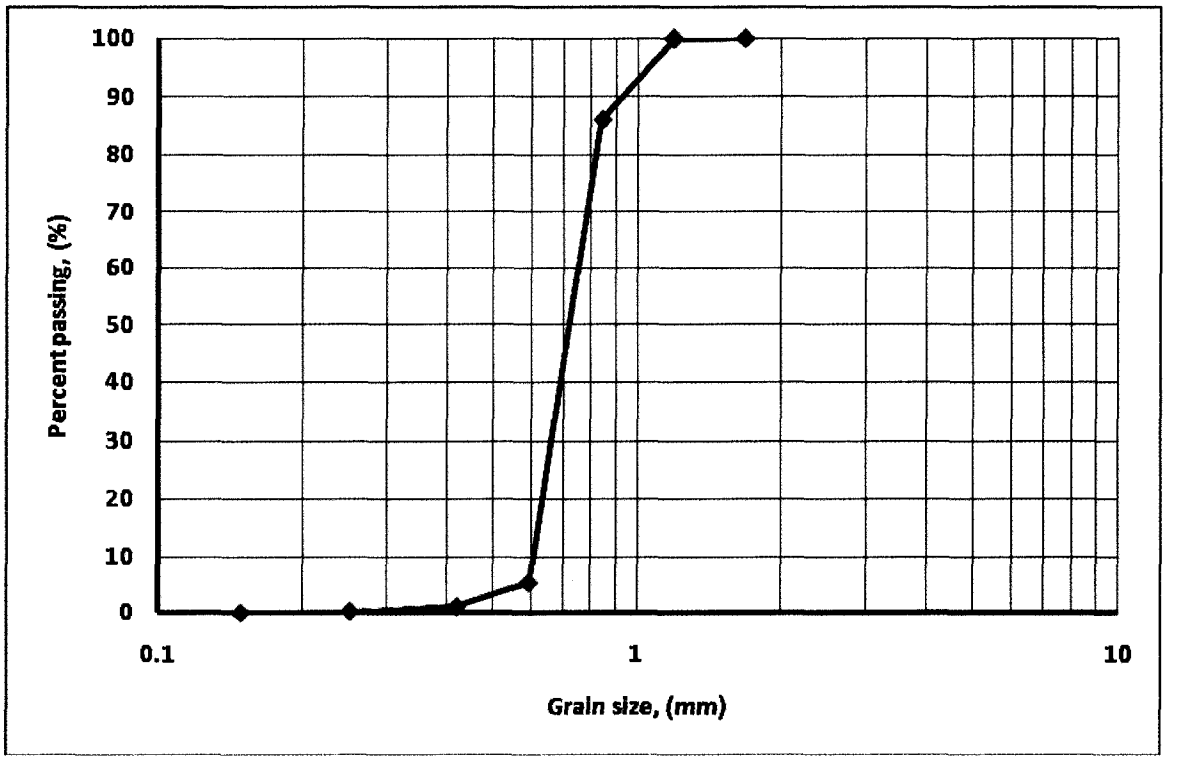

Figure 4- 4 Grain size distribution of Ottawa sand

4.3.2. Suction Profile

Suction profile of Ottawa Sand was measured using suction profile set. The sand in the soil column of the suction profile set was compacted to achieve the same density as the compacted sand in the soil container used for determining the bearing capacity of model footings. Two

Tensiometers were installed in suction profile set to measure the variation of suction in sand above water table. Several series of such tests were conducted varying the depth of water table. In all these tests, two Tensiometers were placed at different depths for measuring matric suction varying the depth of water table. The first Tensiometer was installed 40 mm below the soil (sand) surface and the second one was installed at 90 mm below the soil surface. After saturating Ottawa Sand using the procedures described in the earlier section, water table was lowered to 40 mm below the soil surface and allowed for a period 24h to reach equilibrium conditions with respect to matric suction values. The water table for other series of tests were lowered to 140 mm, 240 mm, 340 mm, 440 mm and 540 mm, in the suction profile set apparatus and tests were repeated to determine the variation of suction with respect to depth. Measured suction profile is plotted in Figure 4- 5. The capillary height was also measured in Ottawa Sand which was equal to 120 mm.

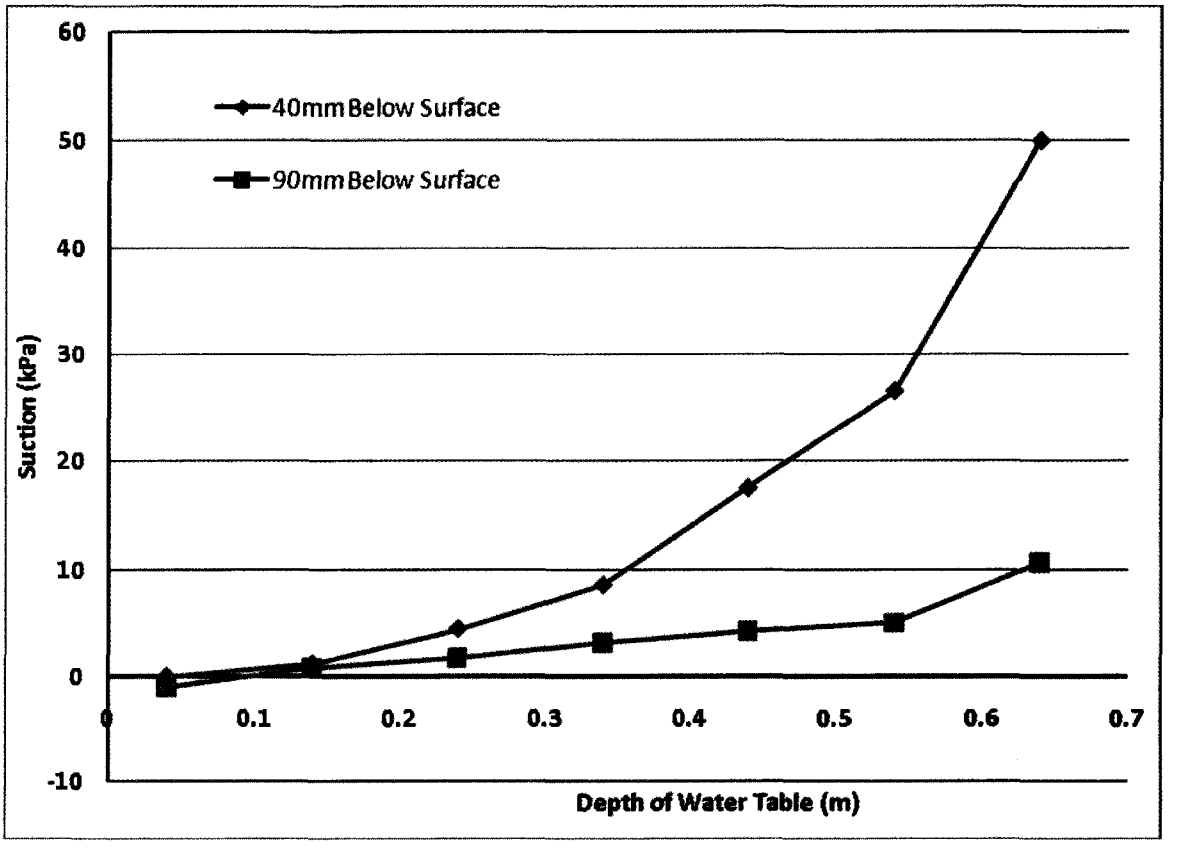

Figure 4- 5 Suction profile of Ottawa sand

The matric suction in Ottawa sand near soil surface (40 mm below the soil surface) increases steeply as the depth of water table increase similar to the Unimin 2075 sand. However, the matric suction values in the Ottawa sand (90 mm below the soil surface) increases slowly with an increase in the depth of water table. Evaporation of water from the soil column at the surface plays an important role contributing towards increase of matric suction values.

4.3.3. Shear Strength

Shear Strength properties of Ottawa sand were measured using direct shear apparatus under both saturated and dry conditions. Two different strain rates were used to understand the influence of strain rate on the shear strength behavior. The faster shear strain rate was equal to 1mm/min and the slower shear strain rate was equal to 0.02mm/min.

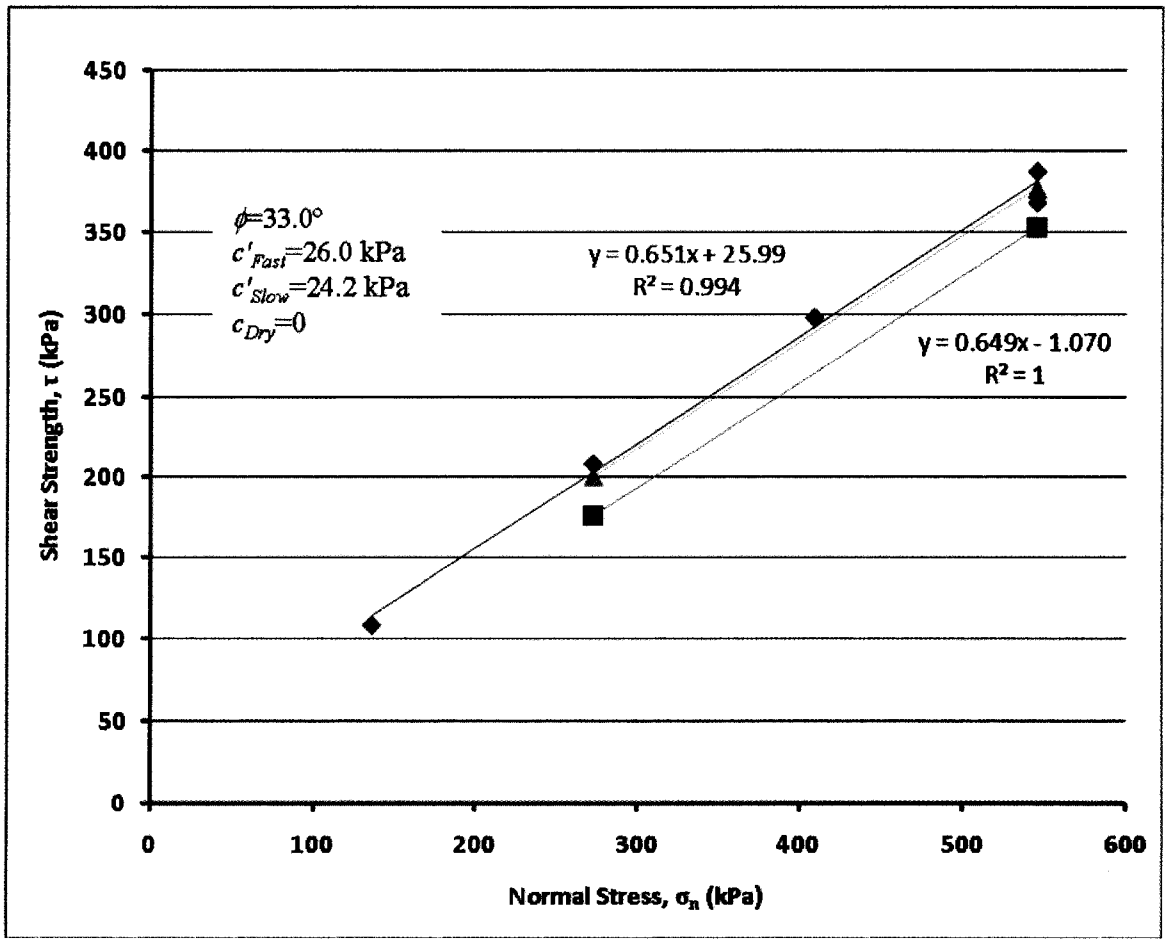

Figure 4- 6 Direct shear test results of Ottawa sand

The test results are shown in Figure 4- 6. The angle of internal friction angle, ϕ' of Ottawa sand was equal to 33° for both saturated and dry conditions. For the dry sand, cohesion value was equal to 0; however, under saturated condition, the sand exhibited an apparent cohesion value which was equal to 25 kPa, which may be attributed to the contribution of water tension. On the other hand, the cohesion value from direct shear tests conducted at a faster rate of strain was equal to 26.0 kPa, which is 1.9 kPa higher than the cohesion value of 24.1 kPa conducted at a slower rate of strain. The test results on Ottawa sand suggest that the rate of strain has no influence on the ϕ' value and no significant effect on the cohesion values.

4.3.4. Soil Water Characteristic Curve (SWCC)

Soil Water Characteristic Curve (SWCC) was measured using Tempe Cell extending the axis-translation technique. The axis-translation technique facilitates the measurement of SWCC relationship for suction values greater than 100 kPa. In this technique, the origin of reference of the pore-water pressure is simply translated from the standard atmospheric condition to the final air pressure in the chamber. As a result, the water pressure in the measuring system does not become highly negative and the problem associated with cavitation is avoided. Extending the axis-translation technique, the SWCC can be measured using the Tempe cell for the matric suction range from 0 to 500 kPa.

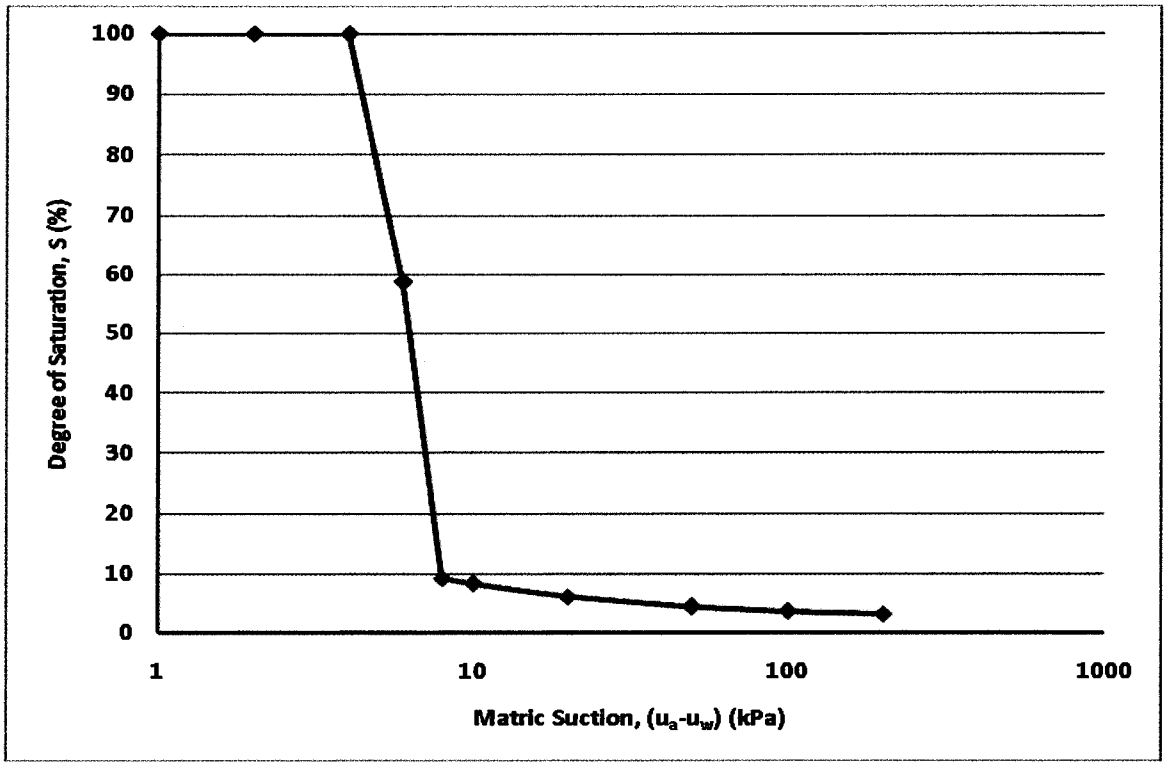

a. SWCC of Ottawa sand in the suction range of 0 to 200 kPa

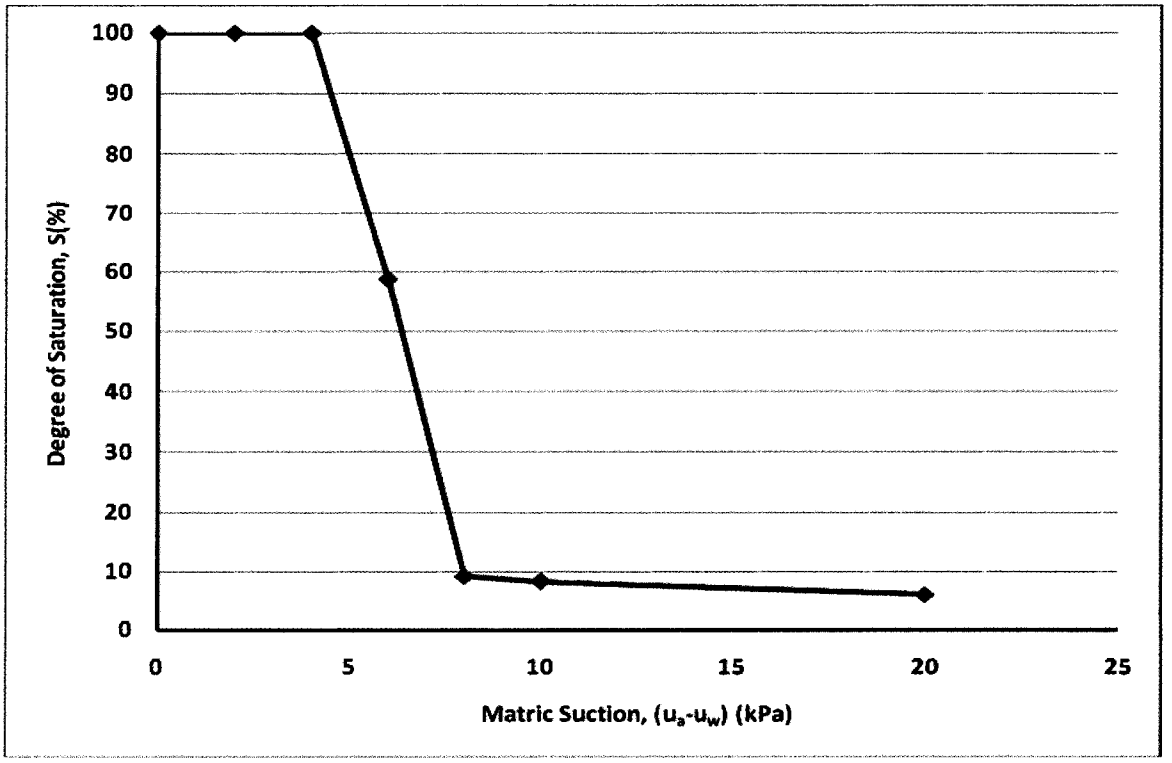

b. SWCC of Ottawa sand in the suction range of 0 to 20 kPa

Figure 4- 7 Soil Water Characteristic Curve of Ottawa sand

Figure 4- 7 shows the measured SWCC of compacted Ottawa sand for two different suction ranges, to demonstrate the rate of desaturation. Ottawa sand desaturates at a fast rate as the soil particles are relatively coarse-grained in nature. More than 90% of the water was drained when the matric suction in the tested specimen reached a value of 8 kPa. Measured SWCC shows that the air entry value of Ottawa sand is 4 kPa.

The SWCC were measured on a specimen with dry density equal to 17.65 kN/m^3. The water content at saturated condition was 17.83%. The bearing capacity of the model footings was also determined by compacting the Ottawa sand to the same initial density. The water content at saturation conditions was found to be same as in the specimen used for determining the SWCC.

4.4. Unimin 7030 Sand

The Unimin Silica Sand 7030 was commercial sand obtained from Merkley Supply Ltd. from Ottawa. All the soil required for the study was obtained in a single batch. The sand is named No. 7030, meaning 30% retained on 70 mesh (0.212mm) and the measured geometric mean of the sand particles was equal to 0.20 mm. Mohamed (2006) had undertaken several conventional tests in the Geotechnical laboratory of University of Ottawa.

4.4.1. Soil Properties

The air-dried sample of Unimin 7030 was sieved and analyzed using ASTM, Standards D422 (1994b). The grain size distribution properties of Unimin 7030 sand are summarized in Table 4-4 and plotted in Figure 4-6.

Table 4- 4 Properties of Unimin sand 7030

Property	Description or Value
Specific gravity, G_s	2.65
D_{60} *(mm)*	0.22
D_{30} *(mm)*	0.18
D_{10} *(mm)*	0.12
Coefficient of uniformity, C_u	1.83
Coefficient of curvature, C_c	1.23
Average dry unit weight of the compacted soil in the tank, kN/m^3	16.05
Void ratio, e (after compaction)	0.62 – 0.64
Unified soil classification system *(USCS)*	SP

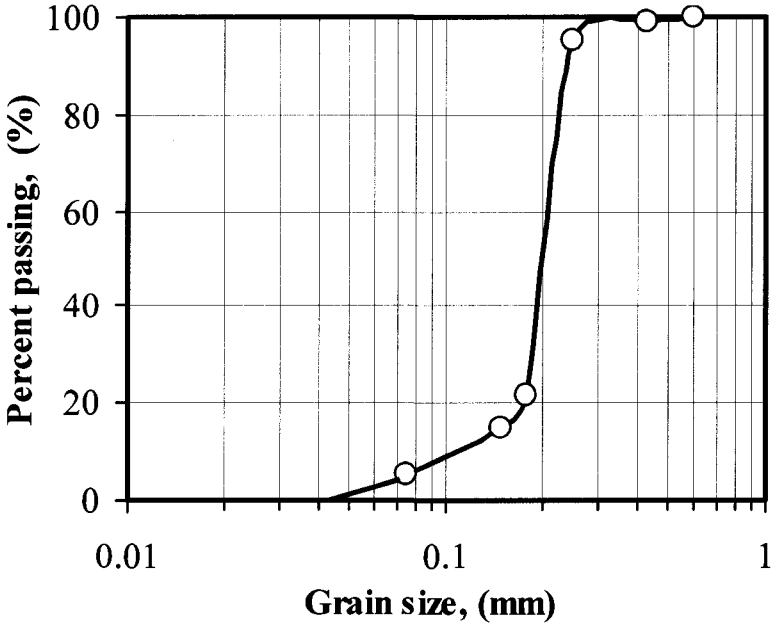

Figure 4- 8 Grain size distribution of Unimin sand 7030

4.4.2. Compaction Test

The compaction test results conducted following the ASTM Standards D698 (1994c) is summarized in Figure 4-7. The optimum moisture content was14.6 % and the maximum dry

density was equal to 16.8 kN/m³. More details of the test procedures are available in Mohamed (2006).

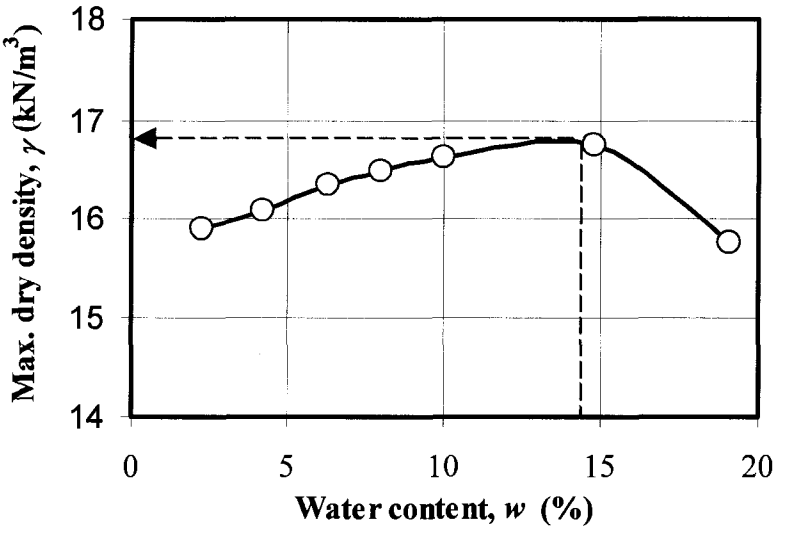

Figure 4- 9 Compaction test results of Unimin sand 7030

4.4.3. Direct Shear Test

Shear strength of Unimin 7030 sand were determined using direct shear apparatus under different normal stresses at a strain rate of 1.2 mm per minute. The two different series of direct shear tests were conducted using two different ranges of normal stresses (i.e., low and relatively high normal stress) to under the influence of different normal stress ranges on the shear strength properties. All the test results are plotted in Figure 4-8; the shear strength results are also summarized on the figure.

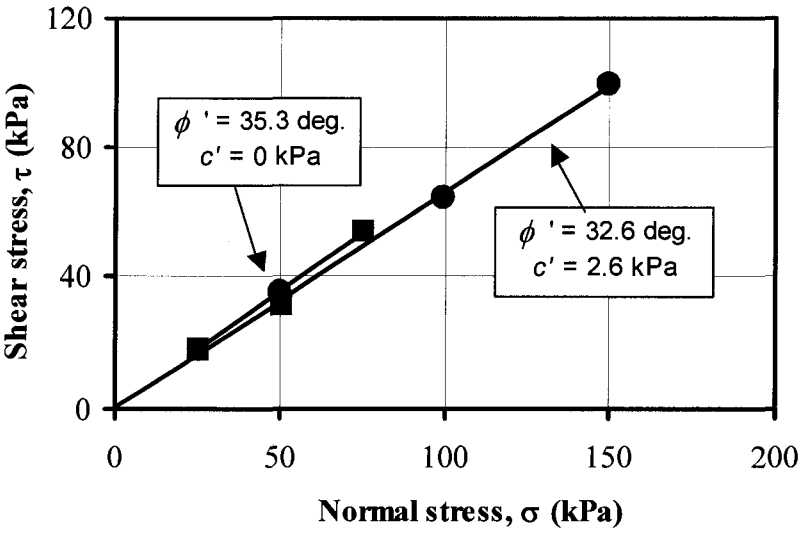

Figure 4- 10 Direct shear test results of Silica sand 7030

4.4.4. Soil Water Characteristic Curve (SWCC)

Figure 4-9 shows SWCC of Unimin 7030 measured using the Tempe cell following the procedures discussed in the earlier chapter.

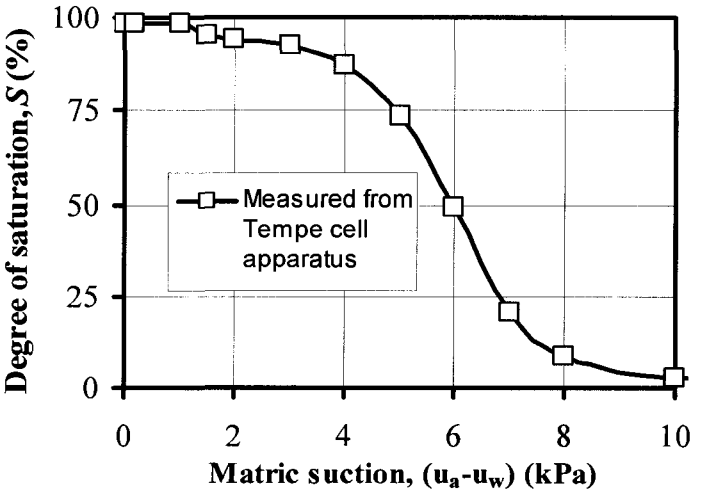

Figure 4- 11 Measured SWCC from the Tempe cell

4.4.5. Suction Profile

The results of the relationship between matric suction and depth of water table for Unimin 7030 are summarized in Figure 4-10. Similar procedures were used as discussed earlier for other sands studied for collecting this data. Therefore, these procedures are not discussed.

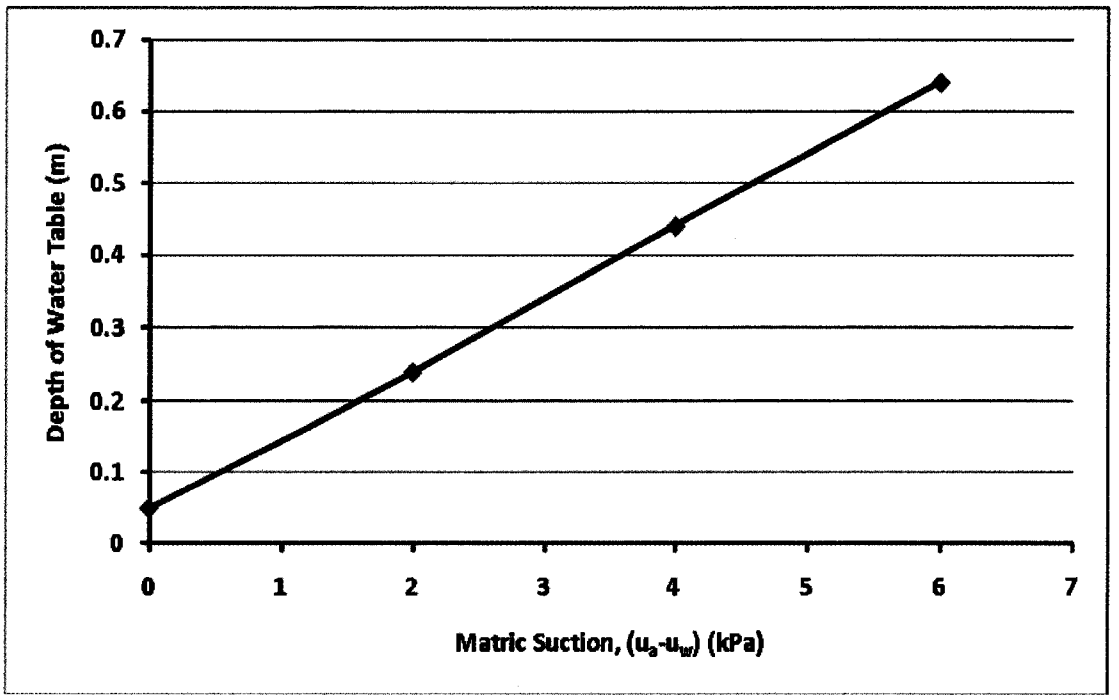

Figure 4- 12 Suction profile of Unimin sand 7030

4.5. Sil-co-sil 106

Sil-co-sil® 106 ground silica is fine grained commercial sand obtained from U. S. SILICA COMPANY in Ottawa.

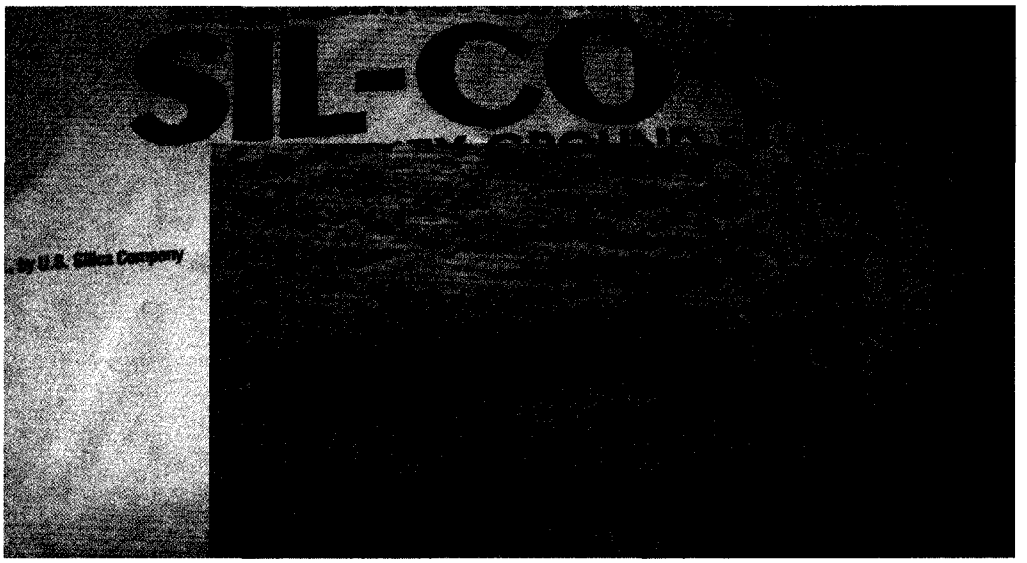

Figure 4- 13 Silica Sand Sil-co-sil 106

Tables 4-5 through 4-7 summarize the properties of the Sil-co-sil® 106 supplied by manufacturer.

Table 4- 5 Typical physical properties of Sil-co-sil 106

Hardness (Moh' s number)	7	Reflectance (%)	79.5
Melting point (degrees F)	3100	Yellowness Index	4
Mineral	Quartz	Specific Gravity	2.65
pH	7		

Table 4- 6 Typical chemical analysis of Sil-co-sil 106, (%)

SiO_2 (Silicon Dioxide)	99.8	MgO (Magnesium Oxide)	<0.01
Fe_2O_3 (Iron Oxide)	0.035	Na_2O (Sodium Oxide)	<0.01
Al_2O_3 (Aluminum Oxide)	0.05	K_2O (Potassium Oxide)	0.02
TiO_2 (Titanium Dioxide)	0.02	LOI (Loss on Ignition)	0.1
CaO (Calcium Oxide)	0.01		

Table 4- 7 Grain size distribution of Sil-co-sil 106

USA std. sieve size		Typical values		
		% retained		% passing
Mesh	Microns	Individual	Cumulative	Cumulative
70	212	0.0	0.0	100.0
100	150	0.1	0.1	99.9
140	106	1.4	1.5	98.5
200	75	5.5	7.0	93.0
270	53	11.0	18.0	82.0
325	45	7.0	25.0	75.0

4.6. Summary

The soil properties summarized in this chapter were used in the analyzing the test results conducted using two different bearing capacity test systems with different model footings. The next two chapters discuss the results of bearing capacity tests.

CHAPTER 5

SILICA SILT COMPACTION AND STRENGTH CHARACTERISTICS

5.1. Introduction

An attempt is made in this Chapter to study how the compaction and strength behavior of silica silt is influenced under static and vibration loading conditions. The silt used in the present study is Sil-co-sil silica silt, which has 98.5% of its particle sizes less than 0.1mm and is non-plastic. The silica silt with an initial water content of 23% was statically compacted using 4,000 kPa. The compacted silt offered significant resistance under static loading conditions in spite of achieving low dry density of 14.9 kN/m^3. However, the same soil with a much lower initial water content of 13% showed tendencies of collapse under the impact of vibration. The dry density of the silica silt was approximately equal to19 kN/m^3 after collapse under the impact of vibration.

Experimental studies have demonstrated that collapse conditions initiate in some pockets of the loose silt with initial water content values greater than 19%. Once collapse initiates in some pockets of the silt which has a high degree of saturation and low suction, it proliferates to other regions in spite of low initial water content. The volume of silica silt decreases dramatically and compacts remarkably during the collapse process under vibration. Suction in the compacted silica silt after collapse is sensitive and decreases significantly when subjected to vibration. The study also demonstrates that bearing capacity and settlement behavior of initially compacted silica silt (i.e., Sil-co-sil 106) is significantly influenced due to vibration or dynamic loading conditions.

This chapter will review and explain the above interesting phenomena of the silica silt tested. The impact of the research findings will also be discussed with respect to the performance of

foundations in silty soils which are initially in a state of unsaturated condition when subjected to vibration or earthquakes.

5.2. Compaction

Conventionally, soils are compacted to achieve favorable engineering properties (i.e., high strength, low coefficient of permeability and reduced settlement). However, compaction is influenced by several parameters such as the initial compaction water content, applied energy, soil structure, percentage of fines and clay mineralogy (Mitchell, 1993). Many practical problems in engineering practice are associated with improper compaction methods and may lead to unnecessary repair costs or in some cases structural damages will occur. Methods and techniques on how to properly compact soil which may collapse can be critical as they influence engineering properties such as strength and volume change.

For many soils, favorable engineering properties may be expected when they are compacted at optimum moisture content. Figure 5- 1 shows typical compaction curves for a variety of soils commonly used in engineering practice. However, the same trends of behavior may not to be valid for some soils, such as the silica silt (i.e., Sil-co-sil 106) studied in the present research program.

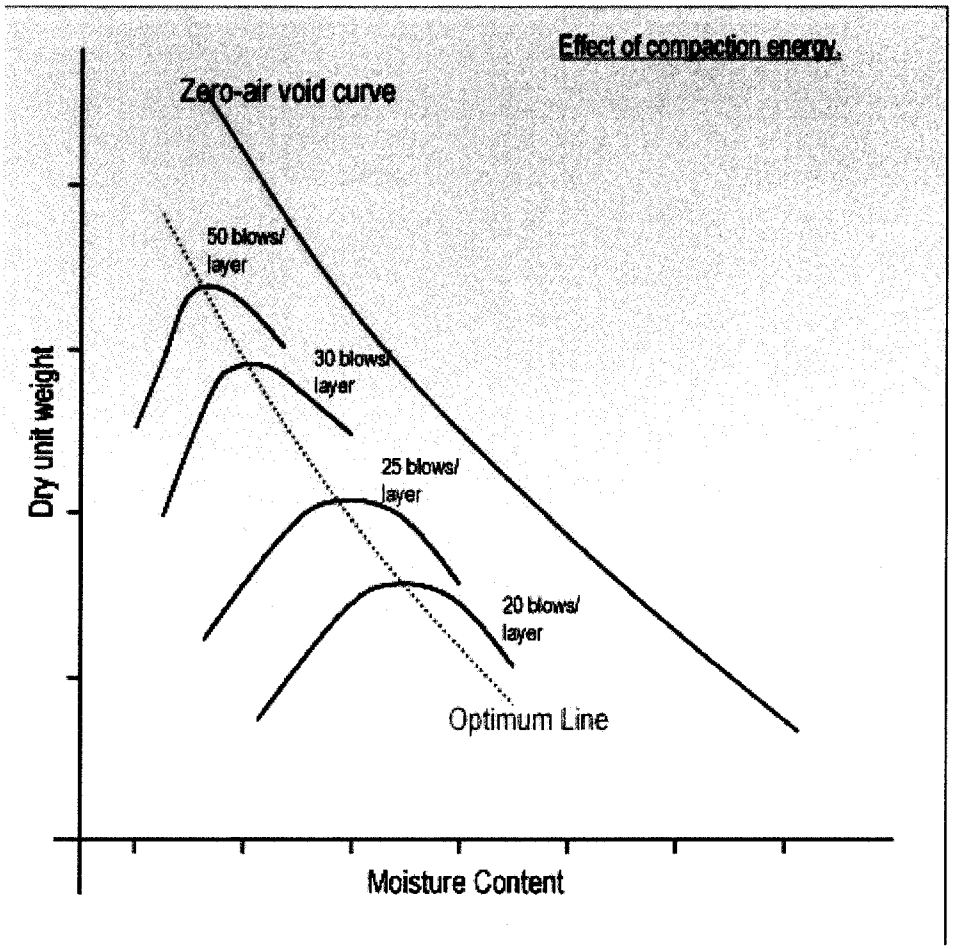

Figure 5- 1 Effect of compaction effort
source: http://www.landpac.com/main.htm

5.2.1. Static Compaction

A total of 19 Sil-co-sil 106 specimens of 50mm in diameter and 19.5mm in height were statically compacted using different water contents. Static compaction energy equal to 4000 kPa was used in the preparation of specimens. Table 5-1 summarizes the results of this study.

Table 5- 1 Static compaction test of Sil-co-sil

Water Content Prepared (%)	Bulk Density (kN/m^3)	Dry Density (kN/m^3)	Water Content Measured (%)
7	14.21	13.25	7.29
8	14.32	13.28	7.85
9	14.47	13.29	8.89
10	14.74	13.40	10.05
11	14.94	13.46	11.03
12	15.11	13.50	11.91
13	15.31	13.54	13.03
14	16.18	13.79	17.34
15	15.76	13.70	15.02
16	15.91	13.73	15.85
17	16.28	13.92	16.96
18	16.44	13.95	17.88
19	16.85	14.17	18.87
20	17.32	14.37	20.48
21	17.64	14.58	20.94
22	17.75	14.56	21.95
23	18.37	14.93	23.00
24	18.63	15.22	22.43
25	18.98	15.49	22.55

The measured water content of the compacted specimens after tests was equal to the water content added to the soil sample for preparing the specimens. However, measured water content was lower than 23% for specimens compacted with prepared water content of 24% and 25%. This is attributed to specimens reaching saturated conditions; some water was squeezed out from specimens during the compaction. In spite of expulsion of water, the compacted specimen appears relatively dry.

Figure 5- 2 Statically compacted silt specimen (i.e., Sil-co-sil 106)

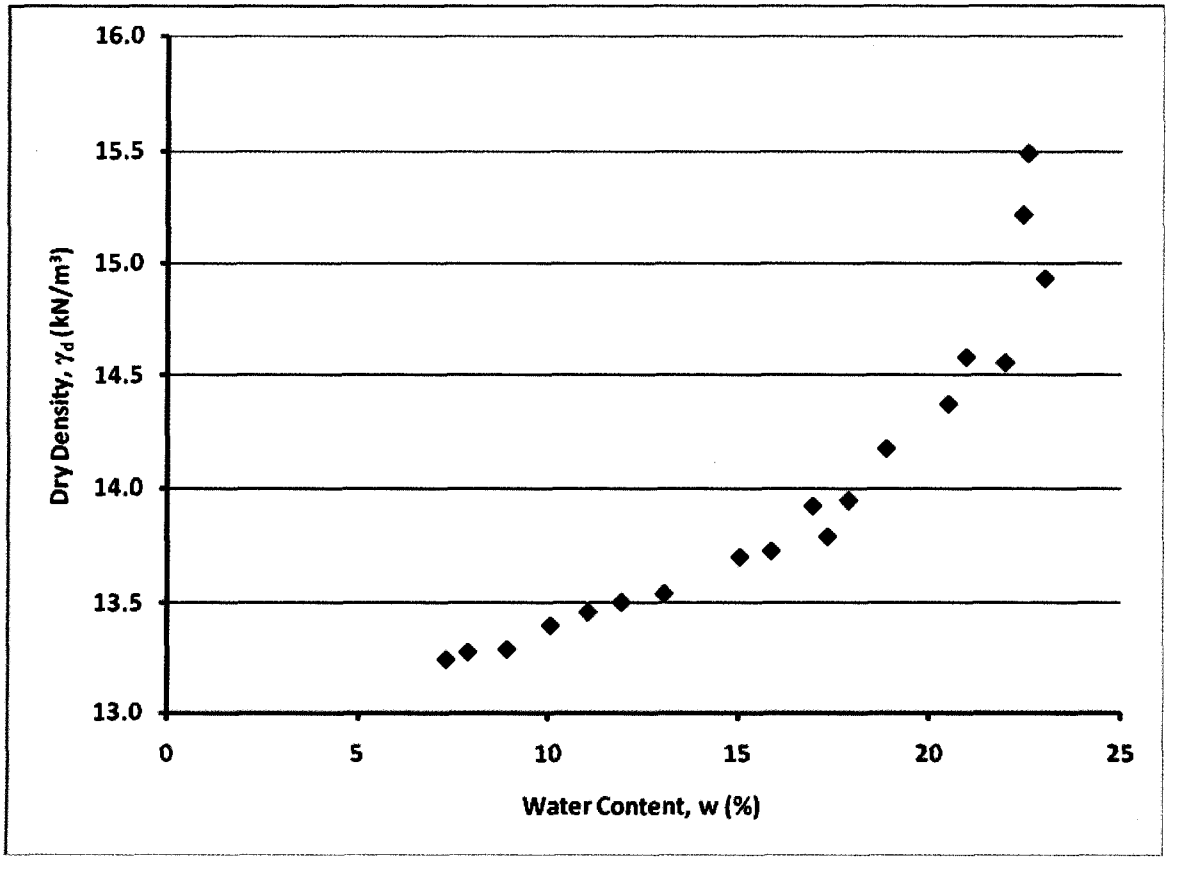

Figure 5- 3 Variation of dry density with water content of statically compacted Sil-co-sil

The static compaction results show that there is no defined optimum moisture content value for the tested Sil-co-sil 106. The dry density of compacted soil increases as the water content increases. In spite of reaching saturation conditions, dry density increases with an increase in water content. Although a compaction stress of 4000 kPa was employed (which is higher energy than the standard proctor's), the average dry density of the compacted silt has a relatively low value of 14.01 kN/m^3. The highest dry density value was only equal to 15.49 kN/m^3. From Figure 5- 2, many visible voids can be observed which demonstrates the reasons associated with low dry density values.

5.2.2. Vibratory Compaction

During static compaction, the author found that although the specimens were compacted with water contents greater than 20% (with degree of saturation values greater than 90% and higher), the specimens appear to be dry with no visible water to the naked eye. However, these specimens collapse and sink under the impact of vibration. The specimen after collapse compacts effectively to achieve high dry density values in comparison to the static compaction conditions. These observations inspired author to use vibratory method to compact this silica silt.

Two vibratory methods; namely, manual vibration and machine (or mechanical) vibration were used in the present for compacting the specimens.

Manual vibration involved shaking the soil container with the specimen in hand lead such that silt gradually collapses and compacted. The procedure used for vibration was to fill half of the container with silica silt with water content values greater than 20% and manually shake the container until the sample is compacted. Water squeezed out during this process collects on the surface of the sample. More dry silt was gradually added on top of the silica silt and subjected to manual vibration until no water squeezes out. Figure 5- 4 shows different pictures to demonstrate this phenomenon.

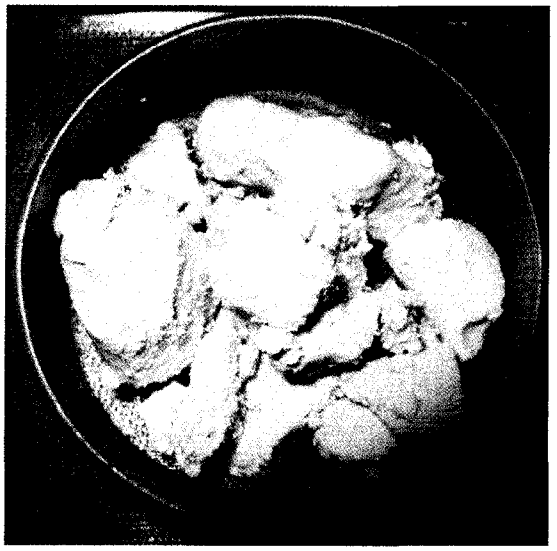

a. Silica silt with high saturation

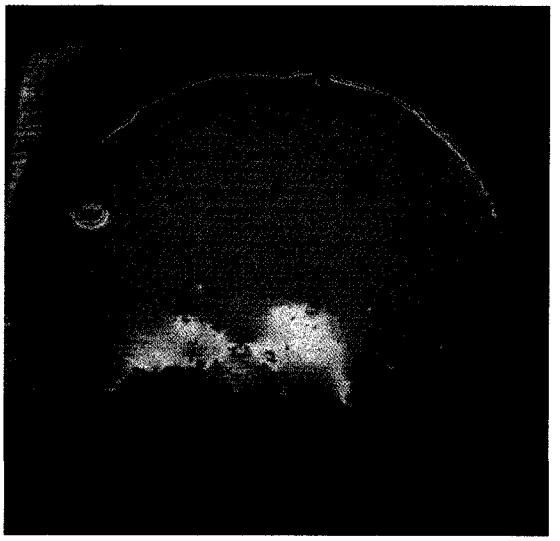

b. Compacted silica silt with visible water on the surface

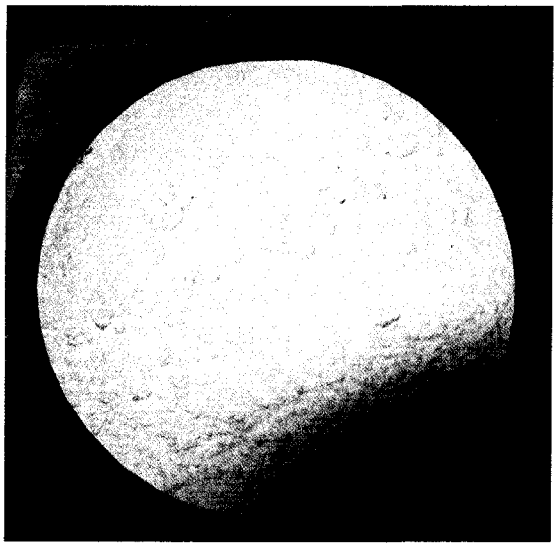

c. Addition of dry silt to the compacted silica silt

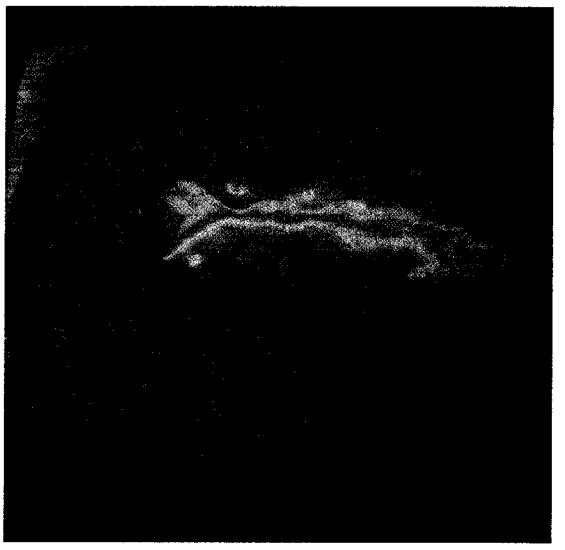

d. No visible water after manual shaking

Figure 5- 4 Manual vibratory compaction process

Table 5- 2 summarizes the results of some key properties of three samples studied after conducting experiments using the described procedure.

Machine (or mechanical) vibration technique involved placing the soil container with pre-determined water content and subjected to mechanical vibration. The compaction procedure is similar to the manual vibration technique detailed earlier. Initially fill the container with some saturated silica silt and vibrate the container until the silt fully collapse and is compacted. After

squeezing out extra water, more wet silt with an initial water content of 13% was added on to the top of compacted silt and subjected to vibration. This is repeated several times adding wet silt with water content of 13% until the soil container is almost full. Finally dry silt was added on the top until no water squeezed out. Four samples were compacted, and their dry densities are listed in Table 5- 2.

Two samples were subjected to mechanical vibration (i.e, MV1 and MV2) in small containers and subject to vibration for a relatively shorter period of time (i.e., 45 mins). Relatively low dry densities were achieved using this vibration technique. The other two samples (MV3 and MV4) were vibrated in long tubes subjecting to longer periods of vibration (i.e., 2 days). Relatively high dry densities were achieved using this technique.

5.2.3. Compaction Comparison

Table 5- 2 provides a summary of the results using the two different techniques of vibration (i.e., manual vibration (mV) and mechanical vibration (MV). The dry density values achieved using mechanical vibration technique was higher than the manual vibration technique. Based on the results of 8 tests conducted using static and different types of vibration (manual and mechanical) methods; mechanical vibration compaction method was found to be a better technique towards achieving higher dry density values or lower void ratio values for the Sil-co-sil tested.

Table 5- 2 Comparison of compaction method

Compaction Method	Dry Density γ_d (kN/m^3)	Water Content w (%)	Void Ratio e	Saturation S (%)
Static compaction (4000 kPa)	14.9	23.0	0.741	82.3
Manual vibration – (mV1)	18.5	14.4	0.408	93.6
Manual vibration – (mV2)	17.5	15.6	0.486	85.1
Manual vibration – (mV3)	17.5	15.2	0.488	82.7
Mechanical vibration - (MV1)	17.0	15.0	0.532	74.7
Mechanical vibration – (MV2)	17.5	15.2	0.484	83.3
Mechanical vibration – (MV3)	19.0	13.0	0.369	93.2
Mechanical vibration- (MV4)	18.9	13.0	0.376	91.5

The dry densities values vary from 17.0 kN/m^3 to 19.0 kN/m^3 using mechanical vibration technique (see Table 5-2). Reviewing the experiment process of vibratory compaction, The author would like to express the opinion based on the results of the studies undertaken, that results are influenced both by frequency used for vibration and the period of vibration. However, the influence of frequency vibration and length of vibration compaction time need further studies. Because of limitations with respect to time, this thesis did not pursue further studies in this direction.

5.3. Collapse

Four samples compacted with different initial water contents of 16%, 18%, 20%, and 22% were tested. All the samples were vibrated on the same platform for a period of three hours. The sample prepared with a water content of 22% collapsed within 3 minutes; the sample with water content of 20% compacted in 10 minutes; the samples with water content of 16% and 18% did not collapse during 3 hours vibration. Therefore, collapse of Sil-co-sil 10$\check{6}$ can initiate only when its water content is higher than 19%. From these experimental studies, it was observed that collapse conditions initiate in some pockets of the loose silica silt with initial water content 19% or higher.

Once collapse initiates in some pockets of the silt with high degree of saturation and low suction, it proliferates to other regions in spite of low initial water content. Figure 5- 5 demonstrates the observed behavior at various stage of vibration. Figure 5- 6 provides possible explanations for the observed behavior.

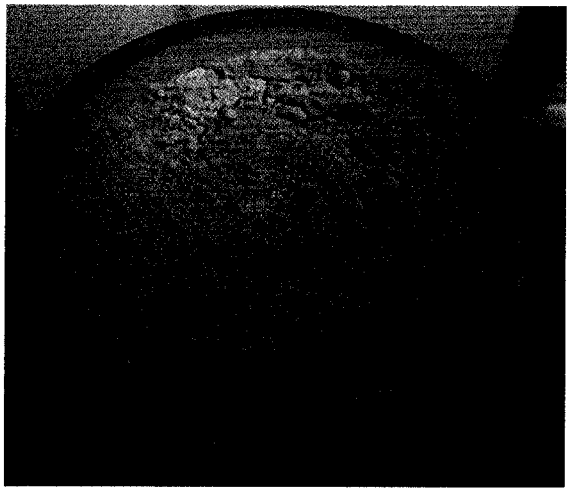

Before collapse

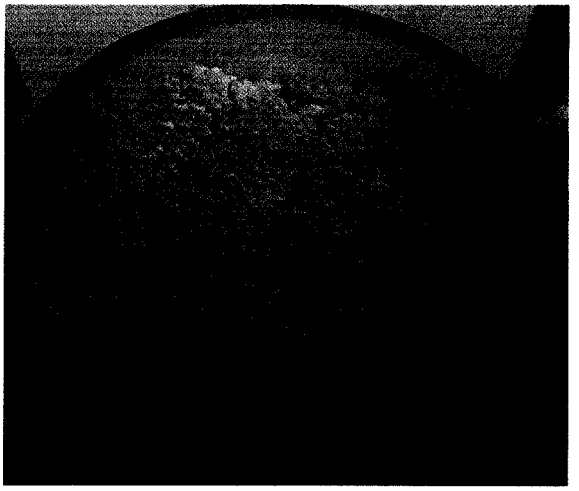

Initiation of collapse

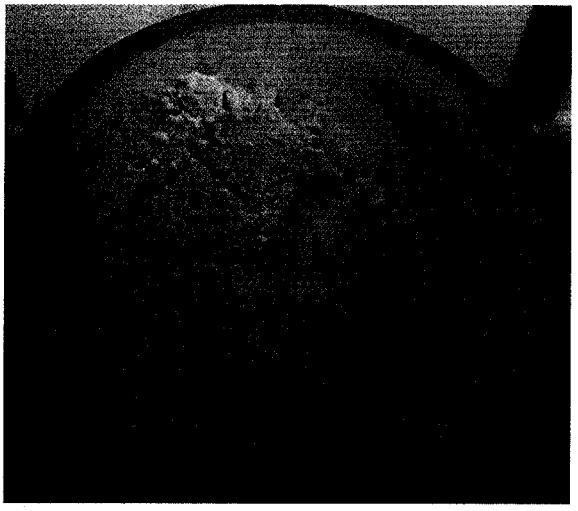

Intermediate stage of collapse

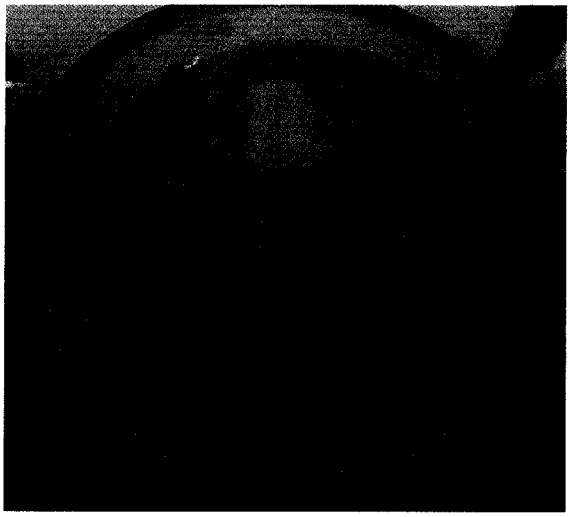

After collapse

Figure 5- 5 Sil-co-sil 106 during different stages during collapse

At the time of collapse initiation during vibration, soil suction or effective stress is low and the soil volume and void ratio dramatically start to reduce. At this stage, extra water gradually squeezes out under impact of vibration and flows into to other non-compacted regions of low initial water content. The density gradually increases due to a decrease in volume associated with an increase in the effective stress. The suction and effective stress is initially high in the non-compacted region of low water content, however, when extra water flows, water content increase and suction and effective stress decreases; hence soil collapses under the impact of

vibration. This process of collapse moves to the other regions of low water content if its water content is over 13% which equal to the water content of the compacted silt.

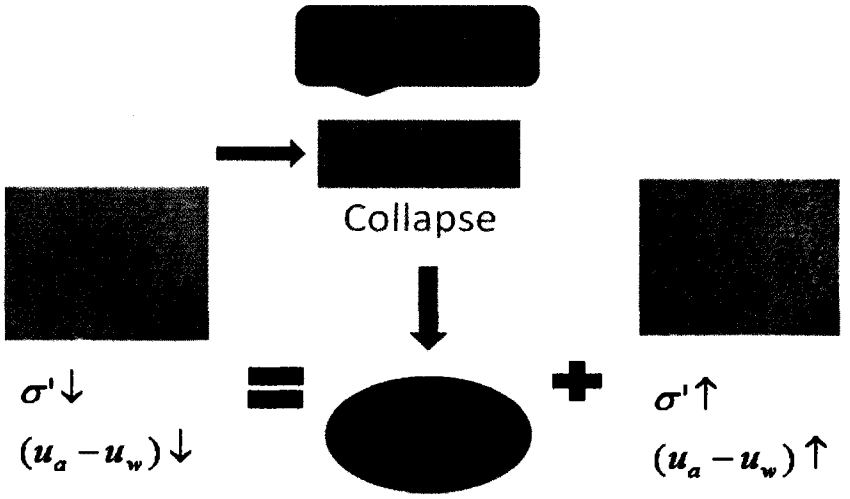

Figure 5- 6 Illustration of collapse process of Sil-co-sil

5.4. Soil-Water Characteristic Curve (SWCC) and Suction

5.4.1. SWCC of Sil-co-sil 106

The SWCC of the dense specimen after collapse was measured using a Tempe cell (Figure 5- 7). The soil dry density and saturated water content of the tested specimen was equal to 19 kN/m^3 and 13.77% respectively. The air-entry value of the specimen, the point at which specimen starts to desaturate is approximately equal to 70 kPa which is a typical characteristic of several compacted fine-grained soils.

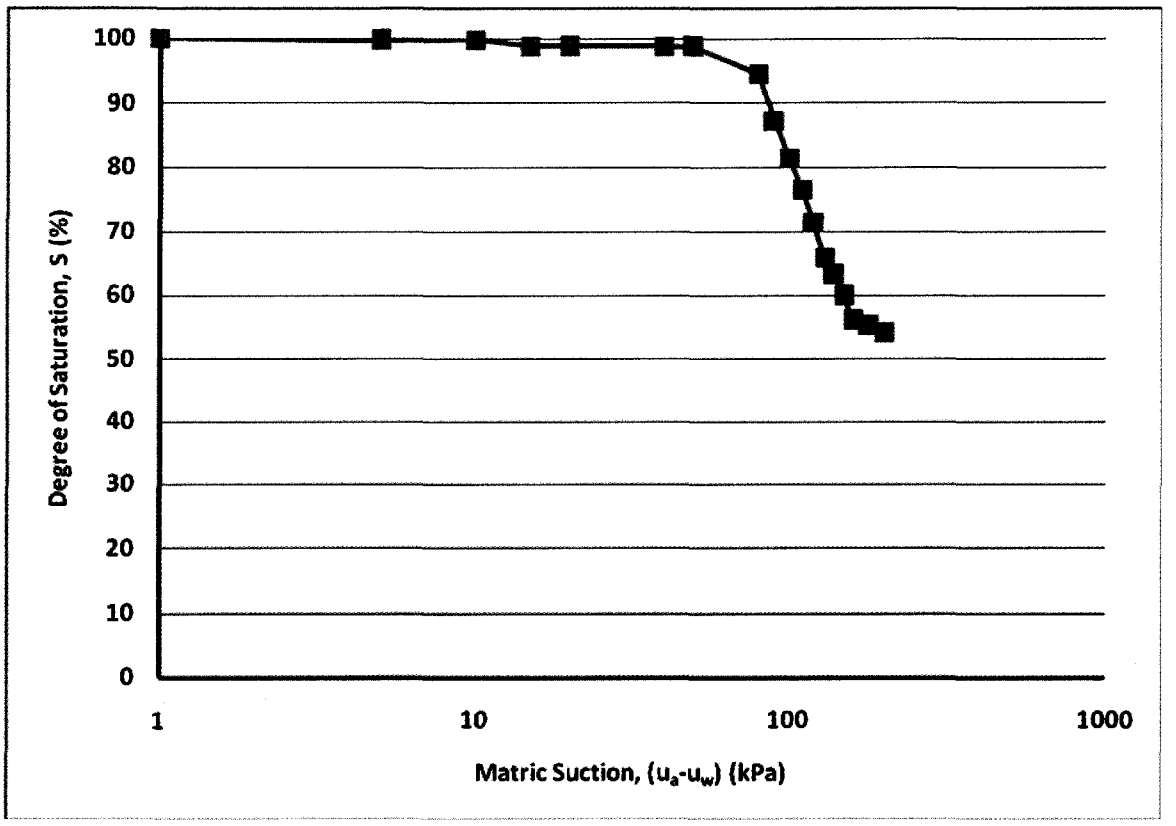

Figure 5- 7 Soil Water Characteristic Curve of Sil-Co-Sil 106

5.4.2. Suction Profile

Suction profile of compacted Sil-co-sil 106 was measured using 5 Tensiometers with the suction profile set by lowering the water table to different depths. The procedure related to the measurement of suction with respect to the depth of water table was discussed in earlier chapter. Measured suction profile for a depth of 1.5m below the ground surface is shown in Figure 5- 8.

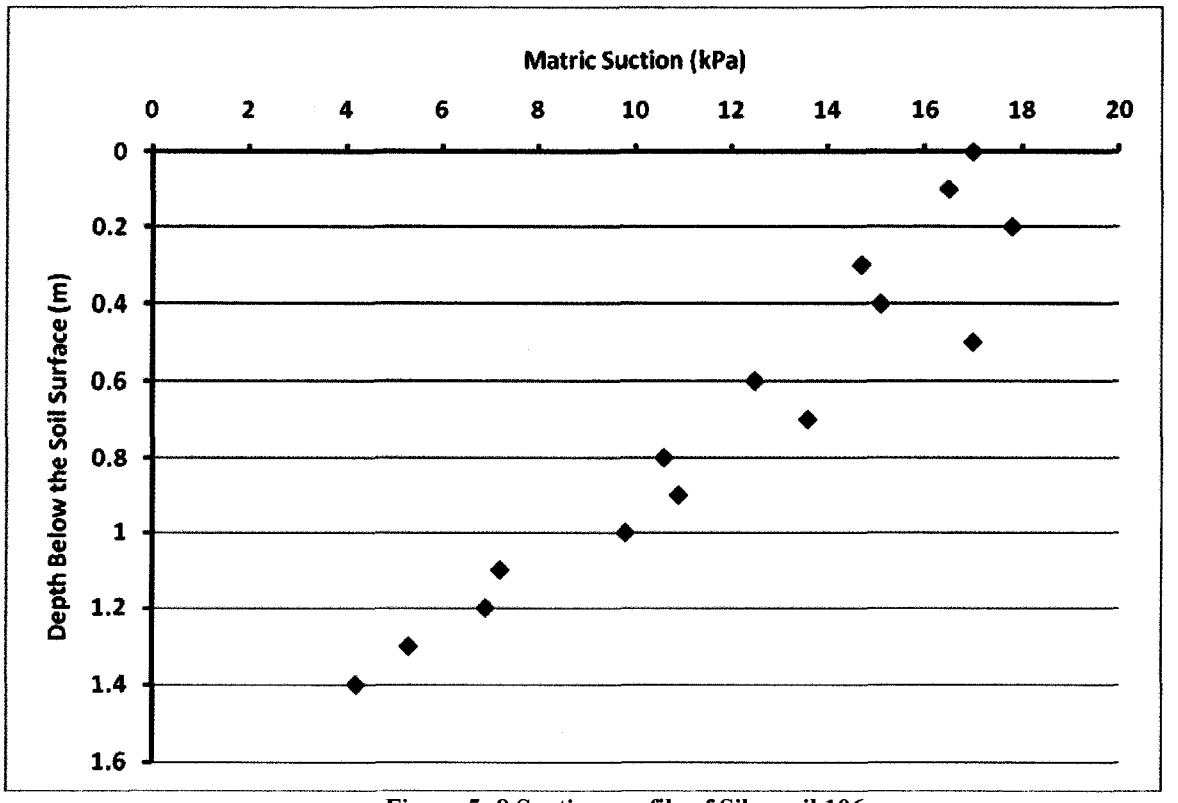

Figure 5- 8 Suction profile of Sil-co-sil 106

5.4.3. Suction vs. Vibration

Experimental results suggest that the suction of Sil-co-sil 106 is highly sensitive to impact loading. The suction values in the compacted specimens of the soil column are significantly influenced due to vibration. Figure 5- 9 shows the suction changes before and after vibration. In this figure, the static suction is suction at the depth of 0 to 0.4 m below the ground surface at equilibrium conditions when the water table is 1.5m below the ground surface; after subjecting to shock (i.e., a hammer knock on the soil column) suction is reduced in a few minutes. With several knocks using hammer on the soil column with the water table maintained at the same level, it can be observed that the suction value of 16 kPa reduced and positive pore water pressures were measured.

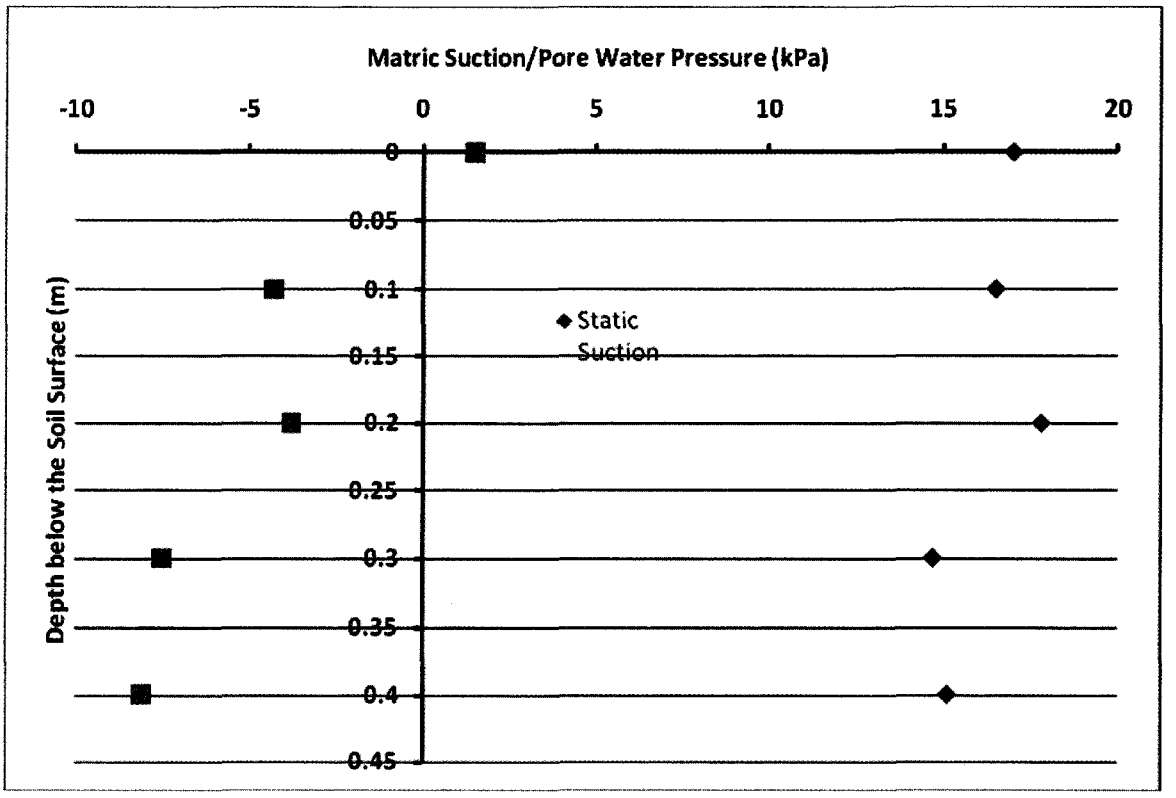

Figure 5- 9 Suction sensitivity of Sil-co-sil 106 to vibration

5.5. Bearing Capacity

The experiments conducted also demonstrate that bearing capacity and settlement behavior of initially compacted silt is significantly influenced due to vibration or dynamic loading conditions.

Compacted silt is stiff and brittle under static loading condition, but it is weak and flowable under the impact of vibration. Figure 5- 10 and Figure 5- 11 illustrate this characteristic of Sil-co-sil 106. Compacted saturated silt was difficult to be spaded up, and after it was spaded up by strong force, it broke into pieces and shows no visible water (see Figure 5- 10a). While the above broken silt subjected to vibration, it collapsed again and flowed back as one smooth mass (see Figure 5- 10b).

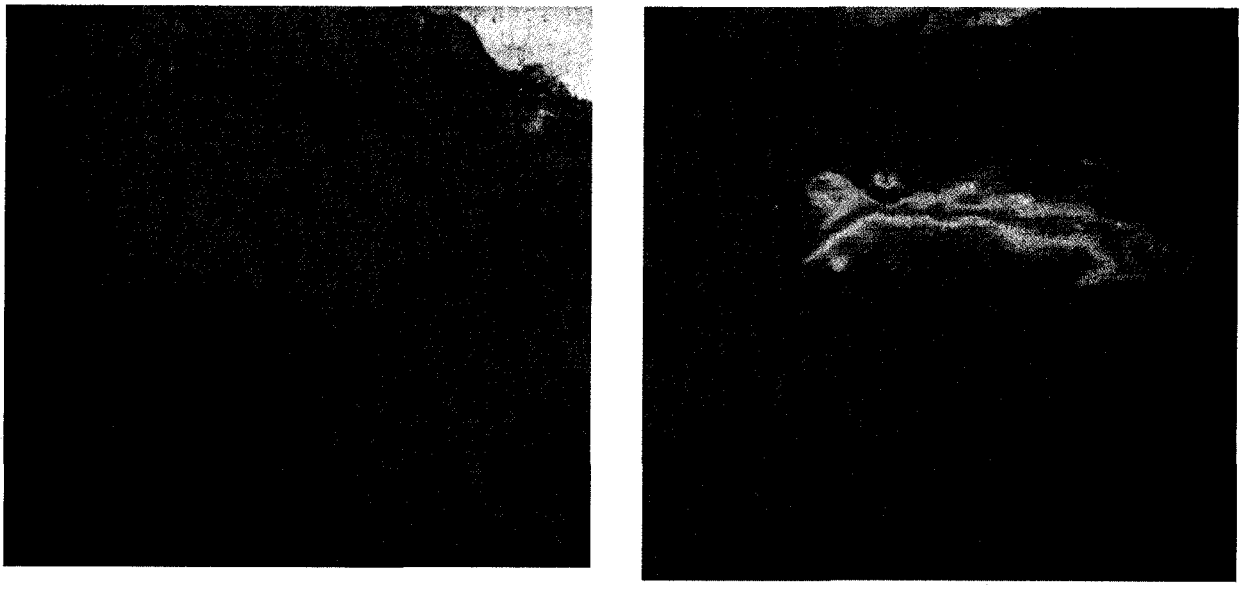

a. Clumps of compacted silt b. Compacted again under vibration

Figure 5- 10 Behavior of compacted Sil-co-sil 106 in static and vibratory conditions

Figure 5- 11d shows a test pit after bearing capacity test subjected to 12000 kPa in static condition. In the photo, the hardness and strength of compacted silt are further proved because the shallow test pit can resist a load of 12000 kPa; the cracks demonstrate the brittleness of the silt. However, under vibration, the silt collapsed again and test pit was refilled (see Figure 5-11a).

5.5.1. Bearing Capacity in Static Condition

Three footing tests were repeatedly conducted on same compacted silt in a small container using 20 mm square footing. Figure 5- 11 illustrates the footing test process with photographs. Before the test and at beginning of the test, there is water on the surface of the soil and it indicates the soil is in a state of saturated condition or close to saturated condition. During the test, soil was absorbing water and the soil surface appearance was relatively "dry". After the test, there was no visible water on the soil surface or in the punched hole of the test (Figure 5-11, d).

a. Before the test

b. At the beginning of the test

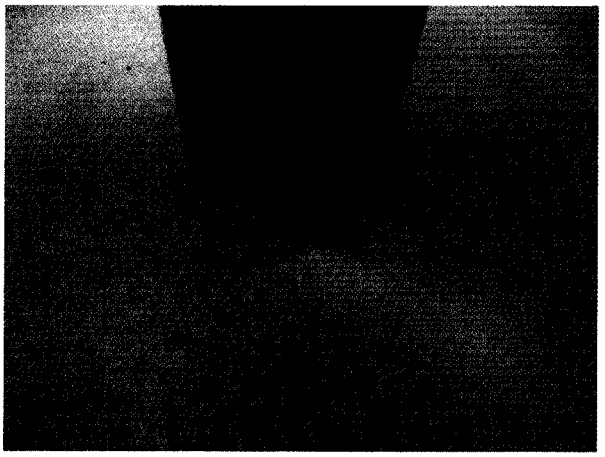

c. In the middle of the test

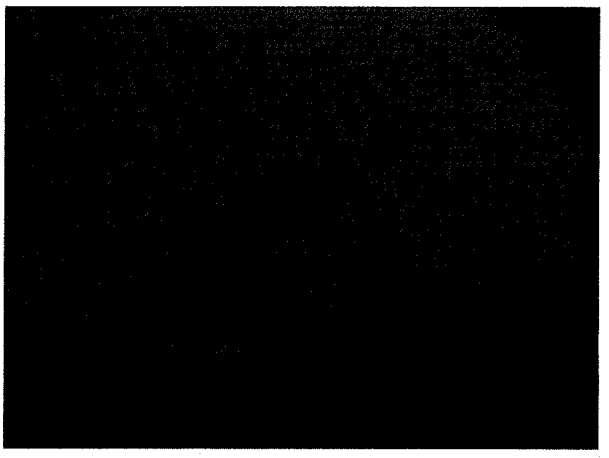

d. Test pit after test

Figure 5- 11 Footing test process of Sil-co-sil in static condition

The applied pressure versus settlement results are shown in Figure 5- 12. These results demonstrate that the silt resistance to the static load increases with an increase in the settlement; however, no defined peak or failure conditions were observed. Three tests (i.e., Test 1, Test 2 and Test 3) were conducted on the same soil in the same container. After completion of Test 1, the soil container was subjected to vibration such that the soil surface is flat again to start the next test (i.e., Test 2). The Test 2 was conducted using similar procedures as Test 1. However, the results of Test 2 suggest that the resistance decreases in comparison to Test 1. Similar results were observed for Test 3 (i.e., further reduction in soil resistance). These results suggest that the previous tests have influence on the stress versus settlement behavior of the later tests. In

addition, it is also likely that the vibration period has a significant influence on the stress versus settlement behavior.

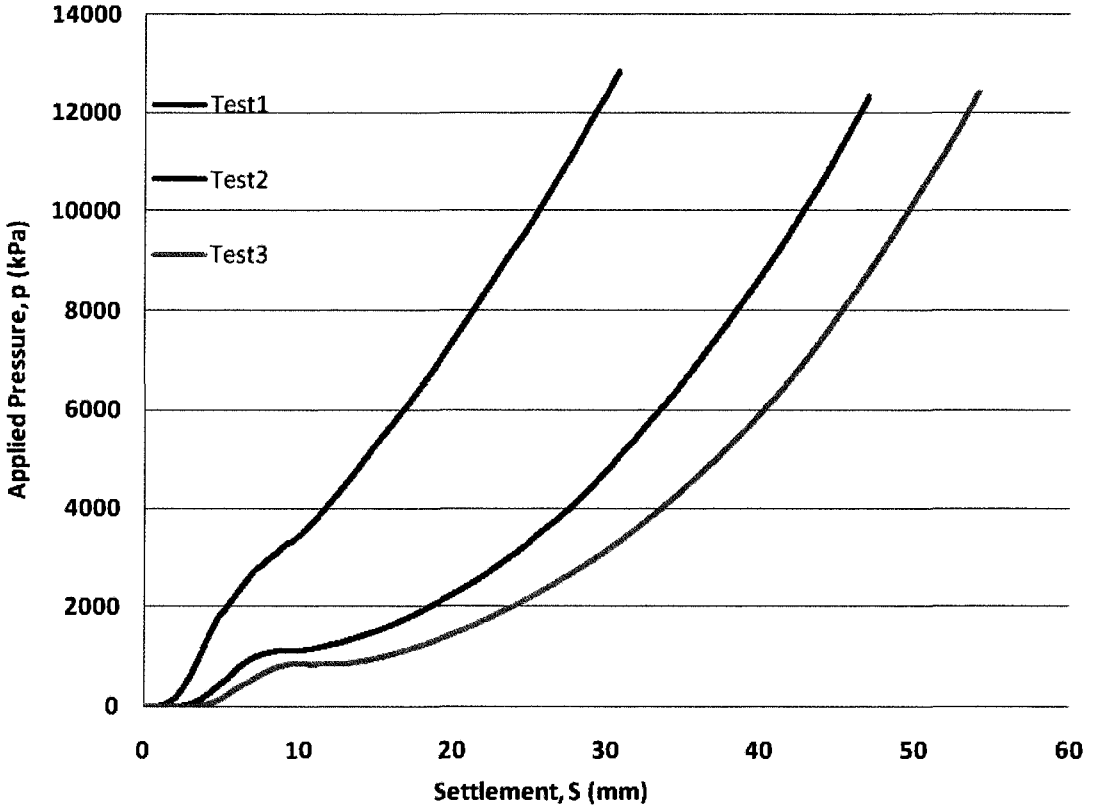

Figure 5- 12 Stress-settlement of compacted Sil-co-sil 106

5.5.2. Creep

A creep test on compacted Sil-co-sil 106 was conducted under static load stress of 250 kPa (a static load of 100 kg on a footing of 20mm × 20mm). The test result shows that the footing settlement occurred during the period of load application. However, no settlement was observed when a constant load was maintained. These results suggest that compacted Sil-co-sil 106 does not exhibit creep behavior under static lading condition (see Figure 5-13**Error! Reference source not found.** and Figure 5- 14).

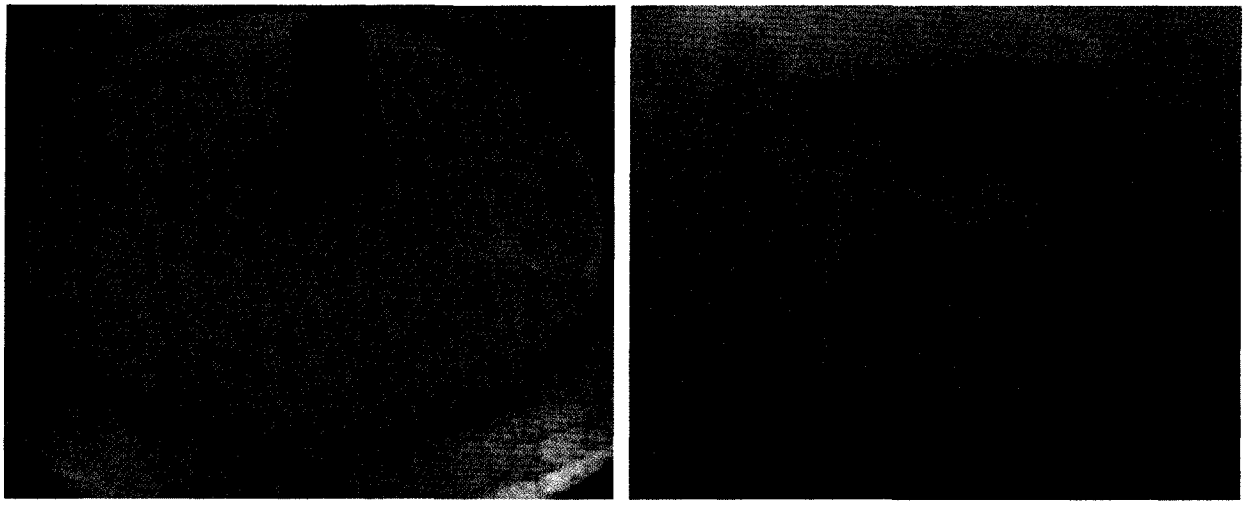

Figure 5- 13 Photos of Sil-co-sil before and after creep test

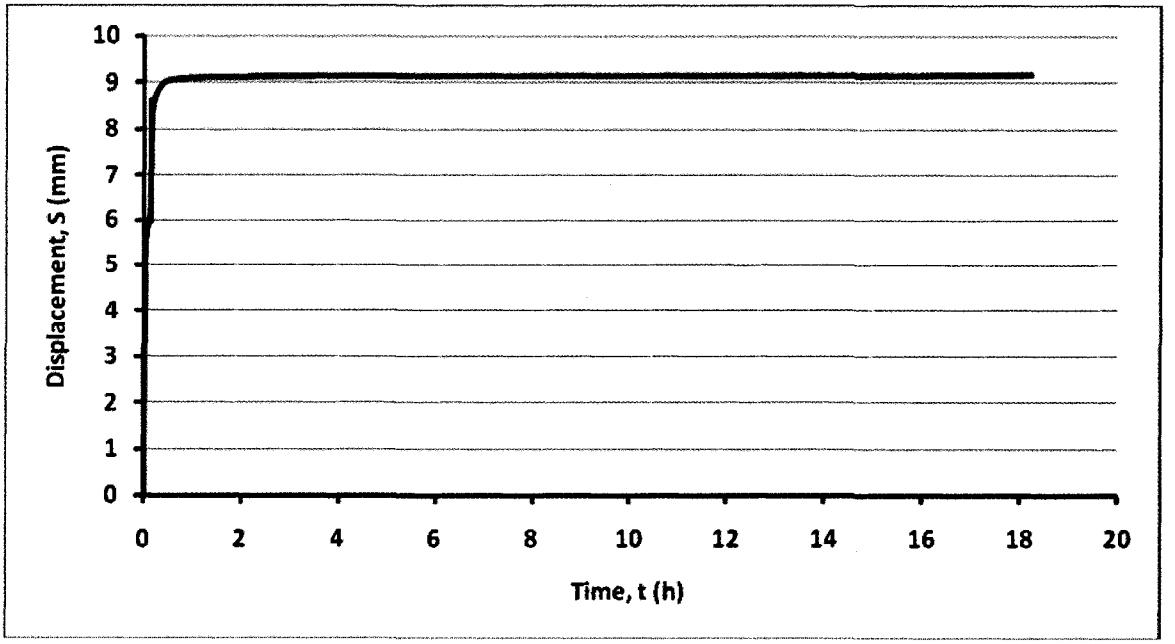

Figure 5- 14 Creep of compacted Sil-co-sil 106 under static load

5.5.3. Bearing Capacity under Vibration

Experiment results show that compacted Sil-co-sil 106 has almost no bearing capacity when subjected to vibration loads. Figure 5- 15 shows the test set-up used for conducting these experiments. A steel bar of 317g in weight and 9.5mm in diameter, which can be assumed to represent a footing was placed on the surface of the soil in the container and subjected to vibration. During the test, the steel bar was held to stand on the soil surface without any extra

force, so the load is just the weight of steel bar itself (i.e., 44 kPa). The settlements (or the displacement of steel bar into the soil) for three tests were 34mm, 42mm and 44mm under 5 minutes vibration. Tests were repeatedly conducted on same compacted silt. After each test, the soil was vibrated to initiate collapse of silt and attain a flat surface. The next test was repeated on the same soil such that the previous test result is influenced by the present test results.

Comparing to stress of 12000 kPa in settlement of 40mm at stress-settlement curve in static condition, the stress of 44 kPa under vibration is much smaller (1/270) than the stress in static condition at the similar settlement.

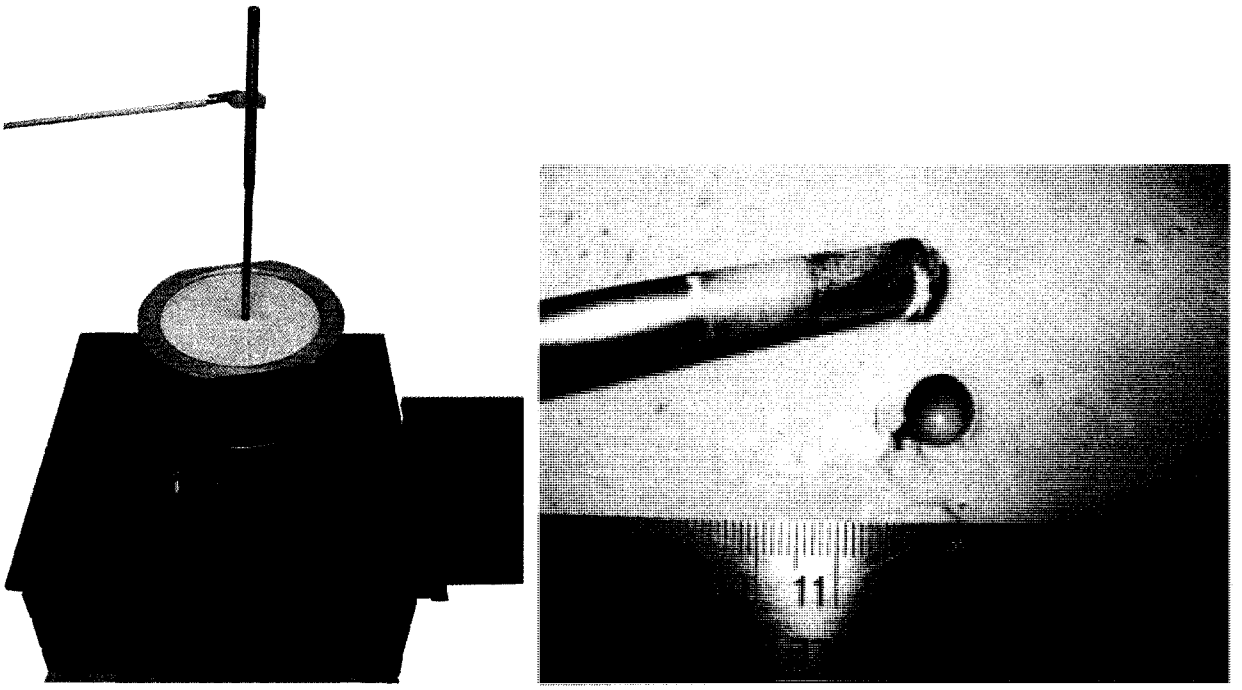

Figure 5- 15 Bearing capacity of compacted Sil-co-sil 106 under vibration

5.6. Shear Strength

Direct shear test results shows that compacted Sil-co-sil 106 has relatively high strength (friction angle ϕ' =52°). Two series of direct shear test were conducted both under saturated and unsaturated conditions using 60mm × 60mm samples. All samples were prepared and compacted using vibration method. Unsaturated direct shear tests were conducted on compacted specimens (Figure 5- 16a) at a shear strain rate of 1mm/minute. The friction angle ϕ was equal

to 51.1° and apparent cohesion, c was equal to 193 kPa for unsaturated specimens. Several sample were tested under submerged conditions to determine the shear strength parameters under saturated conditions (Figure 5- 16b). The sample was sheared at strain rate of 0.02mm/minute. The effective friction angle, ϕ' was equal to 52.6° and effective cohesion, c' was equal to 41.3 kPa. The direct shear test results are summarized in Figure 5- 17a, b, c, and d.

a. Unsaturated condition b. Saturated condition

Figure 5- 16 Direct shear test process of Sil-co-sil 106

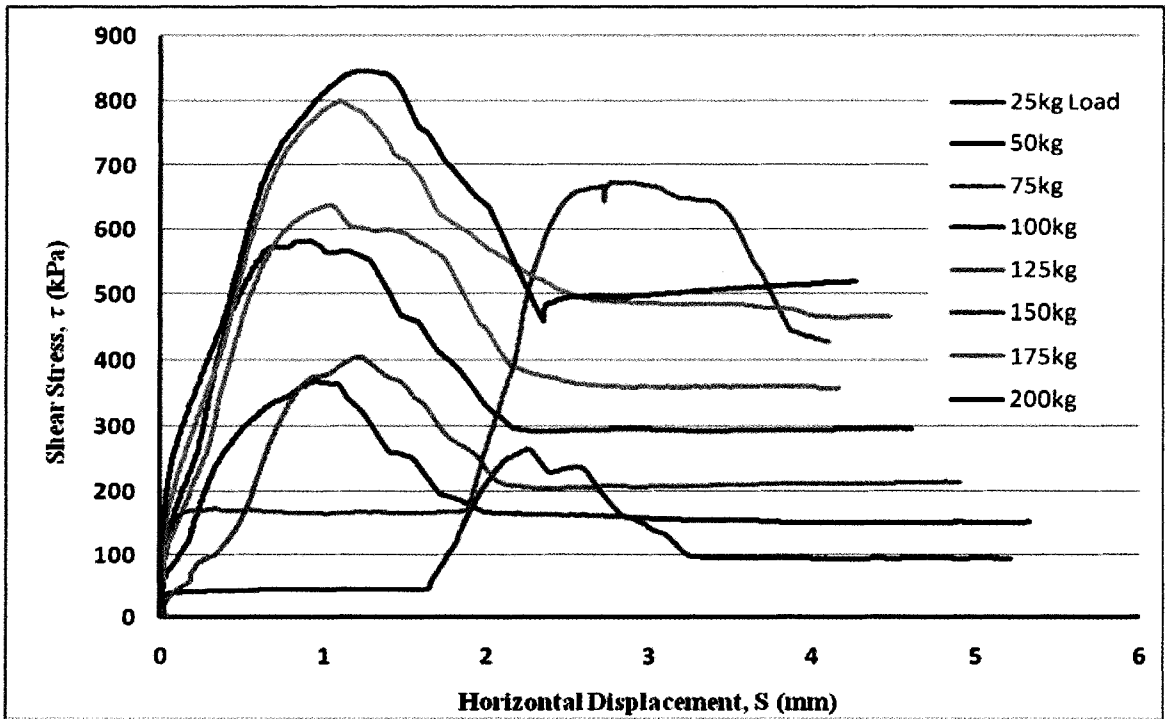

a. Shear strength of Sil-co-sil 106 in unsaturated condition

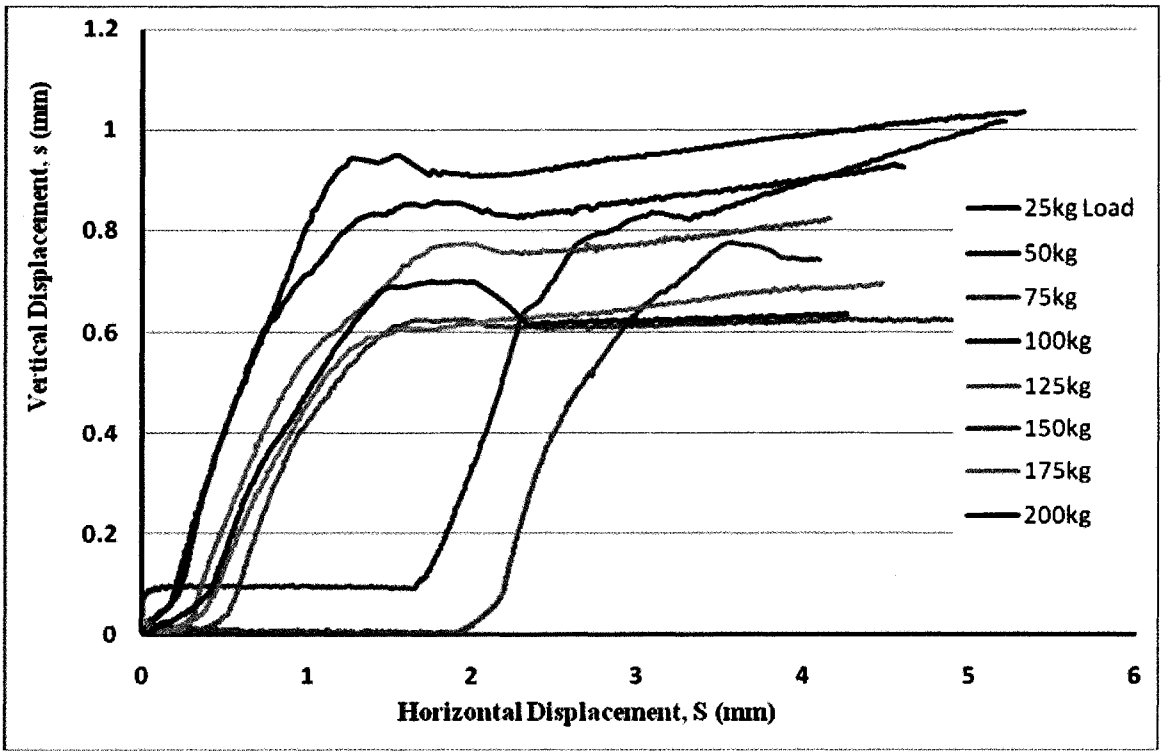

b. Dilatancy of Sil-co-sil 106 during direct shear test in unsaturated condition

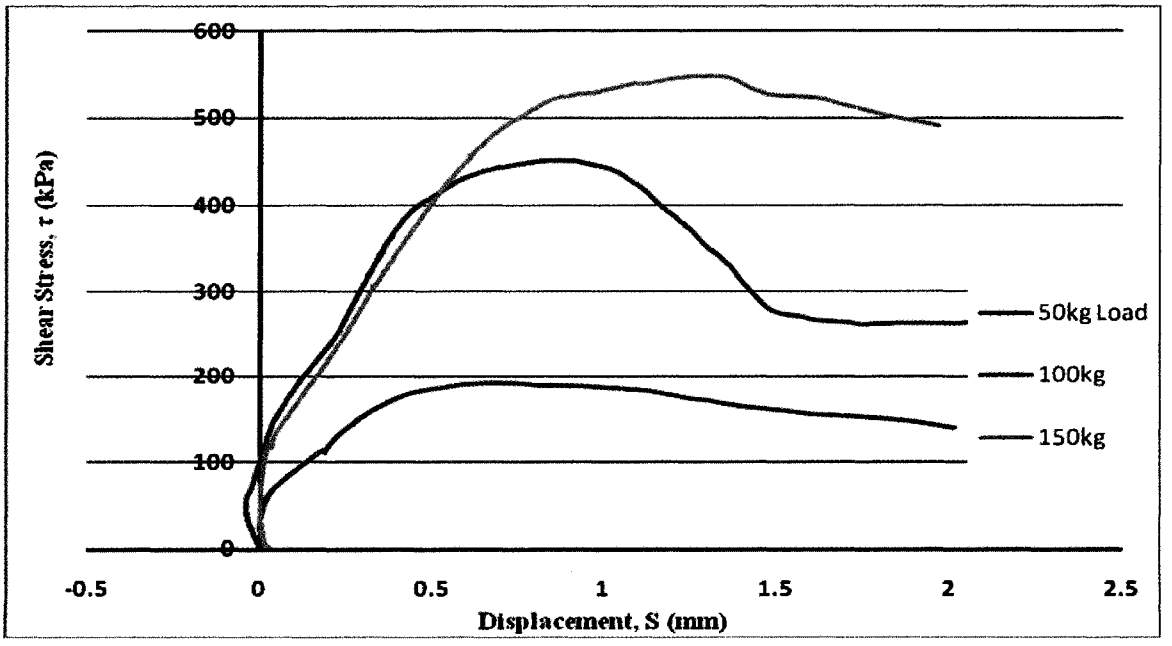

c. Shear strength of Sil-co-sil 106 in saturated condition

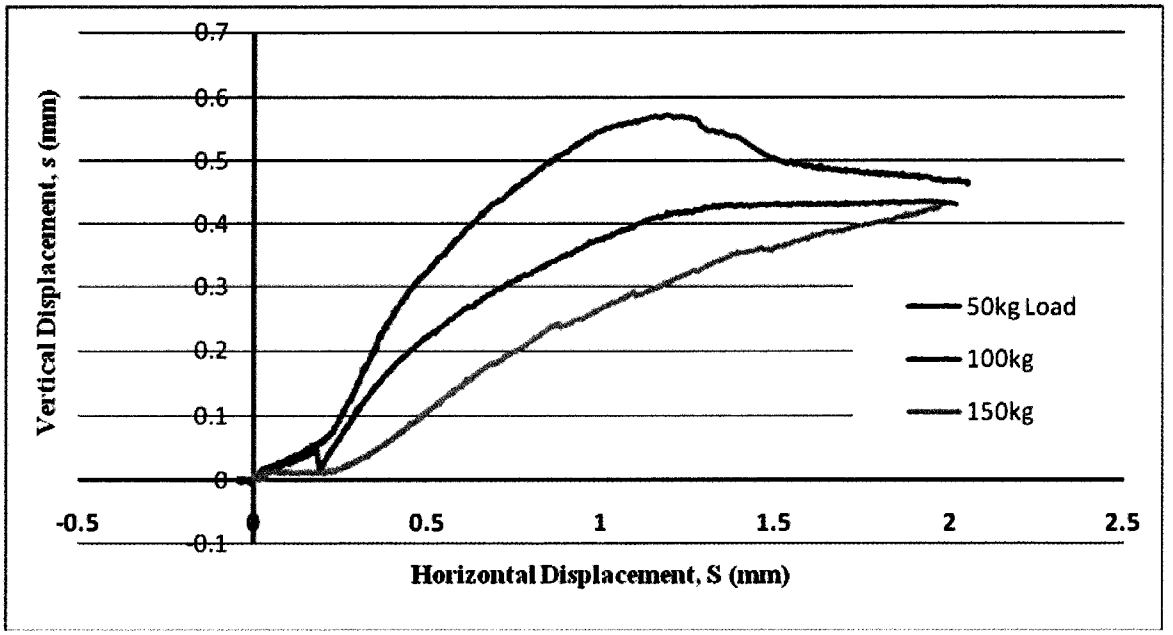

d. Dilatancy of Sil-co-sil 106 during direct shear test in saturated condition

Figure 5- 17 Results of direct shear test

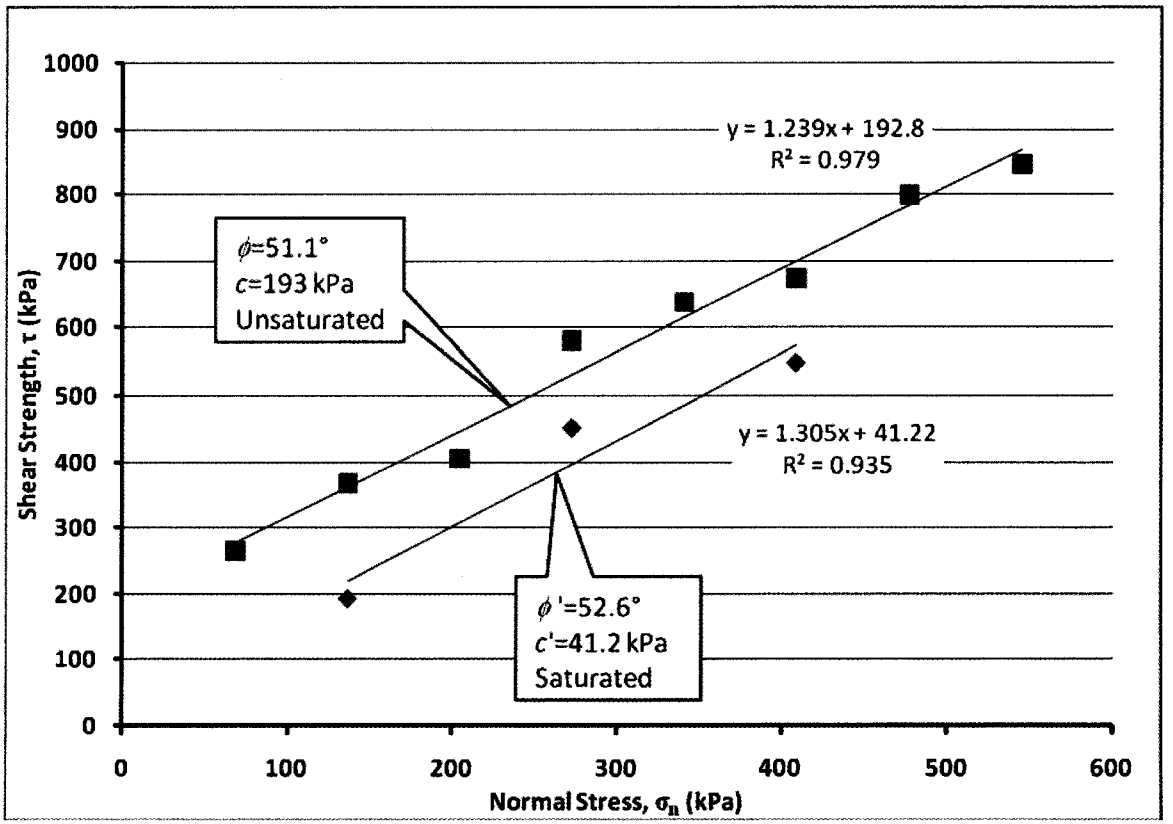

Figure 5- 18 Shear strength of Sil-co-sil 106

The friction angle is the same under saturated and unsaturated conditions for the well-compacted silt Sil-co-sil 106 (Figure 5- 18). However, the measured unsaturated cohesion value is high, 193 kPa, and the saturated cohesion is also relatively high, 41 kPa. These results suggest that the compacted Sil-co-sil 106 has a significant contribution of strength from the cohesion component.

5.7. Microstructure Analysis

The Sil-co-sil 106 demonstrates some interesting characteristics of. In this section, author makes an attempt to explain these characteristics using a visualized microstructure model for Sil-co-sil 106.

Sil-co-sil 106 is ground silt and not natural silt, so it is angular and hence has a relatively high internal friction angle, ϕ'. Sil-co-sil is very fine, 98.5% grain size smaller than 0.1mm, so void size in compacted Sil-co-sil 106 is very small and has very high suction. Therefore, Sil-co-sil 106 is exhibits significant resistance due to the contribution of suction to static loads.

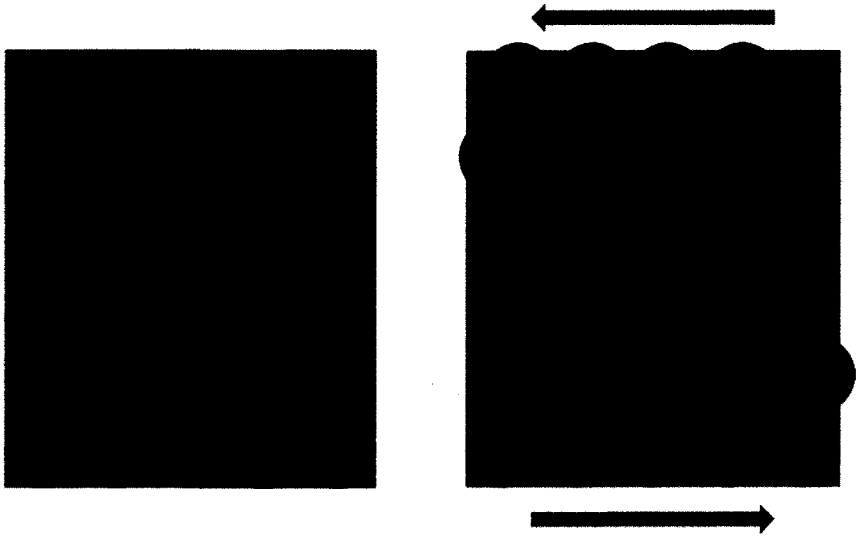

a. No load in static condition b. Under static load

Figure 5- 19 Behavior of silt under static load

In static condition, the stress in the soil is applied one direction; hence soil particles movement is restricted in one direction, which is the direction in which load is applied. In other words, the

one direction load forces the soil particles to try to roll over one another. It is likely that there is an increase in the void ratio of the silt due to dilation arising from absorbing water on the soil surface into the silt (see Figure 5- 19).

Under vibration or cyclic loading condition, stresses in the soil are applied in different directions. Therefore, silt particles have a tendency to move toward the region of higher void ratio or low-suction region. During this process it likely the silt particles squeeze together and the air and water in the voids move upward out of soil. Therefore, soil collapses, sink and get compacted further (Figure 5- 20).

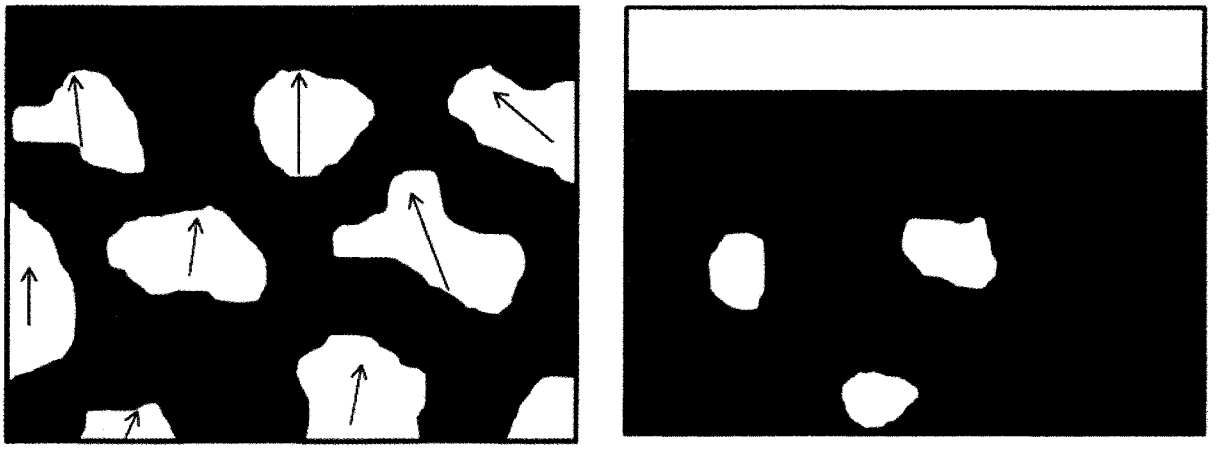

a. Particle movements under vibration b. After liquefaction and compaction

Figure 5- 20 Behavior of silt under vibration

5.8. Engineering Significance

When foundations are placed on soils such as the sil-co-sil, when they are subjected to cyclic loading conditions, such as structures with machinery, railroad and highways, may collapse or have significant settlement problems, even in unsaturated condition. It is a good construction practice to saturate such silts first and compact them rather than compact the silts with lower compaction water content under unsaturated conditions.

CHAPTER 6

ANALYSIS OF BEARING CAPACITY TEST RESULTS

6.1. Introduction

More than 150 bearing capacity tests were conducted on three different sands; namely, Unimin 2075 sand, Ottawa sand, Unimin 7030 sand under both saturated and unsaturated conditions using the two different bearing capacity equipments (i.e., one with the short and the other with the tall soil containers) in the present research program. The bearing capacity of model footings was determined over a matric suction range of 0 to 12 kPa. This range of suction for the three sands studied extends over the boundary effect, transition and residual stages (Vanapalli et al. 1996) for the three different sands studied in the present research program. Four model footings of different sizes (i.e., 20mm×20mm; 25mm×25mm; 37.5 mm×37.5 mm and 50 mm×50mm were used to study the influence of footing size on the bearing capacity of unsaturated sands.

6.2. Soil Preparation and Compaction

6.2.1. Soil Preparation

The procedure used in the preparation of the soil prior to compaction is summarized below:

(i) The optimum moisture content of coarse-grained soil used in the study (i.e., Unimin 2075) was determined in the laboratory following the ASTM procedure. The information about optimum moisture content of the other two sands studied in this research program; namely, Unimin 7030 and Ottawa sand was summarized from the published literature.

(ii) The sand to be tested for bearing capacity using model footing tests was mixed with predetermined amount of water to attain the optimum moisture content of the soil. This soil mixture was placed in plastic bags and stored in a humidifier for a period of

approximately 24 hours to achieve uniform water content conditions through out the sample.

(iii) Prepare the soil container: The base of the soil container with slots was cleaned to ensure free flow of water flow. A lid with perforations was placed on the base of the soil container to cover the slots. A geotextile of the same diameter as the base of the soil container and lid were placed on top of the lid. Lastly, a filter paper was placed on the geotextile, to allow the free flow of water but block the soil particles migration. The base plate of the soil container and cylinder were then fastened with the screws tightly to prevent any leakage of water.

(iv) The soil mixture (i.e., sand mixed with optimum moisture content) was placed into the container in several layers. Each layer was approximately 50mm in depth in the container and compacted using a 5 kg hammer. This procedure helped in achieving a relatively higher value of density index.

(v) A valve connected to the base of the soil container provides access of water to the compacted sand in the container under a controlled head of water. Water flows through slots in container base and rises up from bottom slowly until the sand is fully saturated (i.e. the water table reaches the sand surface in the container). This technique facilitated escape of air from bottom to the surface layers of the sand in the container gradually to ensure a fully saturated condition. The proposed technique was developed after several trial studies.

(vi) The next step constituted the placement of Tensiometers. The Tensiometers were saturated with deaired distilled water following the procedures detailed in Chapter 3. The prepared Tensiometers were then placed in the compacted sand such that the ceramic cup was into the soil approximately at the centre of the depth of stress bulb (which approximately corresponds to 1.5 B of the footing size).

(vii) The loading system and data acquisition system were calibrated prior to loading the footing in the soil containers.

(viii) Different values of matric suction (i.e., 2 kPa, 4 kPa and 6 kPa) were achieved below the model footing following the procedures described in Chapter 3. After achieving equilibrium conditions, the model footings were loaded to failure. In addition, some tests were also conducted on relatively dry sands.

(ix) After the completion of each test (i.e., measurement of the failure load on the model footing), the sand in the top layers of the soil containers where the soil stress were predominant was removed, compacted and saturated again for conducting the next test with different suction values. No attempts were made to determine if the sand particle sizes changed during the loading stage as the failure loads were relatively low. In other words, an assumption was made that the particle sizes of sand do not change during the loading of the model footings. However, it was ensured that the density was maintained constant for all the tests conducted to ascertain "identical" conditions.

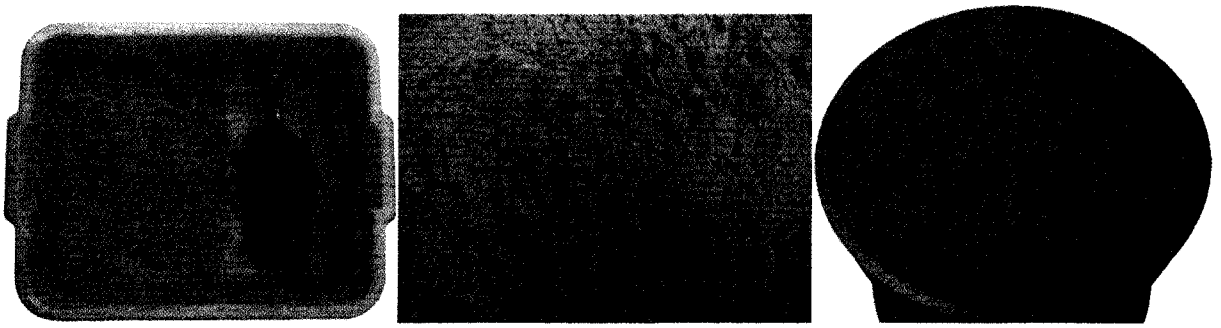

Figure 5- 1 Prepared soil

6.2.2. Soil Compaction in Lab

One of the key objectives of the thesis was to study influence of matric suction on the bearing capacity of sands. However, the experimental studies have shown that the bearing capacity is significantly influenced by soil compaction. Several precautions were taken to eliminate the effects of compaction such that the influence of matric suction can be measured with a greater degree of accuracy. To achieve this objective, the same soil was used to determine the bearing capacity under different values of matric suction controlling the dry density for all the tests to achieve uniform structure or fabric.

Three key factors affect the soil compaction; namely, water content, method used for compaction, and the type of soil being compacted. Based on the experience from the present experimental studies, author found that compaction method has a significant influence on the density for the tested sandy soils in comparison to the other factors.

In the present study, five different methods of compaction were used for Unimin 7030 sand compaction.

6.2.2.1. Method I: Compaction Using 5 kg Hammer

The following procedure was used for static compaction:

(i) The sand to be tested was filled in the soil containers of bearing capacity equipment (i.e., with short and tall cylinder) up to the soil surface.
(ii) Experimental studies by Mohamed (2006) have shown that approximately water content value of 14 % (i.e., optimum water content) value can be achieved by lowering the water table to a depth of 300 mm in the zone of stress bulb due to capillary rise. After achieving this water content, the sand in the soil container was compacted using 5 kg hammer to achieve maximum dry density conditions. The ground water table was then varied to achieve different values of matric suction below the model footing before loading to determine the bearing capacity.
(iii) After completion of the loading test, sand layer up to a depth of 100mm was dug out from the soil test container. A 100 mm depth was chosen to be removed, because this is the predominant depth zone of stress (i.e., stress bulb) for the model footing.
(iv) The removed sand and was then placed in 50 mm layers and compacted using 5 kg hammer as described in the earlier parts of this section.
(v) Soil samples were collected in steel sample rings after compaction to measure the soil density.

The results of bearing capacity and measurements of density of sand have shown that it was difficult to achieve uniform conditions using the method described in this section. The author found that it was difficult to achieve uniform compaction and density conditions (i.e., identical testing conditions for all the tests). The sand structure or fabric appears to be influenced even due to small changes in water content and manual compaction using 5 kg hammer.

6.2.2.2. Method II: Vibration with Concrete Vibrator

A small concrete vibrator was used for sand compaction with a water content equal to optimum moisture content (i.e., 14%) in the soil container for a period 5 minutes. The density of the sand was measured after the test to ensure "identical" conditions.

This method is effective in the reduction of sand volume. However, several trial tests have shown that it is difficult to achieve uniform density conditions in the top layers of the sand layer. Since soil container and footing sizes in this testing program are small, variation in density and matric suction in top layers have a significant influence on the measured bearing capacity values. Due to this reason, this method was also regarded as not a good compaction method for the experimental investigations proposed to be undertaken.

6.2.2.3. Method III: Vibration with Vibratory Machine

The procedures used for compaction are similar to Method I:

(i) The water content in the soil equal to optimum water content using the procedure described in Method 1.However, a vibrator was used for the sand compaction. The vibratory machine was used for a period of 4 minutes for each layer and followed it by gently pressing the sand using a 5 kg hammer. This procedure was followed for different layers; each layer was approximately 50 mm.

(ii) After last layer vibration, the soil surface was leveled and vibrated for an additional 3 minutes.

(iii) The soil density at different layers was measured after performing bearing capacity tests.

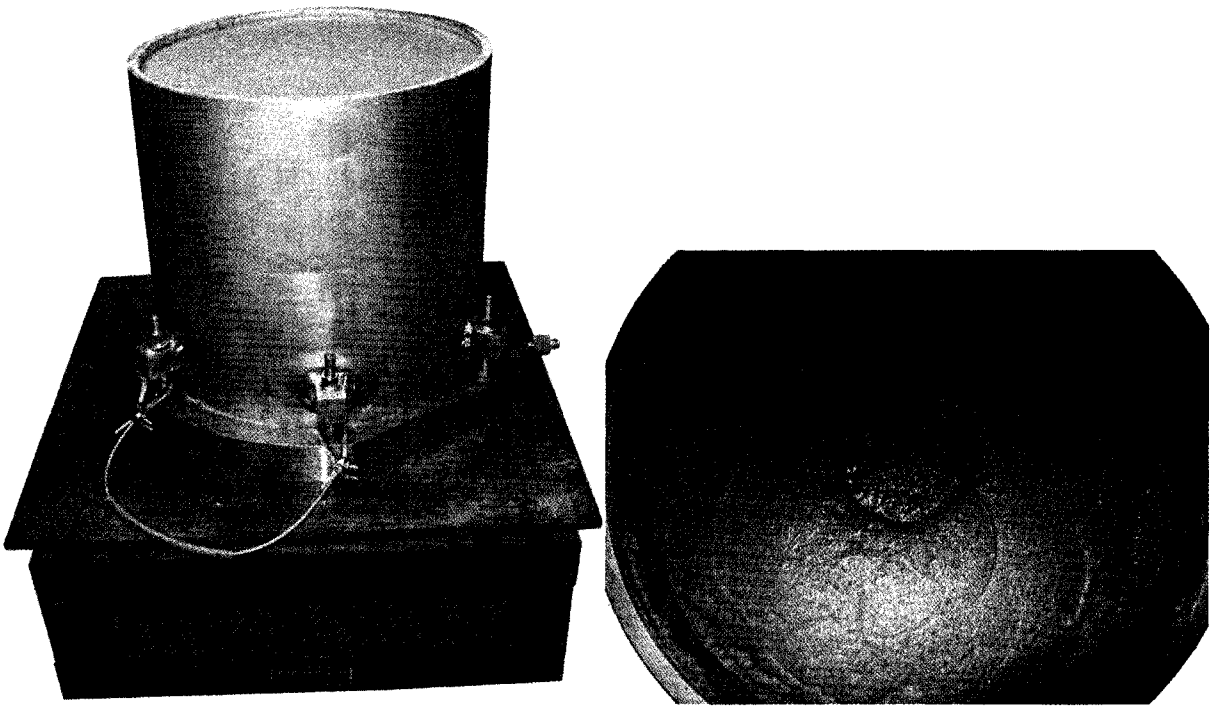

Figure 6- 1 Vibration compaction with vibrator machine

This method was found to be better in comparison to the earlier two methods; however, measured densities show that they still vary, but not erratically as observed in the earlier two methods. It was still difficult to control the density as some scatter was observed.

Based on the experience of several trial studies, the author feels that factors that control the density include the compaction effect, water content, vibratory frequency, and time of vibration. However, author was not able to conduct enough number of tests to investigate in more detail about the influence of al the above parameters.

6.2.2.4. Method IV: Vibration in Saturated Condition

The compaction procedure used in this Method is relatively simple.

(i) The sand is saturated soil using the procedures explained in earlier chapter and then the water table is lowered by 100mm from the soil surface. The sand in the soil container will be in a saturated condition as the capillary height of Unimin 7030 is about 100mm.

(ii) The soil container is placed on the vibratory machine and vibrated it for a period of 5 minutes. The top sand layer is sliced deep down (i.e., stress bulb zone) using a thin blade (Figure 6- 2).

(iii) A level soil surface is prepared by gentle compaction using a 2 kg hammer. This pre-compaction is done for all the tests such that uniform conditions would be achieved with respect to density for all the tests.

(iv) This procedure was assumed to eliminate the influence of structure in sand density in the determination of the bearing capacity of sands from model footing tests.

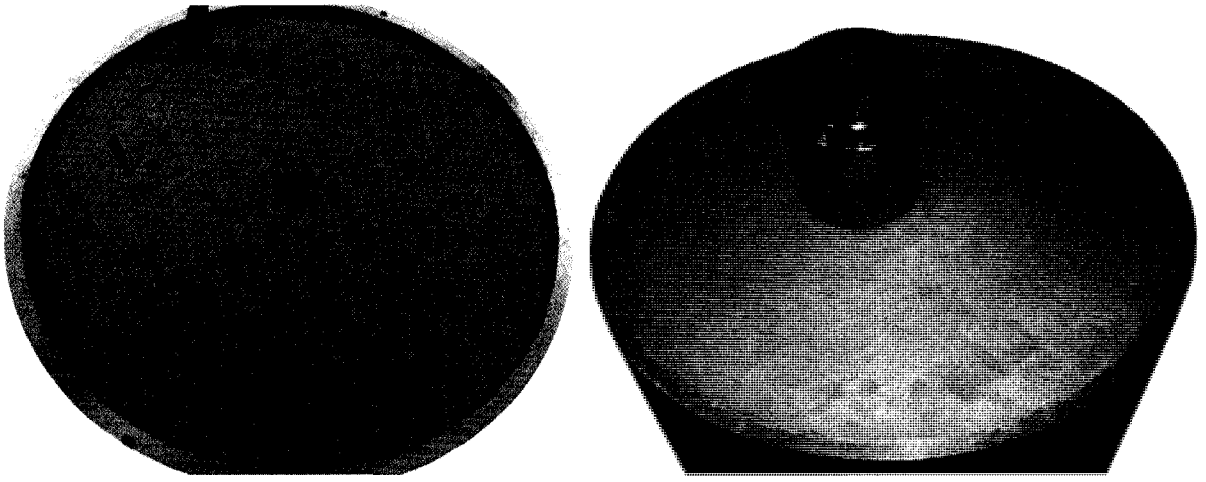

Figure 6- 2 Slice the soil and pre-compaction

In this method, water content is reasonably well controlled through pre-compaction and depth of water table. Due to this reason compaction results is achieved. This method was found to be more suitable using short soil container.

6.2.2.5. Method V: Simple Compaction

The compaction procedures are similar with the method of Vibration in Saturated Condition, but instead of vibration by static impact:

(i) Slice the sand into grid and pre-compact it.

(ii) Saturate the soil and then lower the water table 250mm below the soil surface. According to the author's experience, at this depth of water table, sand on the top layer is in an elastic plastic state, and can stand higher impact without undergoing disturbance.

(iii)Tamp the sand on the surface with 2 kg hummer until the soil surface achieves the same height as the previous test. This ensures that the soil surfaces are in same heights, and sand the sand density will for all the tests will be the same.

This method was used for the tall soil container, because the tall soil container is too heavy to move onto the vibratory machine after each test. This method was found to be an effective compaction method.

6.2.2.6. Compaction of Unimin 2075

Unimin 2075 is manufactured angular sand and is coarser than Unimin 7030. The author has tried to use static impact (Method I) to compact the sand, but the sand was undergoing significant disturbance due to tamping. For this reason, Method IV compaction method was used for these tests (i.e., vibration in saturated Condition) was used for compaction of the Unimin 2075 sand.

6.2.2.7. Compaction of Ottawa Sand

Ottawa silica sand obtained from the St. Peter sandstone is a massive formation from outcrops along the Illinois and the Fox rivers near Ottawa, Illinois. It is clear colorless quartz, pure silicon, with high hardness and rounded grains. Method IV compaction method was used for the compaction of the Ottawa Sand for similar reasons discussed in earlier section. The test results show that vibration compaction (i.e., Method IV) is very effective for Ottawa sand.

6.3. Bearing Capacity

6.3.1. Unimin 2075

The bearing capacity of Unimin 2075 sand using model footings were determined tests varying the depth of water table from the soil surface. The variation of the matric suction with respect to depth below the footing was indirectly estimated using the procedures described in Chapter 5. This technique was used as it is difficult to insert the Tensiometers into the compacted sand for

measuring matric suction due to two reasons. The first reason was associated with the problems of inserting the Tensiometer in compacted Unimin 2075 sand. The second reason was attributed to the shape of the sand particles that were angular and can damage or break the Tensiometer ceramic cup.

The average values of moist density, dry density and void ratio of the tested Unimin 2075 were 19.12kN/m^3, 15.15kN/m^3 and 0.716, respectively. The bearing capacity tests were carried out for four different water table depths (i.e. 0mm (saturated condition), 100mm, 200mm, and 300mm) with a metal footing of 50mm×50mm dimensions. Four duplicate series of tests which equals to a total of 16 tests were conducted. Figure 6- 3 shows the variation of the applied pressure and settlement behavior for one typical series of bearing capacity tests. The other test results are summarized in Appendix A.

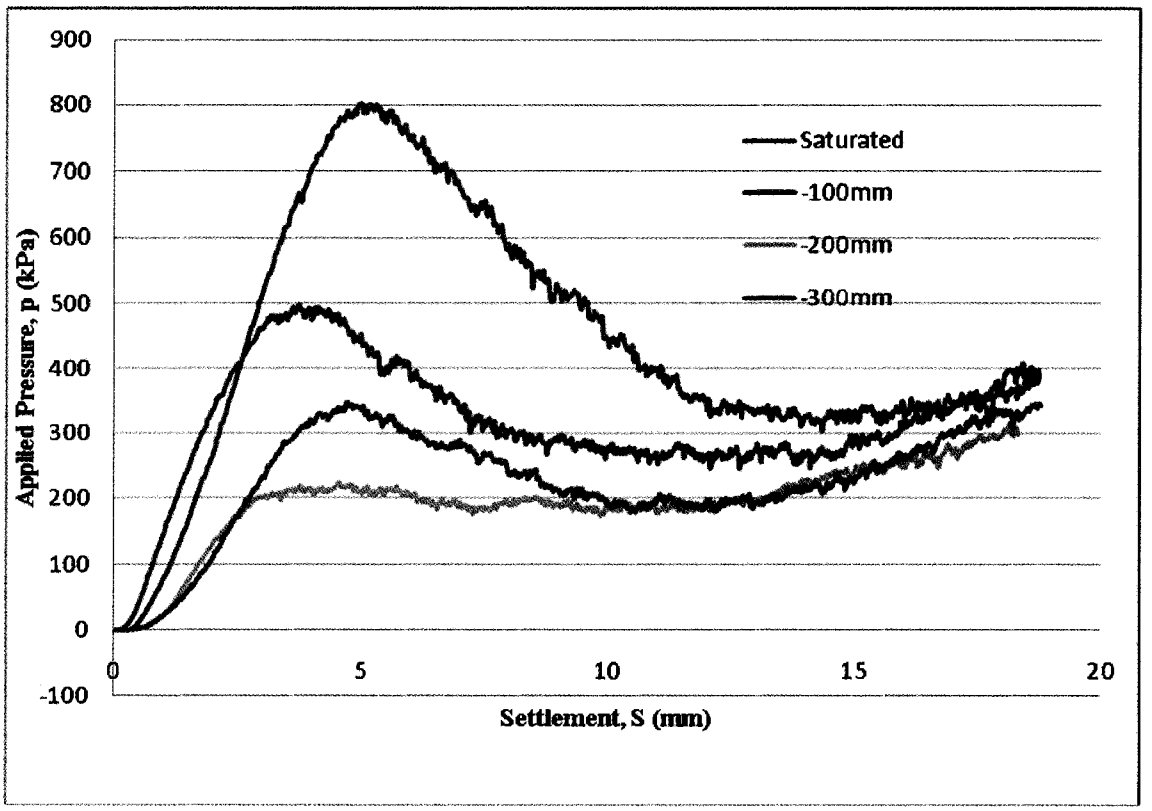

Figure 6- 3 Bearing Capacity Test of Unimin 2075

An expected trend of increase in bearing capacity with an increase in matric suction (i.e., decrease of GWT below the footing) was not observed. However, similar erratic trend was observed for the other series of test results. This characteristic may be attributed to the fact that the matric suction value from the surface to the depth of 50mm is sensitive to the variation of water table, but the variation of suction values deeper than 100mm from the soil surface is relatively small. The variations in measured bearing capacity values in the depth zone of 0 to 100 mm may be attributed to changes in structure or fabric arising due to variations compaction conditions and possible variations in estimated matric suction values. More discussions are offered in the next section about this behavior.

Figure 6- 4 shows the variation of bearing capacity values with respect to matric suction values.

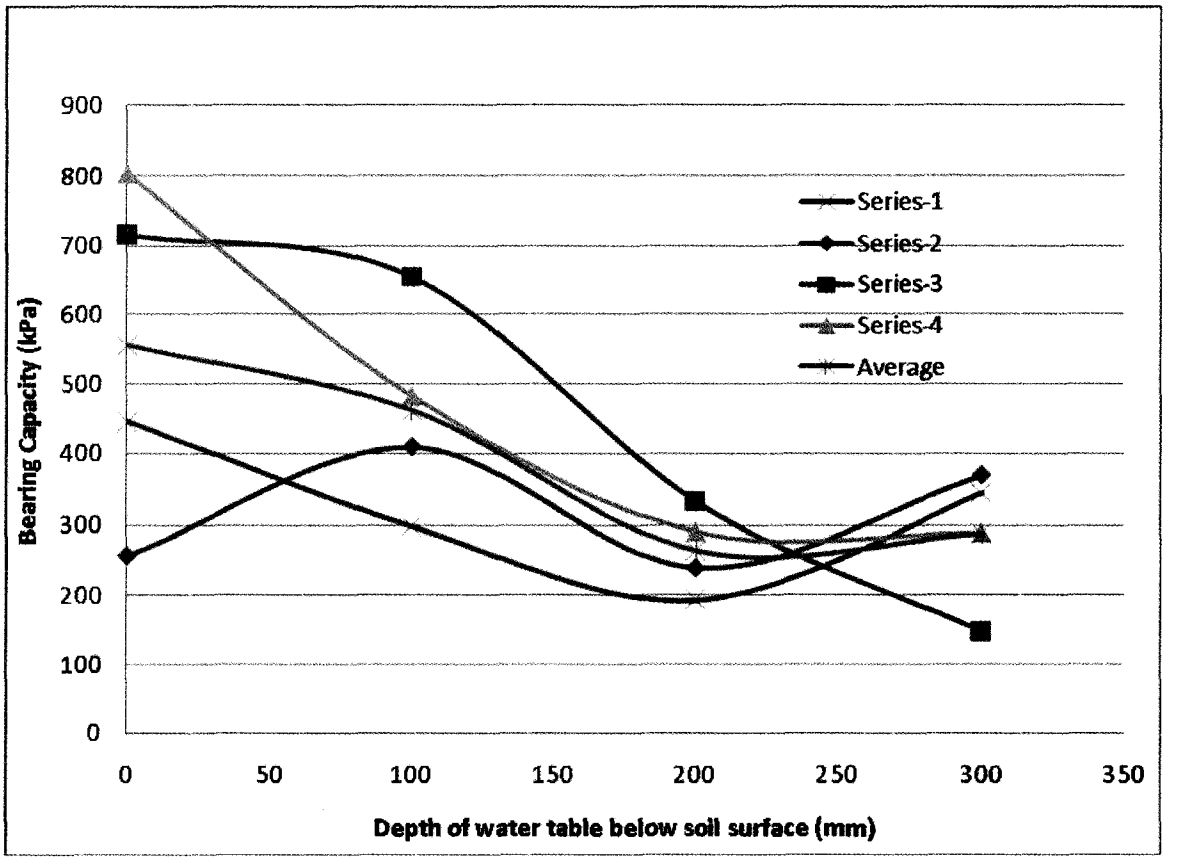

Figure 6- 4 Bearing capacity respect to matric suction

The test results show that bearing capacity decreases with an increasing matric suction values, which is opposite to expected trends of experimental results (Mohamed and Vanapalli, 2006;

Vanapalli et al. 20007). Such a behavior in the present results may be attributed to the difficulties in controlling compacting energy while performing the tests due to the characteristics of the sand used in the present study. In other words, unlike natural sands, Unimin 2075 is too sensitive to compaction energy influencing the density (i.e. void ratio) and soil structure or fabric. In addition, it should also be noted that small variations in environmental conditions also can influence matric suction values. Therefore, it appears that the technique used for estimation of matric suction may not be reliable for the present testing program results

Figure 6- 5 shows bulging failure behavior for Unimin 2075. The diameter of bulged zone for the model footing of 50mm×50mm was in the range of 150mm ~ 200mm, which is less than the diameter of the test container (i.e. 300mm). This implies that boundary conditions have not influenced the model footing failure behavior.

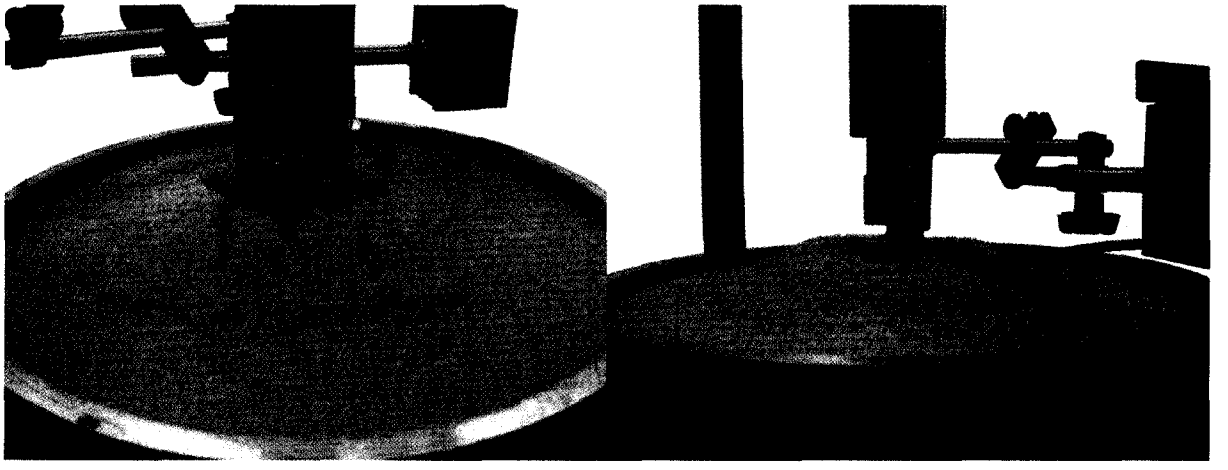

Figure 6- 5 Failure Bulging Shape of Unimin 2075

6.3.2. Ottawa Sand

Three different series of tests which include 35 bearing capacity tests were conducted on Ottawa sand using a model footing of 50mm×50mm. Two Tensiometers were installed separately at the depth of 20mm and 55mm below the soil surface. The average reading of two Tensiometers with in stress bulb zone was used as a representative matric suction value for interpreting the test

results. The relationship between the applied pressure versus settlement for all the other series of tests are presented in Appendix A.

For the first series of tests, the soil specimens were allowed to reach equilibrium conditions over a long period of time (i.e. 20 hours) after lowering the water table to the desired height. A total of 17 tests were carried out and the test results are shown in Figure 6- 6. The bearing capacity decreases with increasing matric suction values. The unexpected trends of results can be attributed to the reason that the matric suction is very sensitive to evaporation of moisture near the soil surface. Although the vertical distance between two Tensiometers is only 35mm (one is installed 20mm below the soil surface and the other is installed 55mm below the soil surface), the difference in matric suction values between the two depths were as much as 10 kPa. The experimental results have shown that the difference in matric suction values becomes larger with increasing the equilibrium periods. In addition, the matric suction profile near the soil surface is generally nonlinear in nature. Hence, using an average reading of two Tensiometers may not well represent the actual matric suction value within stress bulb under the model footing.

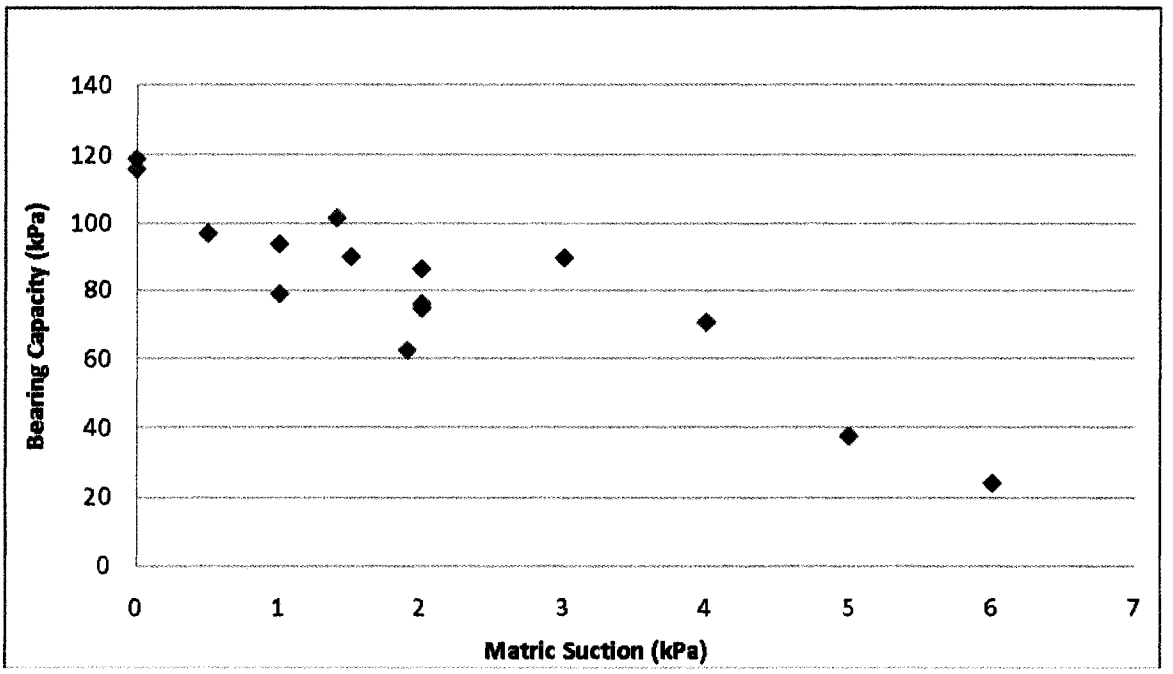

Figure 6- 6 Relationship of bearing capacity versus matric suction for long equilibrium period

For the second series of tests, relatively short equilibrium period (i.e. 1 hour) was used. This procedure was used to eliminate the influence of evaporation on the matric suction values. No

Tensiometers were used for this series of tests since the variation of matric suction values within this depth zone was too small to be measured using Tensiometers. Hence, the remaining 13 tests were conducted varying matric suction values by changing the depth of water table below the model footing. The test results are shown in Figure 6- 7. The variation of bearing capacity versus depth of water table demonstrates an interesting step wise decrease. When the depth of water table is equal to or less than 150 mm, the bearing capacity values fall on the first step (Figure 6- 7). The average bearing capacity value on this step is equal to 120 kPa and represents the saturated zone. This behavior can be explained with the capillary height of Ottawa sand which is 140 mm (measured from suction profile set described in Chapter 5), when the depth of water table is lower than 150 mm. The stress bulb under footing is in saturated condition. In other words, the bearing capacity values in this step are approximately the same as that of saturated condition.

When the depth of water table is deeper than 200 mm, the bearing capacity falls on the second step, which can refer to as the first unsaturated step with average bearing capacity value of 90 kPa. This is because when the depth of water table is 200 mm below the soil surface, the capillary rise height is 60 mm below the soil surface. Therefore, the soil in stress bulb under footing is in a state of unsaturated condition. In addition, the matric suction distribution profile of Ottawa sand deeper than 90 mm shows that the depth of water table has negligible influence on the matric suction value for short equilibrium time. This characteristic behavior resulted in approximately the same bearing capacity values for the tests conducted with the depth of water table between 90 and 350 mm. The bearing capacity values further decreases as the water table becomes deeper than 350 mm below the soil surface.

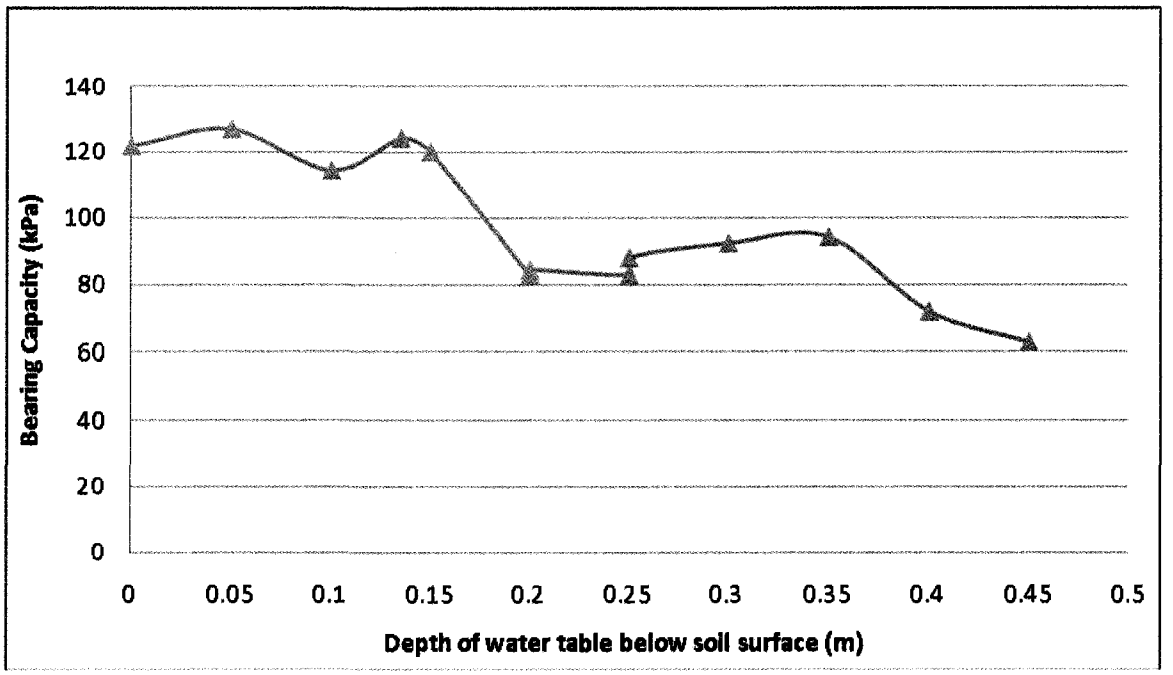

Figure 6- 7 Relationship of bearing capacity versus depth of water table for short equilibrium period

For the third series test, a total of seven tests were conducted under three different conditions; i) saturated condition (water table is at surface of the soil; 1 test), ii) submerged condition (water table is 5mm above the surface of the soil; 2 tests), and iii) high suction condition (almost dry sand, with very little moisture; 4 tests). The test results are shown in Figure 6- 8. The bearing capacity values obtained under saturated condition showed the highest value compared to the results obtained for other soil materials under the same condition. The bearing capacity continuously decreases beyond saturated condition and eventually reaches the values which may be approximated to be the same as that of submerged condition. The results also demonstrate that the lowest bearing capacity value for Ottawa sand can be obtained in either submerged or dry condition. This is because there is no apparent cohesion between sand particles for both dry and submerged condition. In other words, sand moisture is the key factor contributing to the differences in the measured bearing capacity values. It should also be noted that matric suction value has no effect on the tests results for both dry and submerged condition. It is also interesting to note that the difference in the height of water table between the saturated and submerged condition was only 5mm, but the difference of the bearing capacity values are significantly high (i.e. the highest and lowest bearing capacity values). It is difficult to explain this phenomenon with the theory of effective stress since the difference of water height is so

small but the influence on the results are substantial. Hence, the more detailed and controlled studies are required to explain the bearing capacity behavior of sands. It is also suggested that sand microstructure and interaction between water molecules and sand particles are studies for offering better explanations with respect to the observed model footing behavior.

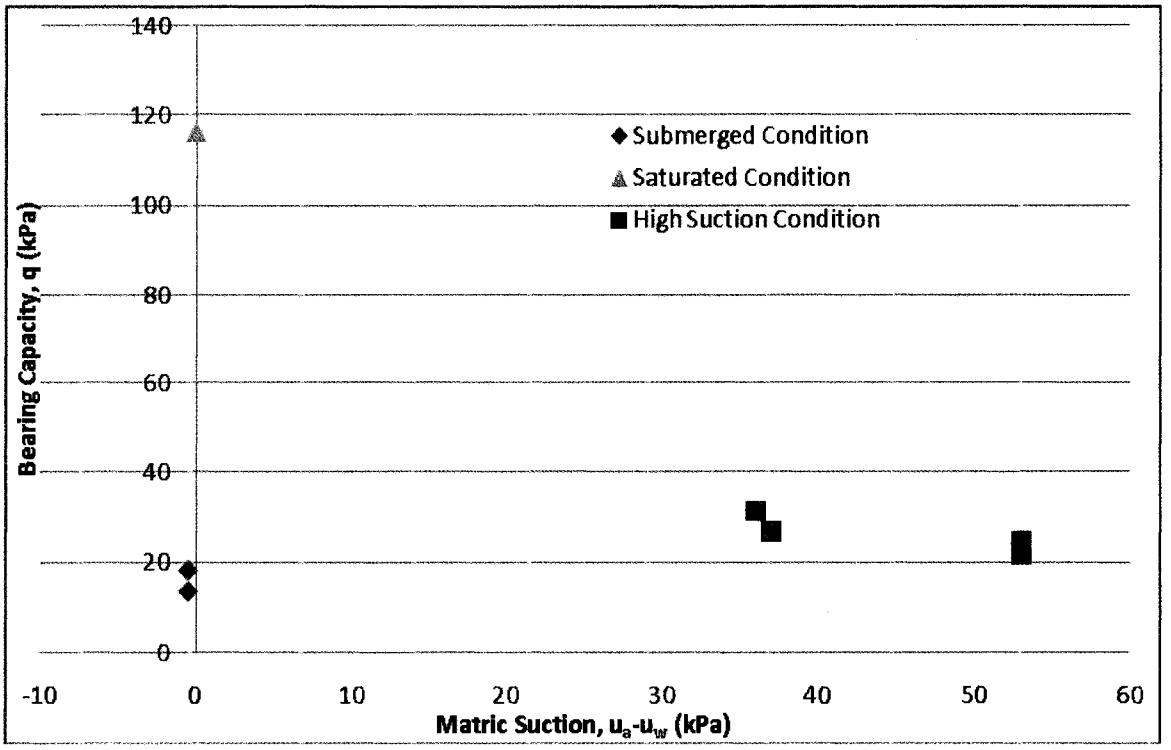

Figure 6- 8 Bearing capacities in submerged and dry condition

The decrease in bearing capacity of Ottawa sand with increasing matric suction can be explained with additional simple test (Figure 6- 9). From Figure 6- 9a, it can be seen that that compacted saturated Ottawa sand can stand by itself without collapse after sample ring is taken away, which demonstrates apparent cohesion between wet sand particles (with low matric suction). However, the compacted dry Ottawa sand collapses into a flat cone pile immediately after removing the sample ring. This behavior demonstrates that there was no apparent cohesion was observed between relatively between dry sand particles (Figure 6- 9b).

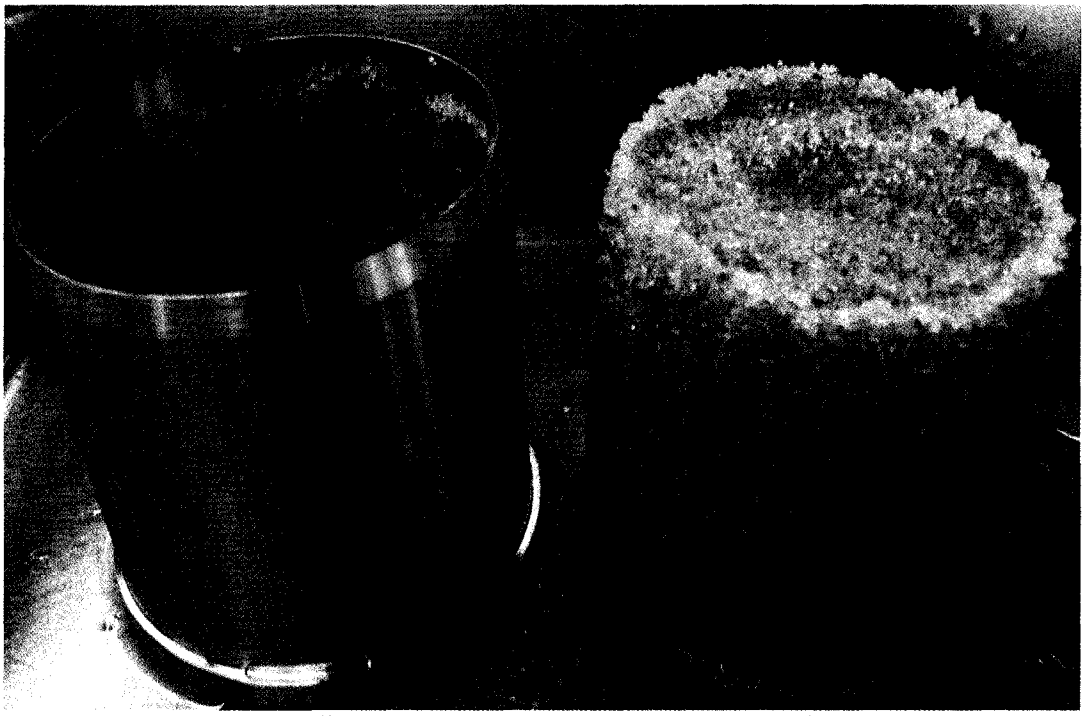

a. Self-standing Column of Saturated Ottawa Sand

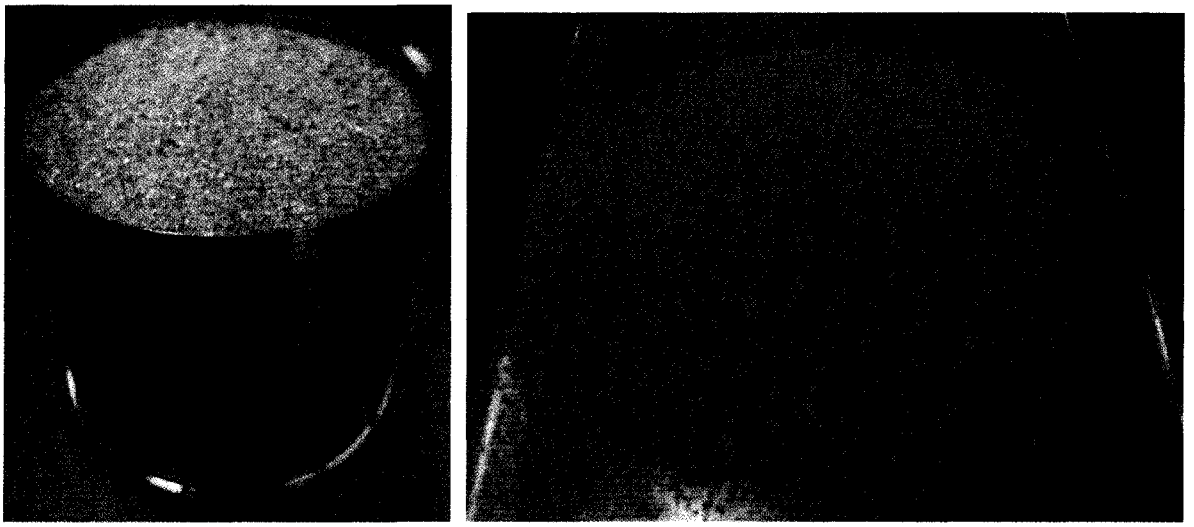

b. Collapse of dry Ottawa sand without sampling ring

Figure 6- 9 Comparison of cohesiveness of saturated and dry Ottawa sand

The matric suction value in the sand likely can increase within stress bulb during the period of conducting bearing capacity test due to dilation. Experimental evidence was obtained for demonstrating this behavior. Two Tensiometers were installed within the stress bulb under the model footing while during loading under saturated condition. The variation of matric suction change within stress bulb was monitored during the period of conducting bearing capacity test.

An average increase in matric suction from the beginning of the test to the failure was measured to be equal to 1 kPa from two different tests conducted.

The dilatancy of sand during bearing capacity test can also be illustrated using Figure 6- 10. Before the bearing capacity test, there is visible water on the surface of Ottawa sand. However, there no water visible on the soil surface and in the indentation left behind after the test. During the bearing capacity test, the sand dilates and void ratio of sand increases. Therefore, more water is needed to fill the voids, which causes the water on soil surface to be imbibed into the sand. This process contributes towards matric suction development during bearing capacity tests.

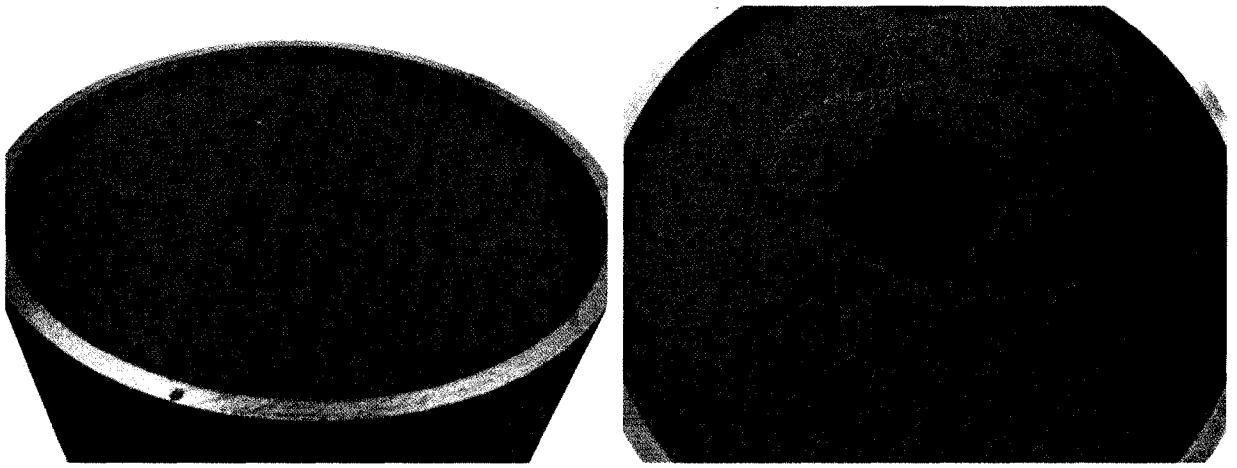

Figure 6- 10 The photos of saturated Ottawa sand before and after bearing capacity test

6.3.3. Unimin 7030

A total of 139 bearing capacity tests were conducted to study the influence of compaction method and footing size on the bearing capacity using Unimin 7030. The measured dry density values from the short and the tall container were 14.9 kN/m^3 and 14.7 kN/m^3, respectively. The details of the tests are summarized in Table 6- 1.

Table 6- 1 Combination of footing size and matric suction for bearing test of Unimin 7030

	Footing Size	Matric suction (kPa)									
Short Soil Container	20mm×20mm	Saturated	2	4	6						
	25mm×25mm	Saturated	2	4	6	8					
	37.5mm×37.5mm	Saturated	2	4	6						
	50mm×50mm	Saturated	2	4	6	8					
Tall Soil Container	20mm×20mm	Saturated	2	4	6	8	10	12	14	18	
	25mm×25mm	Saturated	2	4	6	8	10	12	14	18	Dry
	37.5mm×37.5mm	Saturated	2	4	6	8	10	12			Dry
	50mm×50mm	Saturated	2	4	6	8	10	12			

The matric suction values in the soil container were controlled by adjusting the water head and monitored using Tensiometer when the matric suction reaches equilibrium condition.

The compacted soil in the container was first saturated by controlling the water head until the water table reaches the soil surface. The tests in saturated condition were conducted when the equilibrium conditions were achieved 24 hours after the saturation process was initiated. The bearing capacity of the saturated sand was measured by loading the model footing until its failure. All Tensiometers indicated zero matric suction values both after saturation and during the testing period.

For the tests in unsaturated conditions, the water table in the soil was lowered to different levels of depth to achieve targeted matric suction values by adjusting water head in the water container after the soil was fully saturated by following the procedures described earlier. The average matric suction values within the stress bulb corresponding to the water table depths of 240, 440 and 640mm were 2, 4 and 6 kPa, respectively. To obtain the matric suction of 8 kPa and higher, the water table in the container was lowered beneath the bottom of soil by lowering the water head in the water container below the bottom of the soil container and let the water drain out freely. The value between the water container and soil container was then closed once the matric suction reading the on tensiometer reached the expected value. Equilibrium conditions with respect to matric suction values of 2 kPa, 4 kPa, and 6 kPa in the stress bulb zone (i.e., depth of 1.5B) were typically achieved in a time period of 24 hours. However, more time was needed for

the matric suction of 8 kPa and higher (i.e. one to three days). When the matric suction value of the soil the container reached equilibrium conditions around 7 hours after the expected matric suction values were obtained, bearing capacity tests were conducted on the model footings.

Figure 6- 11 and 6- 12 show the applied pressure versus settlement behaviors obtained from the bearing capacity tests performed in the short container with the model footing of 25mm × 25mm and in the tall container with the model footing of 50mm × 50mm, respectively. The applied pressure versus settlement behaviors of other footings are presented in Appendix A.

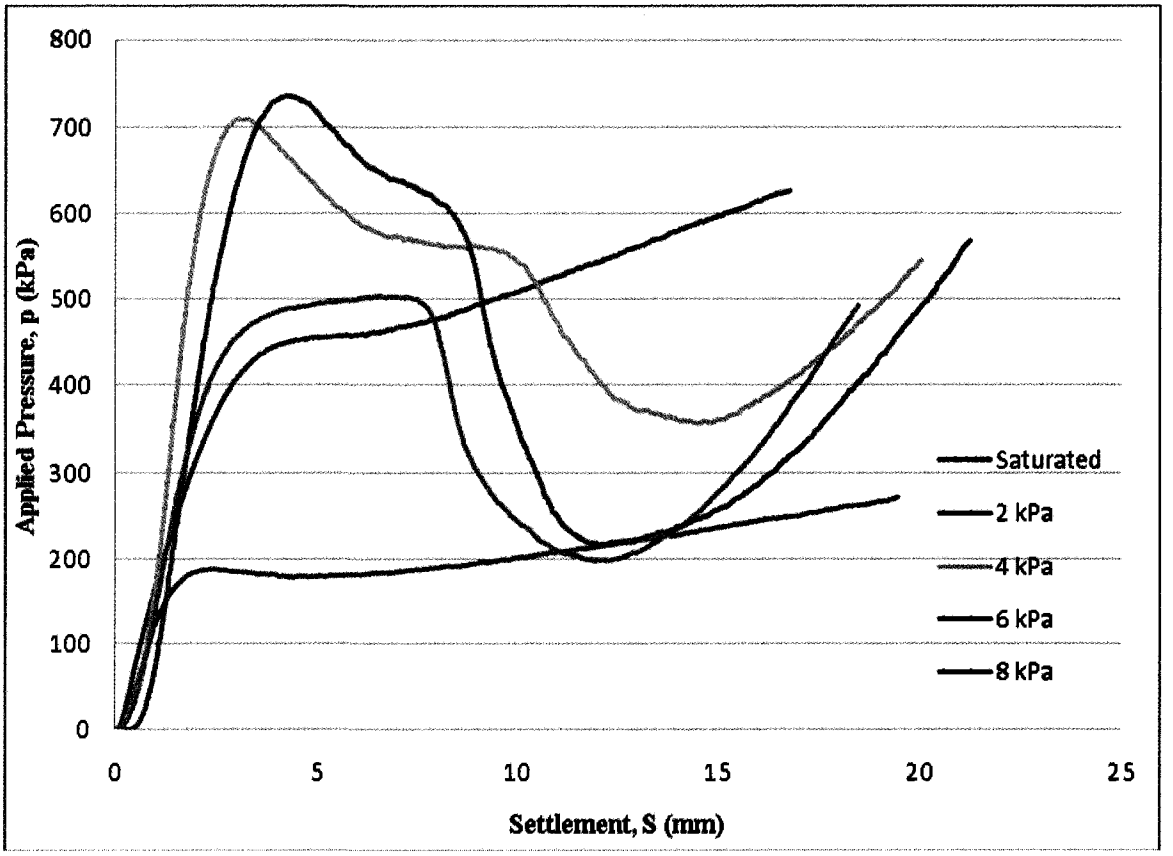

Figure 6- 11 Pressure versus settlement for footing of 25 mm × 25 mm in short soil container

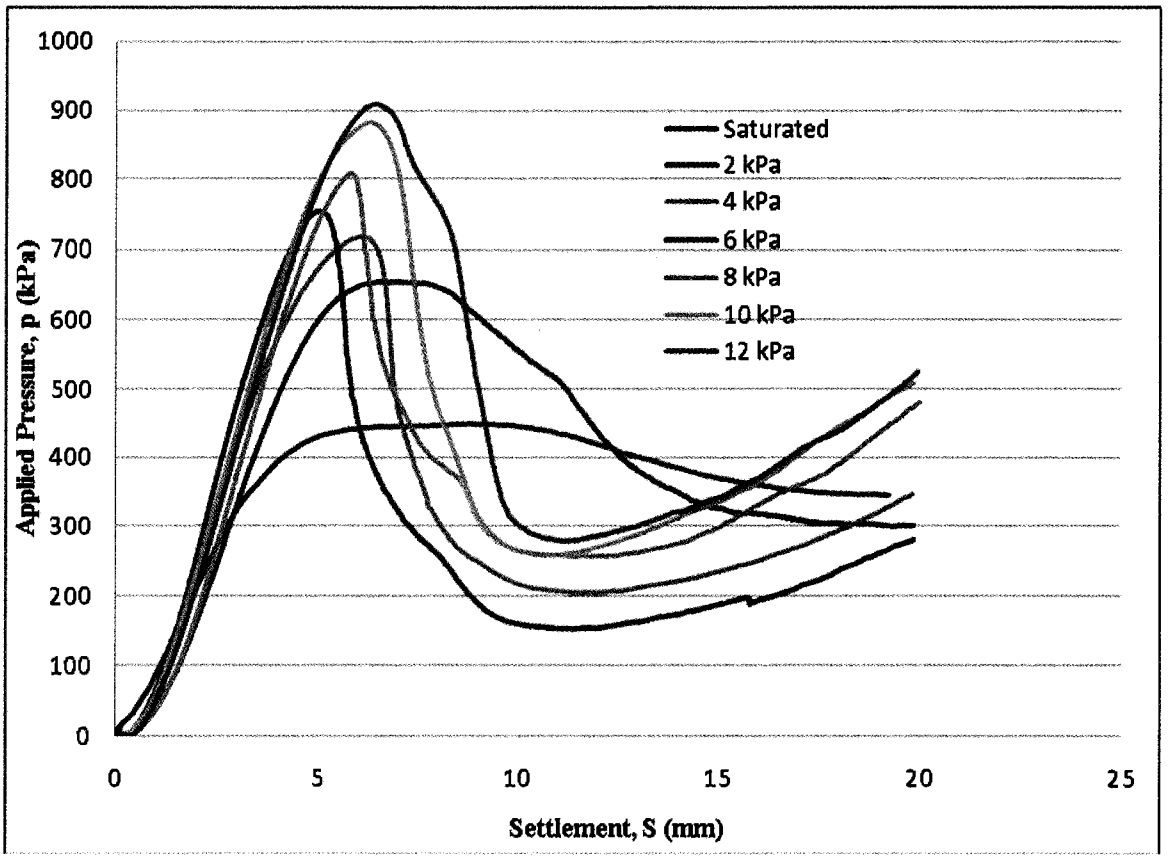

Figure 6- 12 Pressure versus settlement for footing of 50 mm × 50 mm in tall soil container

From the test results, two different modes failure, namely; local shear failure and general shear failure were observed. Local shear failure was observed when the tested sand was in a saturated condition and when the matric suction values below the footings were low (i.e., 2 kPa for short soil container, and 2 kPa, 4 kPa and some 6 kPa for tall soil container). On the other hand, general shear failure was observed when matric suction values were higher. Therefore, in the present study the ultimate bearing capacity was defined as the peak pressure for general shear failure and the inflexion point of pressure as local shear failure.

The variation of the bearing capacity with respect to different matric suction values for four model footings in short and tall container are respectively shown in Figure 6- 13 and Figure 6- 14,. The results demonstrate that there is a significant increase in the bearing capacity due to the contribution of matric suction in the range 0 to 6 kPa. For the matric suction values higher than 8 kPa, the bearing capacity increases in the tall soil container but decreases in the short soil

container. In other words, the matric suction has a little contribution to bearing capacity of Unimin 7030 when the matric suction is higher than 8 kPa.

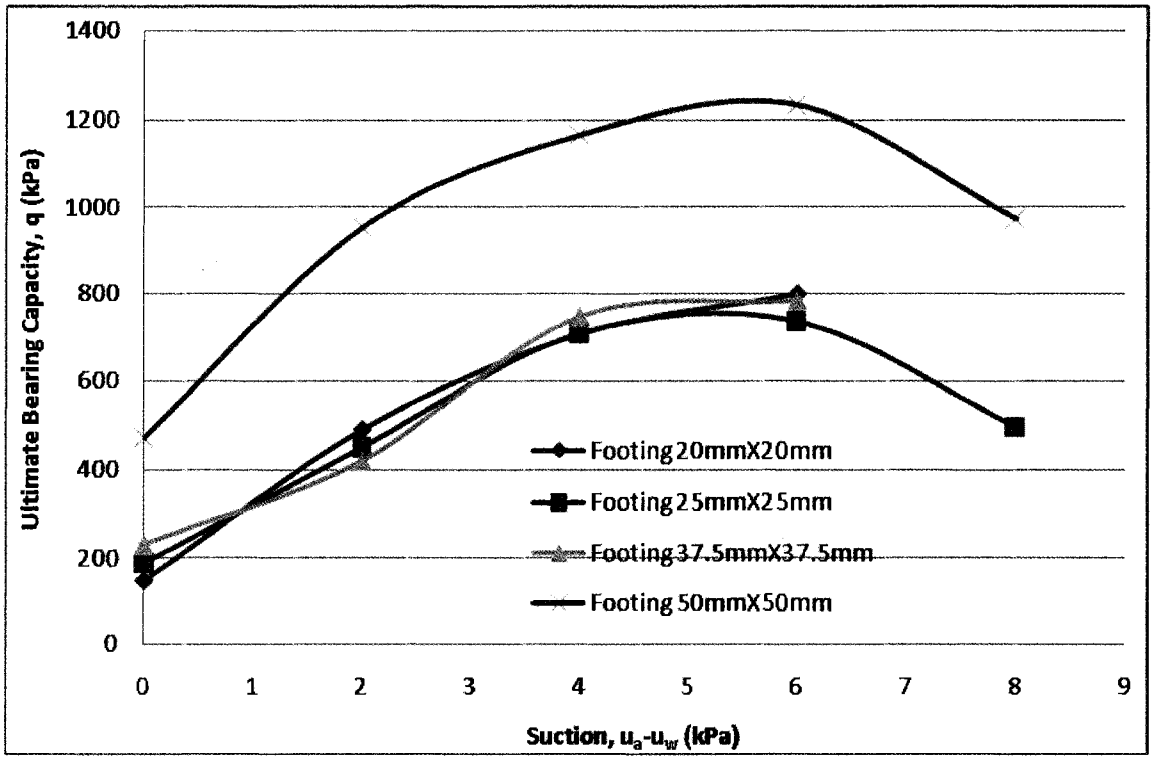

Figure 6- 13 Relationship of bearing capacity versus matric suction for short soil container

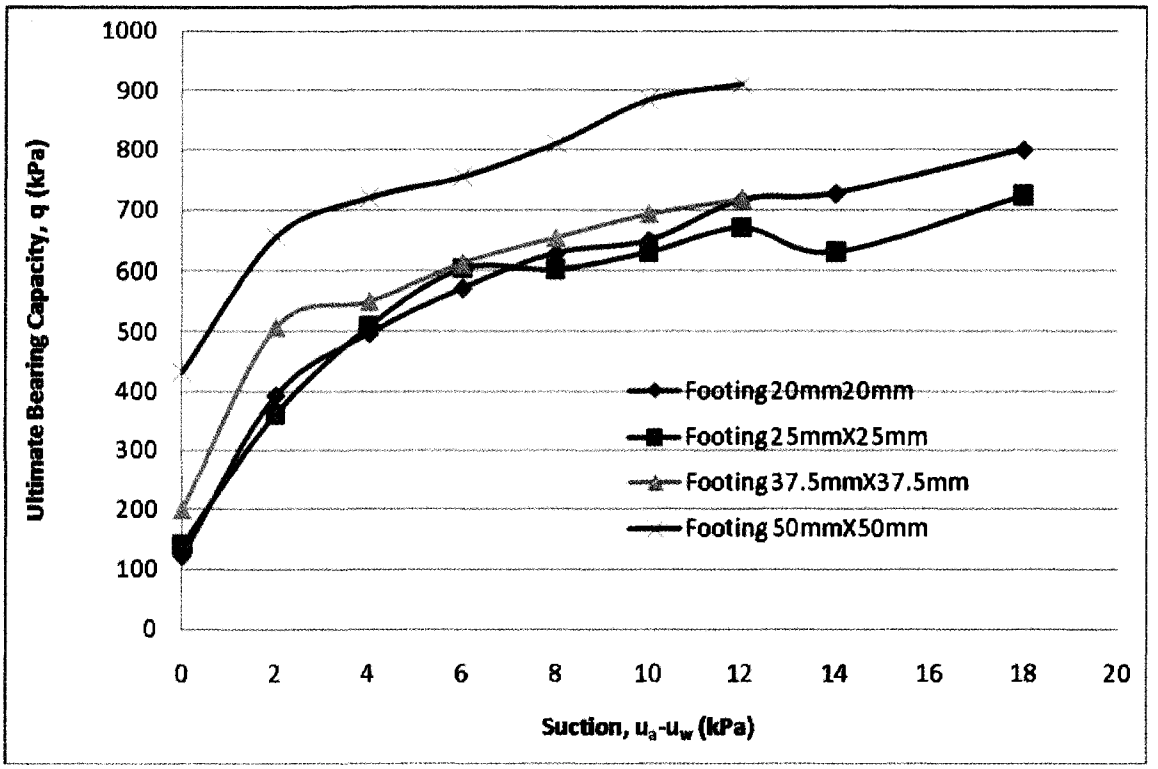

Figure 6- 14 Relationship of bearing capacity versus matric suction for tall soil container

The bearing capacity values for the model footings of 20mm×20mm, 25mm×25mm, and 37.5mm×37.5mm are approximately the same regardless of the matric suction values under similar conditions. However, the bearing capacity values for the model footings of 50mm×50mm show higher values compared to the results for smaller footings. Hence, it is postulated that the size of footing has no influence on the bearing capacity for Unimin 7030 in the present study. The test results however suggest that the boundary condition (the ratio of footing size to the diameter of container) has influence on the measured bearing capacity values.

Mohamed (2006) performed bearing capacity tests with different sizes of model footing (i.e. 100mm×100mm and 150mm×150mm) in the same soil and showed that the bearing capacity values were approximately the same as shown in Figure 6- 15.

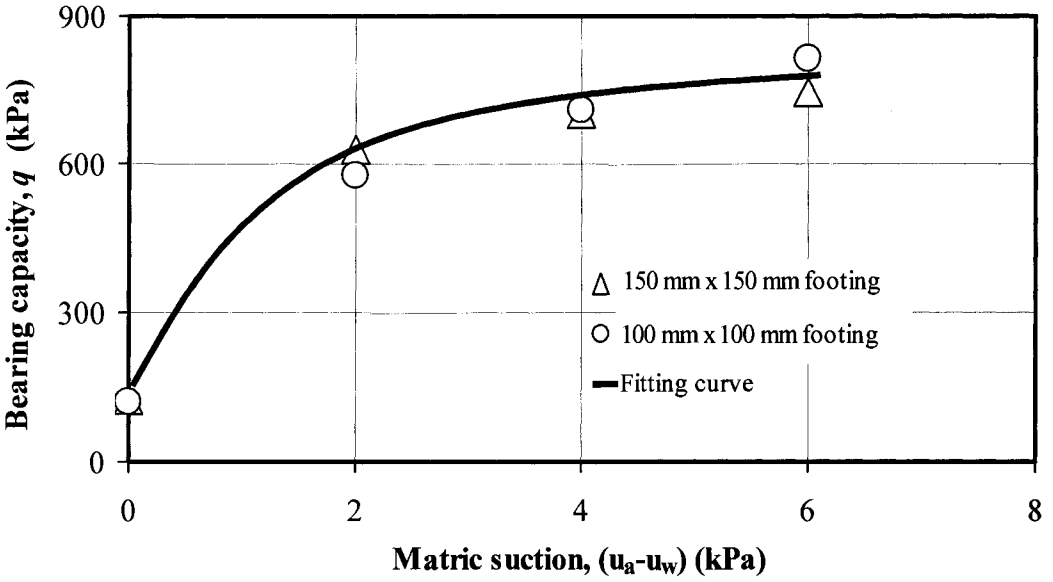

Figure 6- 15 Bearing capacity versus matric suction for two model footings (Mohamed, 2006)

Figure 6- 16 shows a shape of failure surface due to bearing capacity test for the model footing of 50mm×50mm. It can be clearly seen that the failure surface extends to the wall of soil container, which implies that the bearing capacity values for the model footing of 50mm×50mm were overestimated due to the influence of boundary conditions.

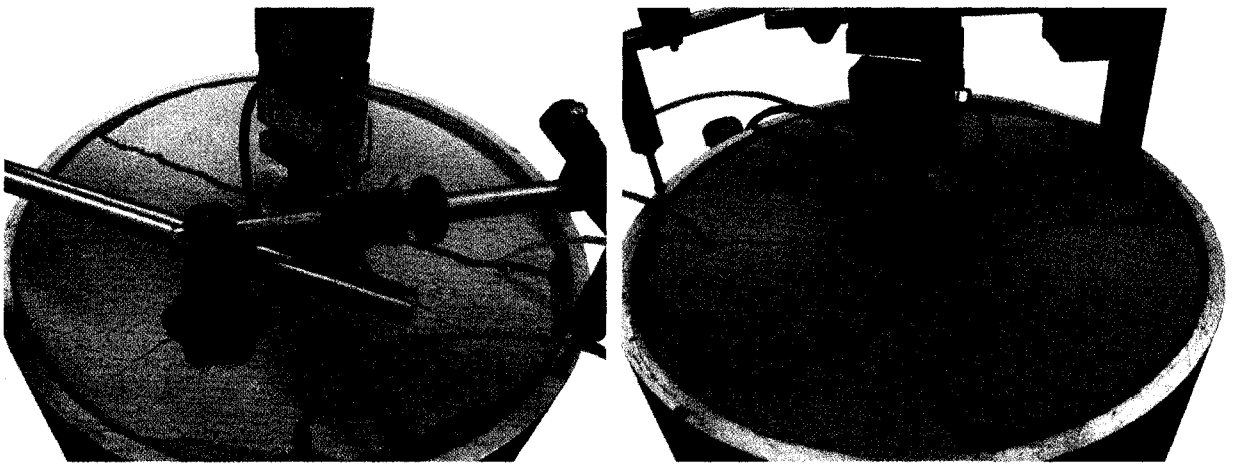

Figure 6- 16 Photo of failure surface and slip movement of footing 50mm×50mm

CHAPTER 7

CONCLUSIONS AND RECOMMENDATIONS

7.1. Summary

The bearing capacity of saturated and unsaturated sands were determined under a controlled laboratory environment on three different compacted sands using four different sizes of square model footings (i.e. 20 mm × 20 mm, 25 mm × 25 mm, 37.5 mm × 37.5 mm, and 50 mm × 50 mm). The research tests were conducted in specially designed equipment which includes two test systems (short container with 300 mm in diameter and 300 mm in height and the tall container with 300 mm in diameter and 700 mm in height) were used in the study. All the equipment was designed by the author and fabricated in the student workshop at University of Ottawa. Using these equipments, the bearing capacity of model footings was determined over a matric suction range of 0 to 12 kPa. This range of suction for the three sands studied extends over the boundary effect, transition and residual stages (Vanapalli et al. 1996) for the three different sands studied in the present research program.

The load carrying capacity of model footings on silica sand (i.e., Sil-co-sil) under different vibration loadings in both saturated and unsaturated conditions were also studied. In addition, different compaction techniques were used to study how bearing capacity behavior will be influenced both under saturated and unsaturated conditions.

Several conclusions were drawn from the present study are summarized in this chapter. Some recommendations are also provided for future research to better understand the bearing capacity behavior of unsaturated soils.

7.2. Sand Compaction

(i) In general, it was difficult to achieve "identical" initial testing conditions for determining the bearing capacity of sands. The bearing capacity values were found to be very sensitive to density and soil structure or soil fabric.

(ii) The vibration compaction was found to be the best compaction method for the tested sandy soils of all the different compaction methods used. Reasonably identical conditions with respect to density and soil structure or fabric were achieved using this method in comparison to other methods.

(iii)The maximum density that can be achieved for sand is by subjected it to vibration for a long period of time. This technique initiates collapse followed with more effective compaction. During this process, some water also drains out from the sand.

(iv)Fine grain sand (i.e., the tested Sil-Co-Sil 106) collapse can initiate (or be triggered) under vibration in loose condition when the initial water content is greater than 19%. This water content is referred as "critical" water content in the present research work.

(v) Once collapse initiates in some pockets of the loose fine-sand (with relatively high degree of saturation), it proliferates to other regions in spite of low initial water content (i.e., 13%).

(vi) Matric suction in fine-grained compacted sand is very sensitive and decreases significantly when subjected to vibration.

7.3. Sand Strength and Bearing Capacity

(i) The degree of saturation or matric suction has no effect on the sand friction angle, ϕ.; however, apparent cohesion, c, is significantly influenced by both these parameters.

(ii) The bearing capacity test increases during the loading of the model footing due to dilation of sand. The matric suction in stress bulb increases due to dilation and contributes towards increase in the bearing capacity.

(iii)The footing size (i.e., 20mm×20mm; 25mm×25mm; 37.5 mm×37.5) appears to have little influence on the measured bearing capacity of the sand.

(iv)The boundary condition (ratio of soil container size to footing size) does have some effect on the bearing capacity of three compacted sands studied in this research program.

(v) Saturated compacted fine-grain silty sand (Sil-Co-Sil 106) has strong resistance to the static load conditons, but has little bearing capacity under cyclic loading conditions (under the impact of vibration)

7.4. Recommendations for further study

(i) The variation of bearing capacity with respect to matric suction in some of the test instead of showing increasing trend has shown erratic trends. These results demonstrate that the bearing capacity of sands is sensitive to density and soil fabric or soil structure. Therefore, model studies should be conducted carefully to obtain results with repeatability.

(ii) More studies are necessary to understand the influence of soil structure or soil fabric on the bearing capacity of saturated and unsaturated sands.

REFERENCE

Alonso, E. E., Gens, A., and Josa, A. (1990). A constitutive model for partly saturated soils. *Geotechnique*, 40(3):405-430.

ASTM Standards (1997). ASTM Designation: D653-97.Standard terminology relating to soil, rock and containing fluids.

Barbour, S. L., and Fredlund, D. G. (1989). Physico-chemical state variables for clay soils. *Proc., XII Int. Conf. on Soil Mechanics and Foundation Engineering, Invited Lecture,* Rio de Janeiro, Brazil, 1839-1843.

Bera, Ashis Kumar; Ghosh, Ambarish, and Ghosh, Amalendu. (2007). Behaviour of model footing on pond ash. *Geotech Geol Eng*, 25:315-325

Bishop, A. W. (1959). The principle of effective stress. Teknisk Ukeblad, 106(39):859-863.

Bishop, A. W., Alphan, I., Blight, G. E., and Donald, I. B. (1960). Factors controlling the shear strength of partly saturated cohesive soils. *ASCE Research Conf. on Shear Strength of Cohesive Soils,* Univ. of Colorado, Boulder, Colo., 503-532.

Bishop, A. W., and Blight, G. E. (1963). Some aspects of effective stress in saturated and unsaturated soils. *Geotechnique*, 13(3):177-197.

Blatz, J. A., and Graham, J. (2003). Elastic-plastic modeling of unsaturated soil using results from a new triaxial test with controlled suction. *Geotechnique*, 53(1):113-122.

Broms B. B. (1963). The Effect of Degree of Saturation on the Bearing Capacity of Flexible Pavements, *Highway Research Record*, 71:1-14

Broms, B. B., (1964). The Effect of Degree of Saturation on the Bearing Capacity of Flexible Pavements. *Highway Research Recoed*, No. 71:1-14.

Cerato, A. B., and Lutenegger, A. J. (2006). Bearing Capacity of Square and Circular Footings on a Finite Layer of Granular Soil Underlain by a Rigid Base. *Journal of Geotechnical and Geoenvironmental Engineering*, 132(11):1496-1501.

Costa, Y.D, Cintra J. C. And Zornberg J. G. (2003). Influence of matric suction on the results of plate load tests performed on a lateritic soil deposit. *Geotechnical Testing Journal*, Vol. 26, No. 2: 219 – 226.

Craig, R. F. (1997). Soil mechanics. E & FN Spon. London.

Croney, D., Coleman, J. D., and Black, W. P. M. (1958). Movement and distribution of water in soil in relation to highway design and performance. *Water and Its Conduction in Soils Special Rep. No. 40, Highway Research Board,* Washington, D.C., 226-252.

Das, Braja M. (1997). Advanced Soil Mechanics. Taylor & Francis Group. Washington.

Das, Braja M. (2004). Principle of Foundation Engineering, 5ed. Thomson Learing. USA.

Derjaguin, B. V., and Churaev, N. V. (1981). Structure of the boundary layers of liquids and its influence on the mass transfer in fine pores. *Progress in surface and membrane science,* D. A. Cadenhead and J. F. Danielli, eds., Academic, New York, 69-130.

Donald, I. B. (1956). Shear strength measurements in unsaturated non-cohesive soils with negative pore pressures. *Proc., 2nd Australia–New Zealand Conf. on Soil Mechanics and Foundation Engineering*, Christchurch, New Zealand, 200-205.

Fredlund, D. G. and Morgenstern, N. R. (1977). Stress state variables for unsaturated soils. *Journal of the Geotechnical and Engineering Division*, ASCE, 103(GT5):447-466.

Fredlund, D. G. and Morgenstern, N. R. And Widger, R. A. (1978). Shear strength of unsaturated soils. *Canadian Geotechnical Journal,* Vol. 15 (3):313-321.

Fredlund, D. G. and Rahardjo, H. (1993). Soil Mechanics for Unsaturated Soils, 1st Ed. Wiley, New York

Fredlund, D. G., and Morgenstern, N. R. (1976). Constitutive relations for volume change in unsaturated soils. *Can. Geotech. J.*, 13(3):261-276.

Fredlund, D.G., Morgenstern, N.R., and Widger, R.A. 1978. The shear strength of unsaturated soils. *Canadian Geotechnical Journal*, 15(3): 313-321.

Fredlund, Delwyn G. (2006). Unsaturated Soil Mechanics in Engineering Practice. *Journal of Geotechnical and Geoenvironmental Engineering*, 132(3): 286-321.

Fredlund, M. D., Stianson, J., and Rykaart, M., (2002a). Application of automatic mesh refinement in the SVFlux and ChemFlux software packages. Proc., *55th Canadian Geotechnical Conf.*, Niagara Falls, Ont., Canada, 25-32.

Fredlund, M. D., Wilson, G. W., and Fredlund, D. G. (2002c). Use of grain-size distribution for the estimation of the soil-water characteristic curve. *Can. Geotech. J.*, 39(5):1103-1117.

Fredlund, M. D., Wilson, G. W., and Fredlund, D. G., (2002b). Representation and estimation of the shrinkage curve. *Proc., 3rd Int. Conf. on Unsaturated Soils, UNSAT 2002*, Recife, Brazil, 145–149.

Gallipoli, D., Gens, A., Sharma, R., and Vaunat, J. (2003). An elastoplastic model for unsaturated soil incorporating the effects of suction and degree of saturation on mechanical behaviour." Geotechnique, 53(1):123-135.

Gan, J. K.-M., and Fredlund, D. G. (1996). Shear strength characteristics of two saprolitic soils. *Can. Geotech. J.*, 33(4):595-609.

Gan, J. K.-M., Fredlund, D. G., and Rahardjo, H. (1988). Determination of the shear strength parameters of an unsaturated soil using the direct shear test. *Can. Geotech. J.*, 25(8):500-510.

Garven, E. and Vanapalli, S.K. 2006. Evaluation of empirical procedures for predicting the shear strength of unsaturated soils. Proc. 4th Int. Conf. on Unsaturated Soils, Carefree (Arizona), ASCE Geotechnical Special Publication, 147(2), 2570–2581

Jommi, C. (2000). Remarks on the constitutive modeling of unsaturated soils. *Experimental evidence and theoretical approaches in unsaturated soils*, A. Tarantino and C. Mancuso, eds., Balkema, Rotterdam, The Netherlands, 139-153.

Lim, P. C., Barbour, S. L., and Fredlund, D. G. (1998). The influence of the degree of saturation on the coefficient of aqueous diffusion. Can. Geotech. J., 35(5), 811-827.

Lyklema, J. (2000). Fundamental of interface and colloid science, Vol. III, Academic, New York.

Matsumoto, M., and Kataoka, Y. (1988). Study on liquid-vapour interface of water. I. Simulational results of thermodynamic properties and orientational structure. J. Chem. Phys., 88(5):3233-3245.

Melinda, F., Rahardjo, H., Han, K. K., and Leong, E. C. (2004). Shear strength of compacted soil under infiltration condition. *J. Geotech. Geoenviron. Eng.*, 130(8):807-817.

Meyerhof, G. G. (1956). Penetration tests and bearing capacity of cohesionless soils. *Journal of the Soil Mechanics and Foundations Division*, ASCE, Vol. 82, No. (SM1): Paper: 866.

Meyerhof, G. G. (1951). The ultimate bearing capacity of foundations. Geotechnique, Vol. 2: 301-332.

Mitchell, J. K (1993). *Fundamentals of soil behavior*, John Wiley & Sons.

Mohamed, Fathi M. O., (2006). A Semi-Empirical Approach For the Interpretation of The Bearing Capacity of Unsaturated Soils. M.A.Sc Thesis, Univ. of Ottawa, Ottawa, On., Canada.

Newman, G. P. (1996). Heat and mass transfer in unsaturated soils during freezing. MSc thesis, Univ. of Saskatchewan, Saskatoon, Sask., Canada.

Nishimura, T., and Fredlund, D. G. (2001). Failure envelope of a desiccated, unsaturated silty soil. *Proc., XVth Int. Conf. on Soil Mechanics and Foundation Engineering*, Istanbul, Turkey, 615-618.

Oloo, S. Y. (1994). A bearing capacity approach to the design of low-volume traffic roads. PhD. Thesis, University of Saskatchewan, Saskatoon, SK, Canada.

Pentland, J., Gitirana, G., Jr., and Fredlund, D. G. (2001). Use of a general partial equation solver for solution of heat and mass transfer problems in geotechnical engineering. *Proc., 4th Brazilian Symp. On Unsaturated Soils, UNSAT 2001*, Porto Alerge, RS, Brazil, 29-36.

Poulos, H.G. and Davis E.H. 1974. Elastic solutions for soil and rock mechanics, John Wiley and Sons, NY (USA).

Powrie, W. (2004). Soil mechanics concepts and applications. Spon Press. London.

Rahman, M. G. (1981). Bearing capacity and settlement of circular footing on sand. MSc thesis, Univ. of Ottawa, Ottawa, Ontario, Canada.

Shin, E. C., Lee, J. B., and Das, B.M. (1999). Bearing capacity of a model scale footing on crude oil-contaminated sand. *Geotechnical and Geological Engineering*, 17:123-132.

Spangler, Merlin G., and Handy, Richard L. (1982). Soil Engineering, 4th Edition. Harper & Row, New York

Steensen-Bach J.O., Foged, N. and Steenfelt, J.S. (1987). Capillary induced stresses – fact or fiction? *9th ECSMFE, Groundwater Effects in Geotechnical Engineering*, Dublin: 83-89.

Terzaghi, K. (1943). Theoretical Soil Mechanics. John Wiley and Sons, New York

Thieu, N. T. M., Fredlund, M. D., Fredlund, D. G., and Vu, H. Q. (2001). Seepage modelling in a saturated/unsaturated soil system. *Proc., Int. Conf. on Management of the Land and Water Resources*, Hanoi, Vietnam, 49-56.

Vanapalli, S. K., Fredlund, D. G., Pufahl, D. E., and Clifton, A. W. (1996). Model for the prediction of shear strength with respect to soil suction. *Can. Geotech. J.*, 33(3):379-392.

Vanapalli, S.K. and Mohamed, F.M.O. (2007). Bearing capacity of model footings in unsaturated soils, Experimental Unsaturated Soil mechanics. *Proceedings of the 2nd International Conference on Unsaturated Soils (Springer Proceedings in Physics)*, Weimar, Germany, 483-493.

Vanapalli, S.K., Fredlund, D.G. & Pufahl, D.E., 1999. Influ-ence of soil structure and stress history on the soil-water characteristics of a compacted till. Geotechnique, 49: 2, pp. 143-159.

Vanapalli, S.K., Oh, W.T. and Puppala, A.J. 2008. A simple method for the prediction of modulus of elasticity for unsaturated soils. Proc. 1st Int. European Conf. on Unsaturated Soils. (Accepted for publication)

Vanapalli, Sai K. and Oh, Won Taek (2007). Determination of the Bearing Capacity of Unsaturated Soils Under Undrained Loading Conditions. *Proc.(CD), 60th Canadian Geotechnical conference*, Ottawa, Canada, T6-A.

Vesić, A. S. (1973). Analysis of ultimate loads of shallow foundations. *Journal of the Soil Mechanics and Foundation Division*, ASCE, Vol. 99, No. (SM1): 45 – 73.

Wheeler, S. J., and Sivakumar, V. (1995). An elasto-plastic critical state framework for unsaturated soil. *Geotechnique*, 45(1):35-53.

Zhu, D.Y., Lee, C.F. and Jiang, H.D. (2001). A numerical study of the bearing capacity factor N_γ. *Can. Geotech. J.* 38:1090-1096

APPENDIX

All stress-settlement curves of bearing capacity tests, except listed in the chapter 6, are listed in following figures.

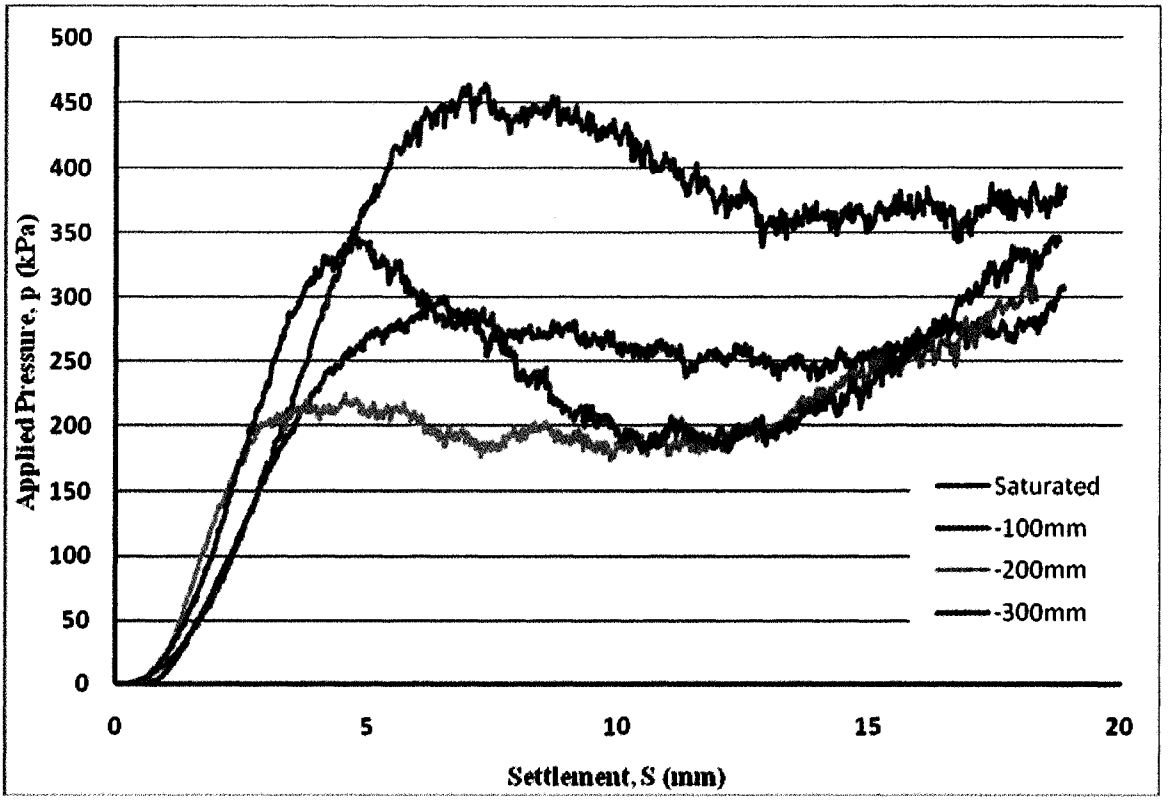

Figure A- 1 Bearing Capacity test of Unimin 2075 - Short Soil Container Footing 50mm × 50mm Series 1

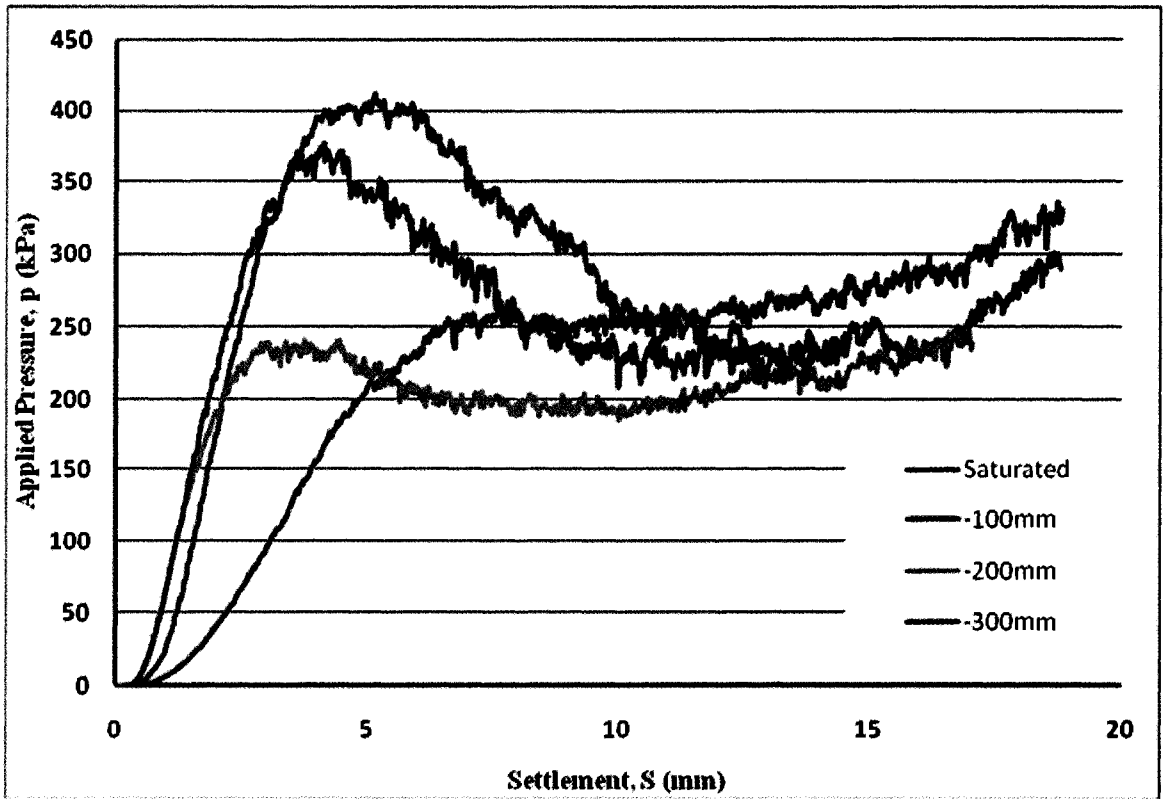

Figure A- 2 Bearing Capacity test of Unimin 2075 - Short Soil Container Footing 50mm × 50mm Series 2

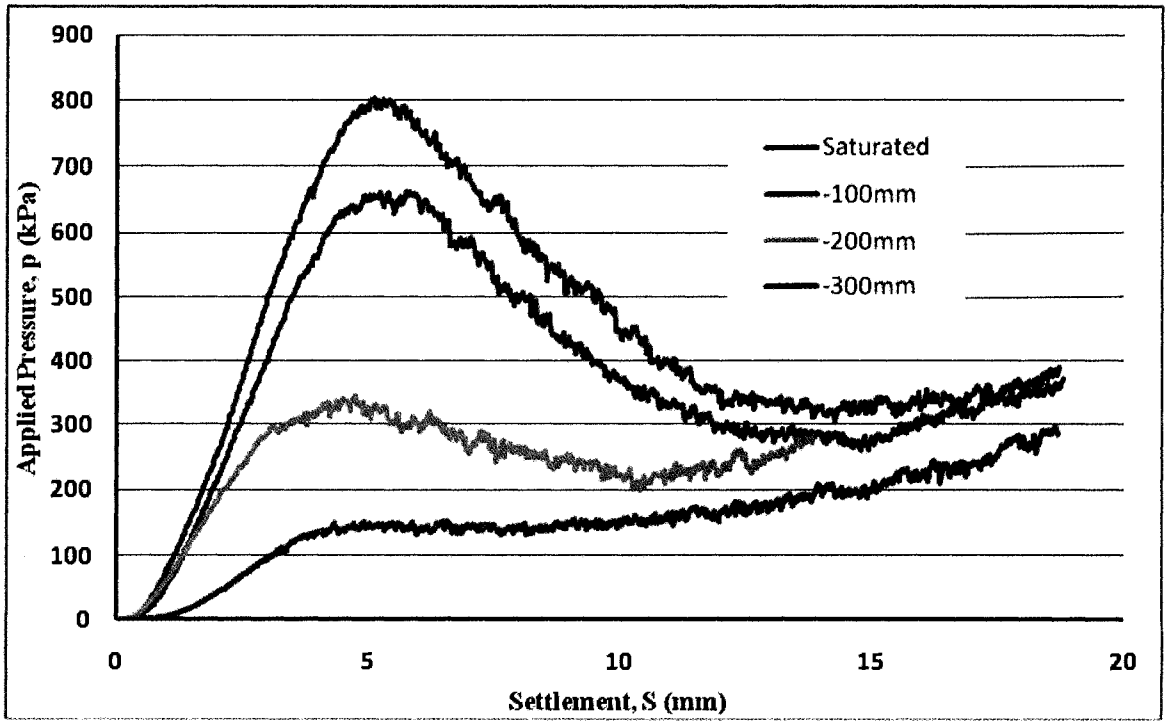

Figure A- 3 Bearing Capacity test of Unimin 2075 - Short Soil Container Footing 50mm × 50mm Series 3

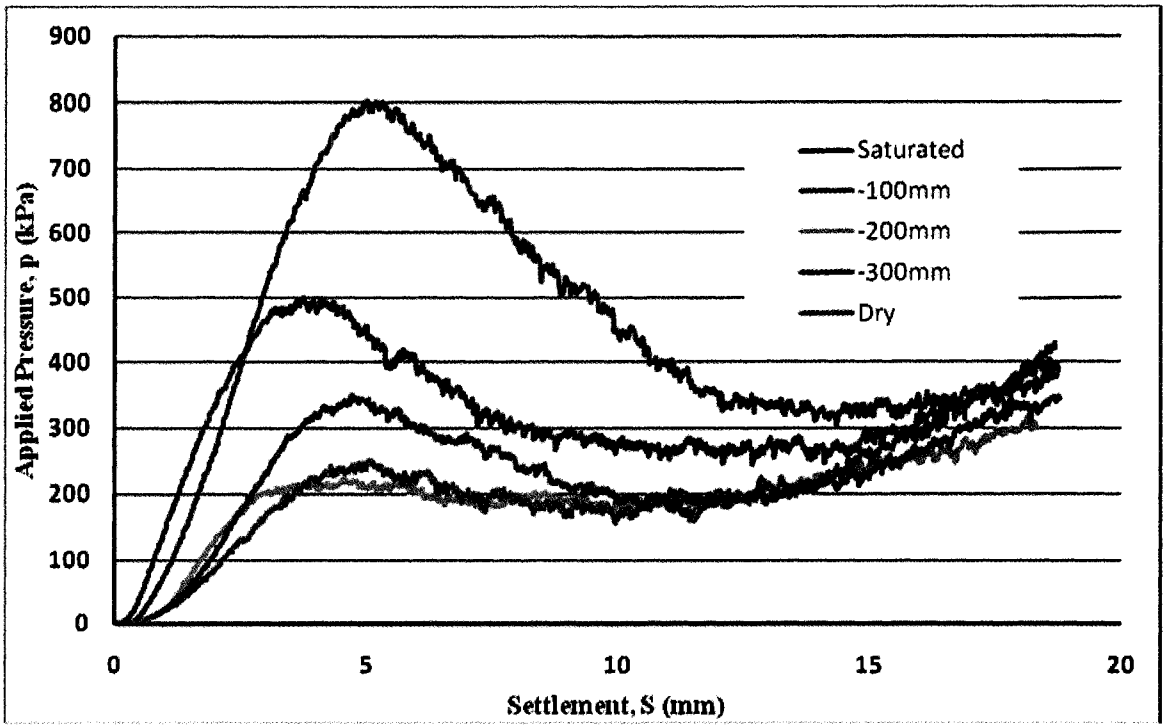

Figure A- 4 Bearing Capacity test of Unimin 2075 - Short Soil Container Footing 50mm × 50mm Series 4

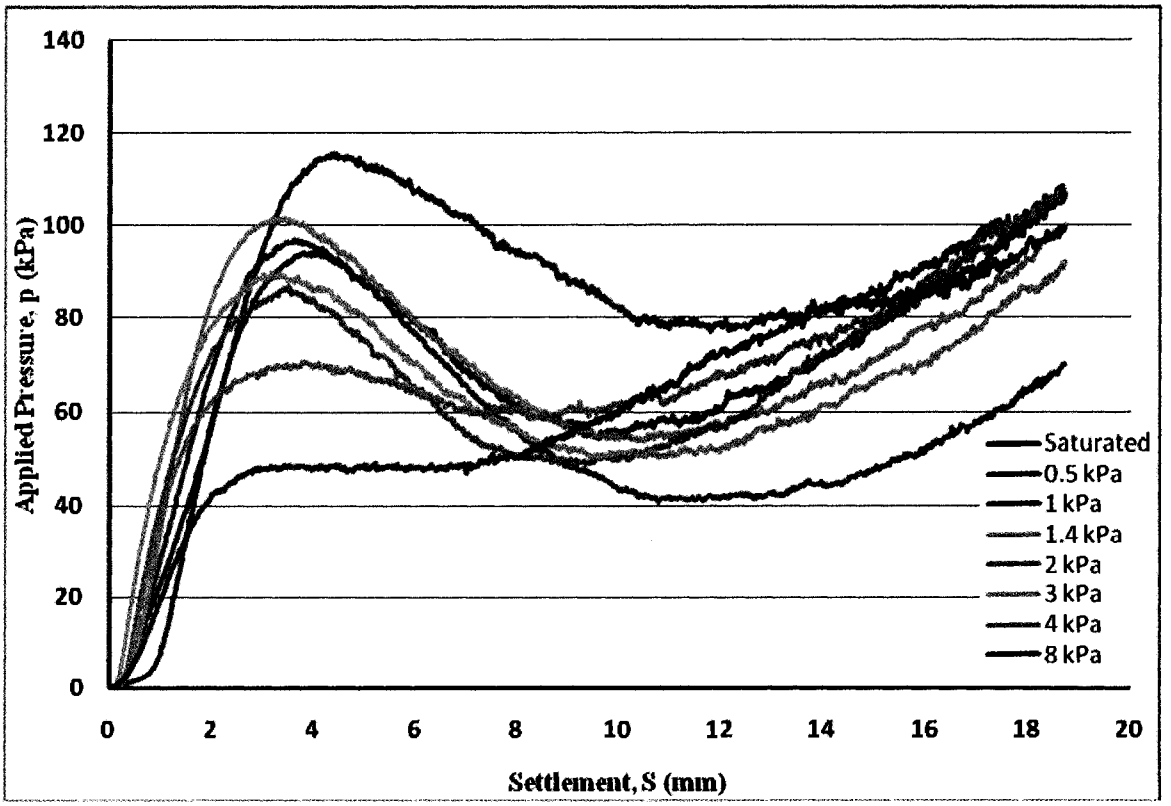

Figure A- 5 Bearing Capacity test of Ottawa Sand – Long equilibrium period Footing 50mm × 50mm Series 1

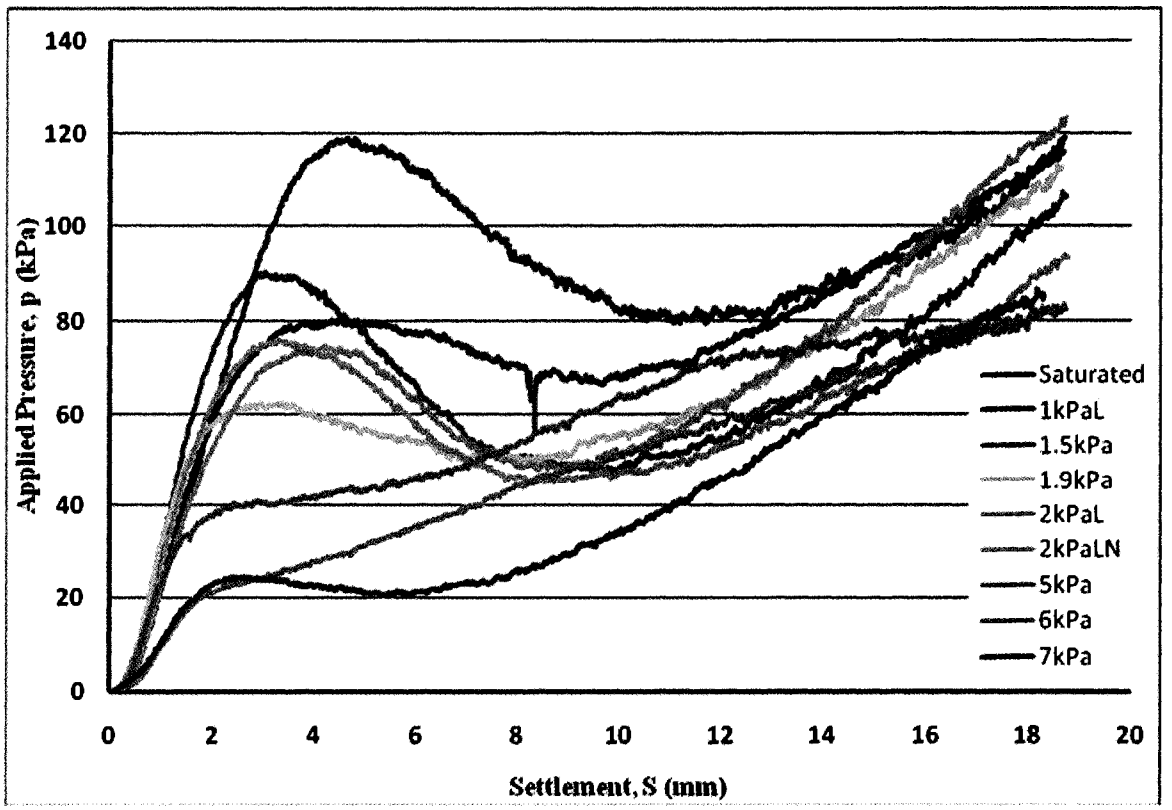

Figure A- 6 Bearing Capacity test of Ottawa Sand – Long equilibrium period Footing 50mm × 50mm Series 2

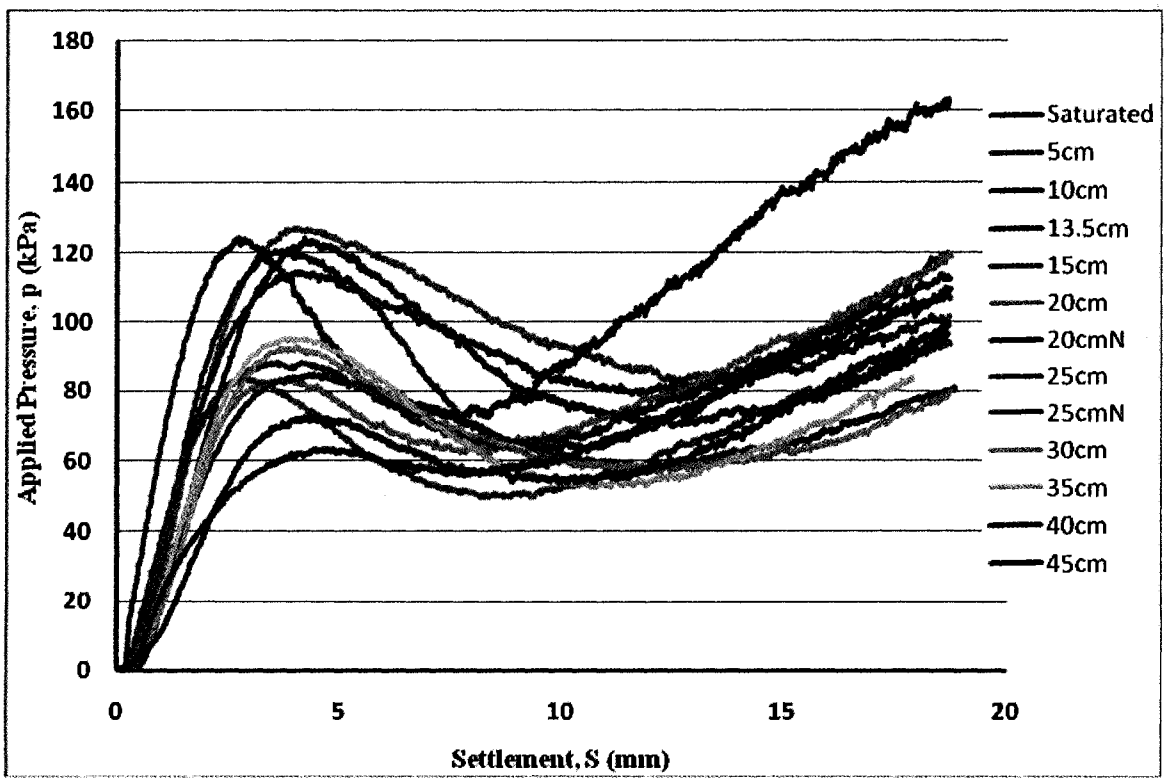

Figure A- 7 Bearing Capacity test of Ottawa Sand – Short equilibrium period Footing 50mm × 50mm

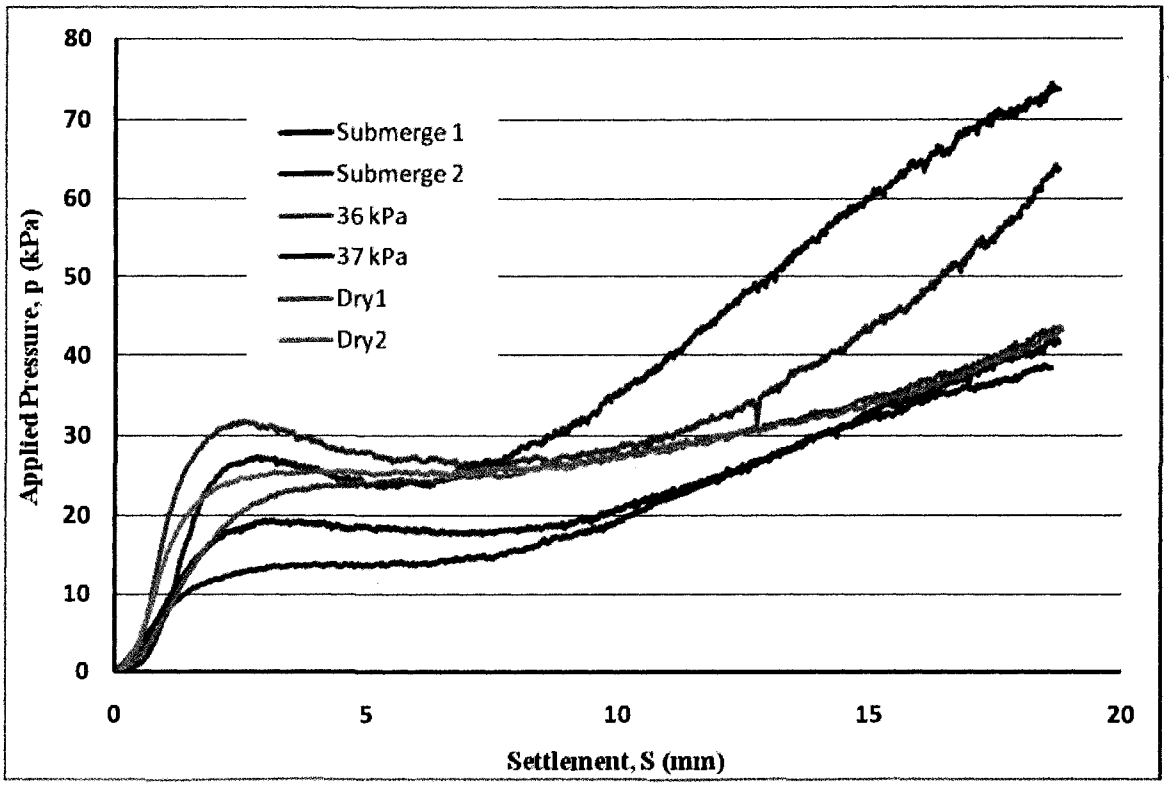

Figure A- 8 Bearing Capacity test of Ottawa Sand – Short Soil Container Footing 20mm × 20mm in Dry and Submerged Condition

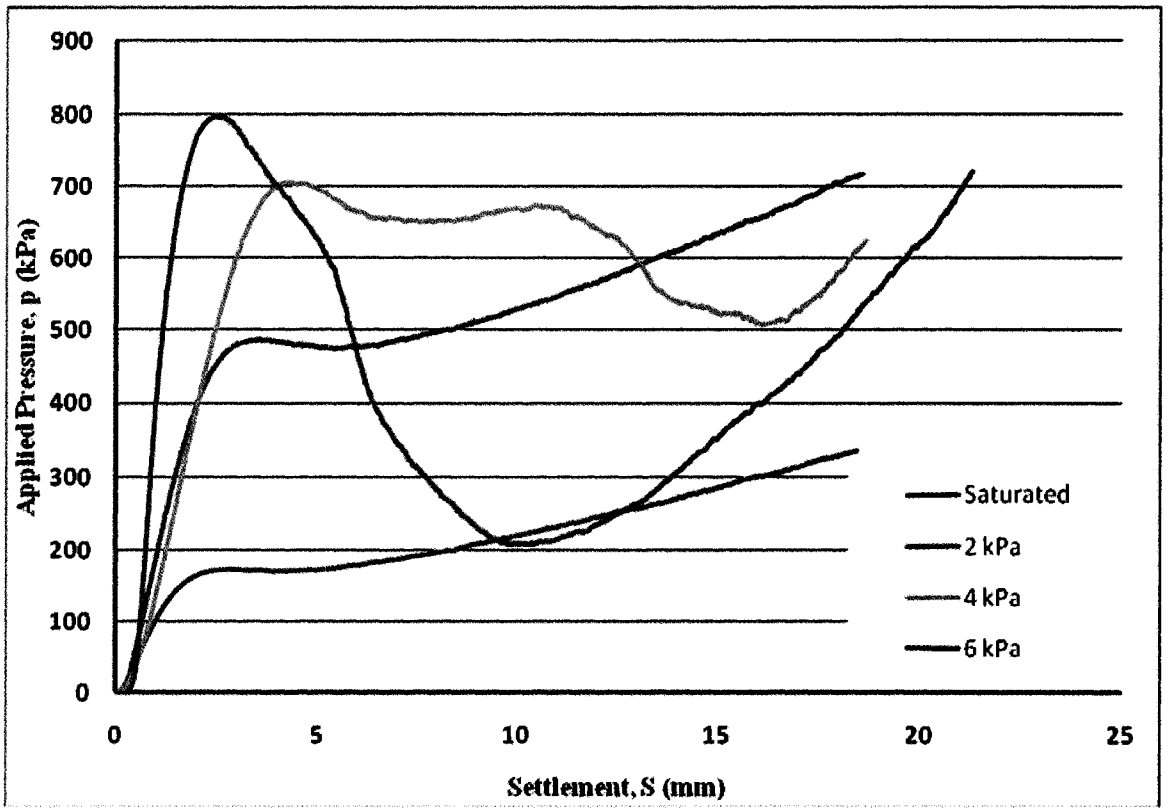

Figure A- 9 Bearing Capacity test of Unimin 7030 – Short Soil Container Footing 20mm × 20mm

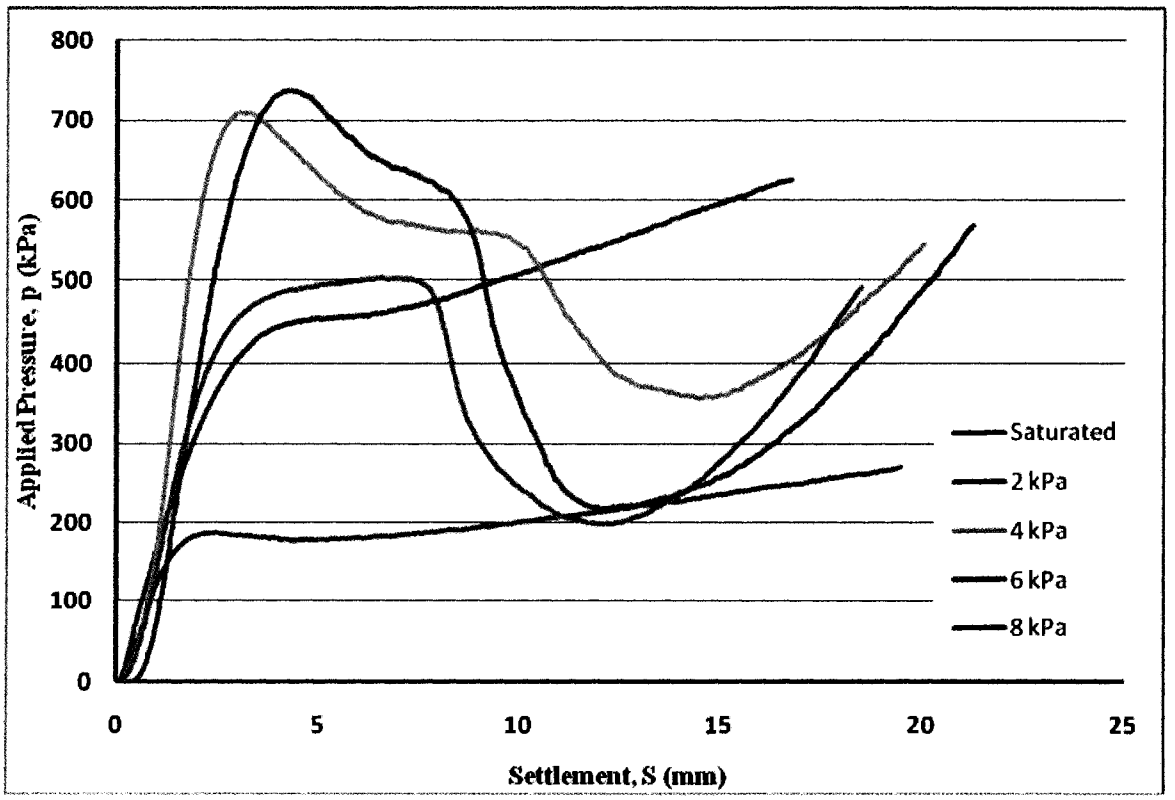

Figure A- 10 Bearing Capacity test of Unimin 7030 – Short Soil Container Footing 25mm × 25mm

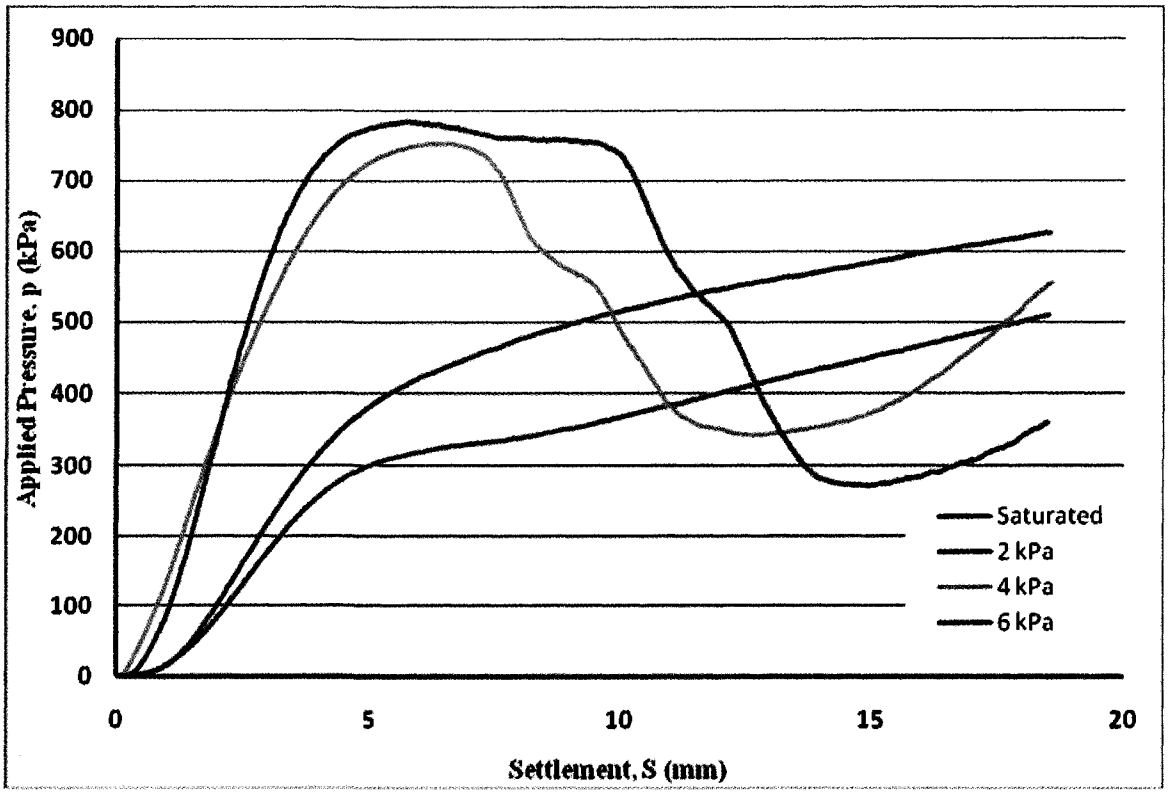

Figure A- 11 Bearing Capacity test of Unimin 7030 – Short Soil Container Footing 37.5mm × 37.5mm

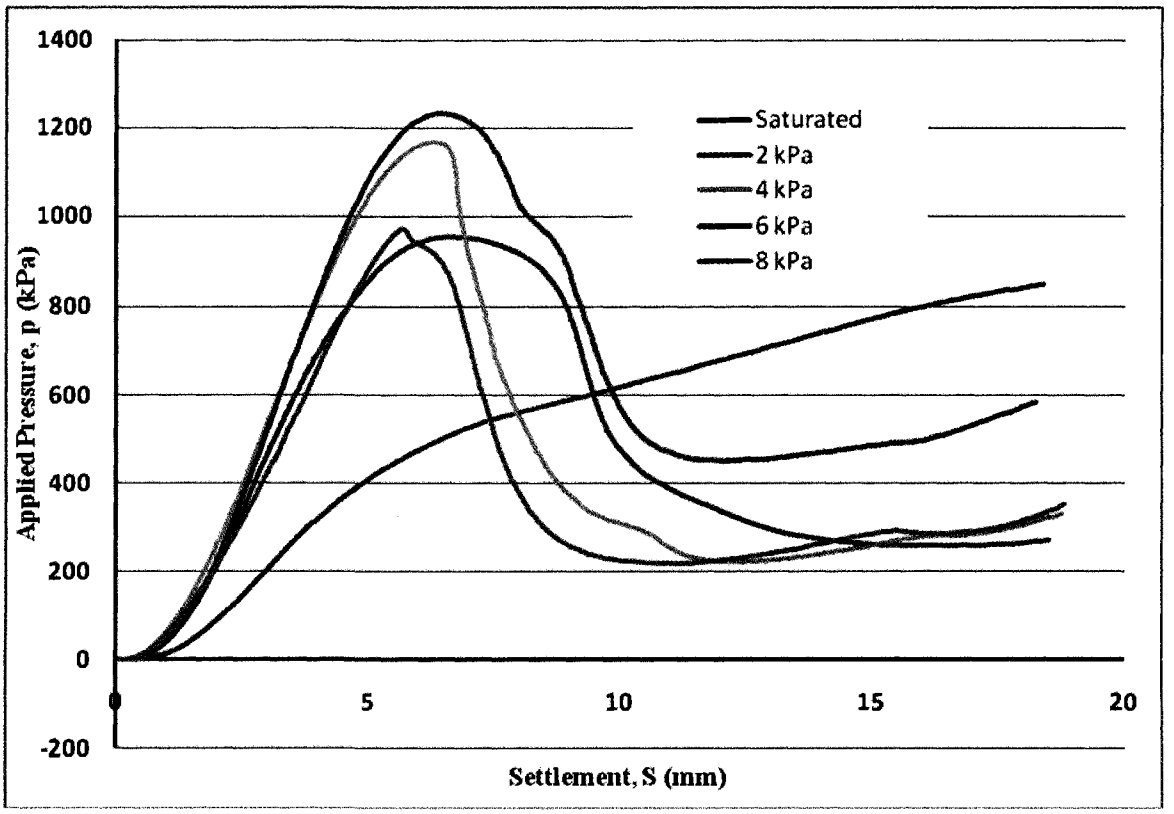

Figure A- 12 Bearing Capacity test of Unimin 7030 – Short Soil Container Footing 50mm × 50mm

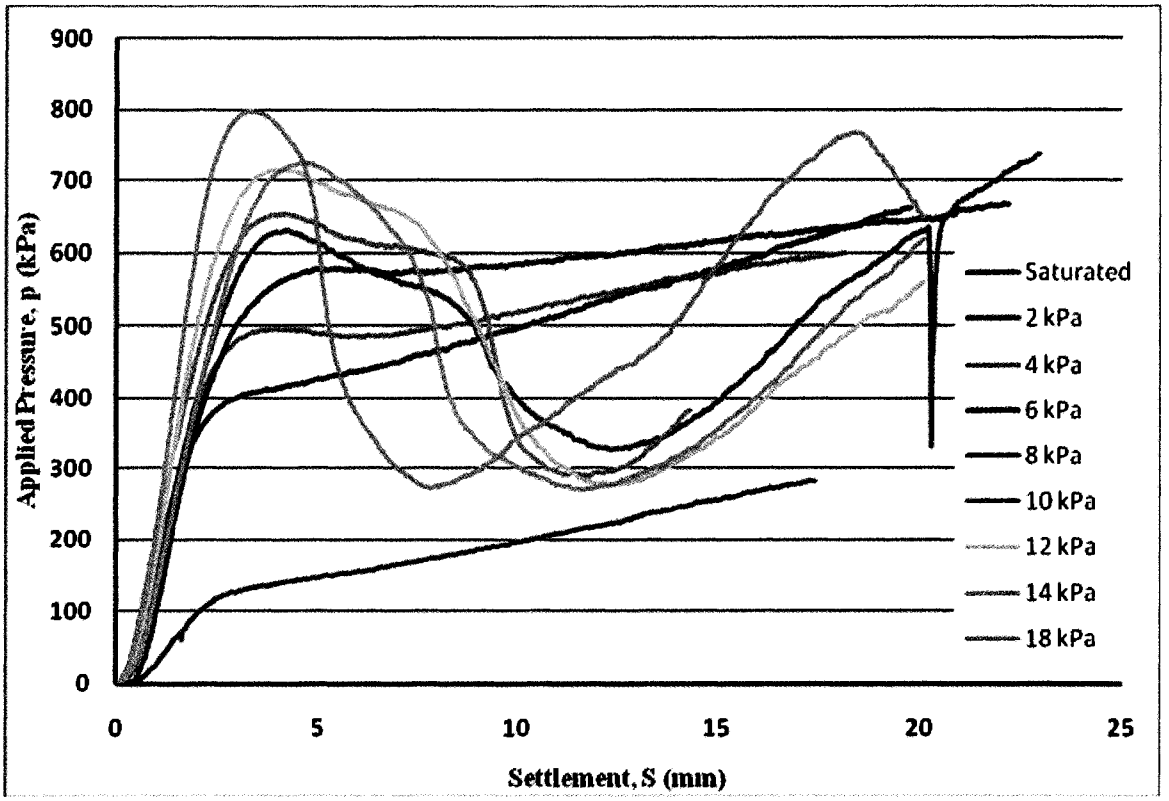

Figure A- 13 Bearing Capacity test of Unimin 7030 – Tall Soil Container Footing 20mm × 20mm

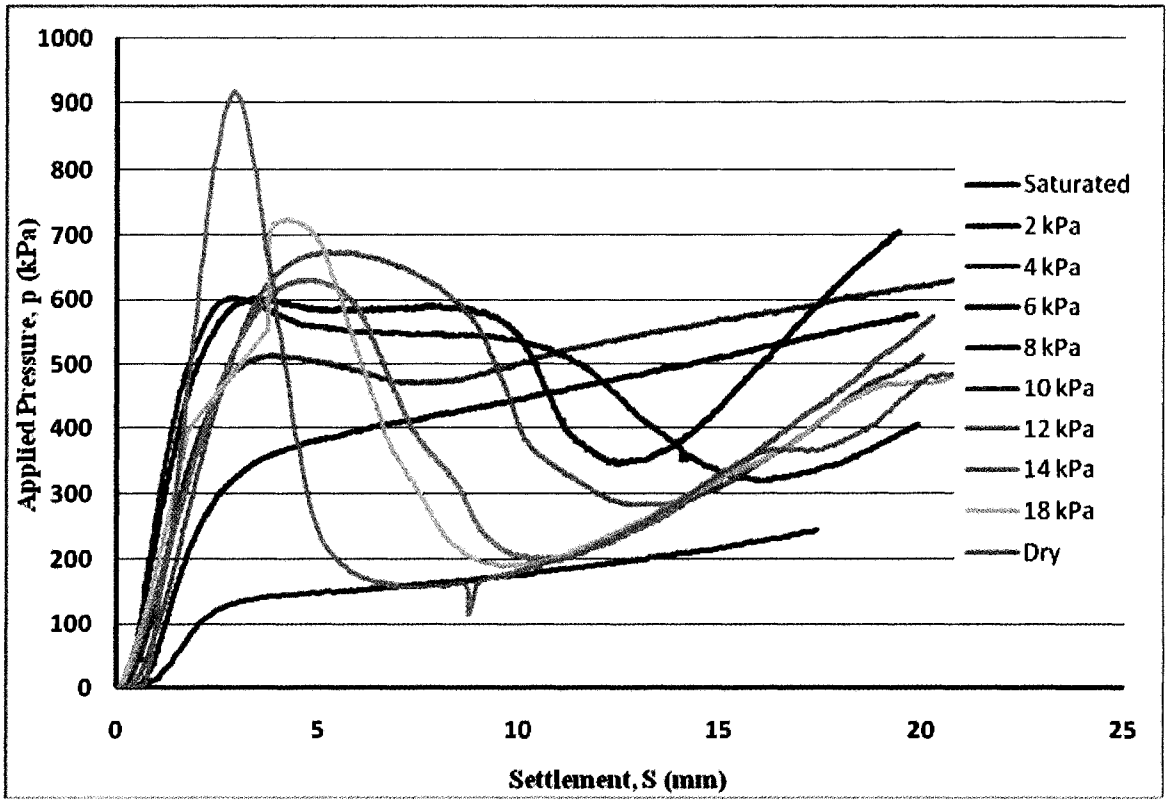

Figure A- 14 Bearing Capacity test of Unimin 7030 – Tall Soil Container Footing 25mm × 25mm

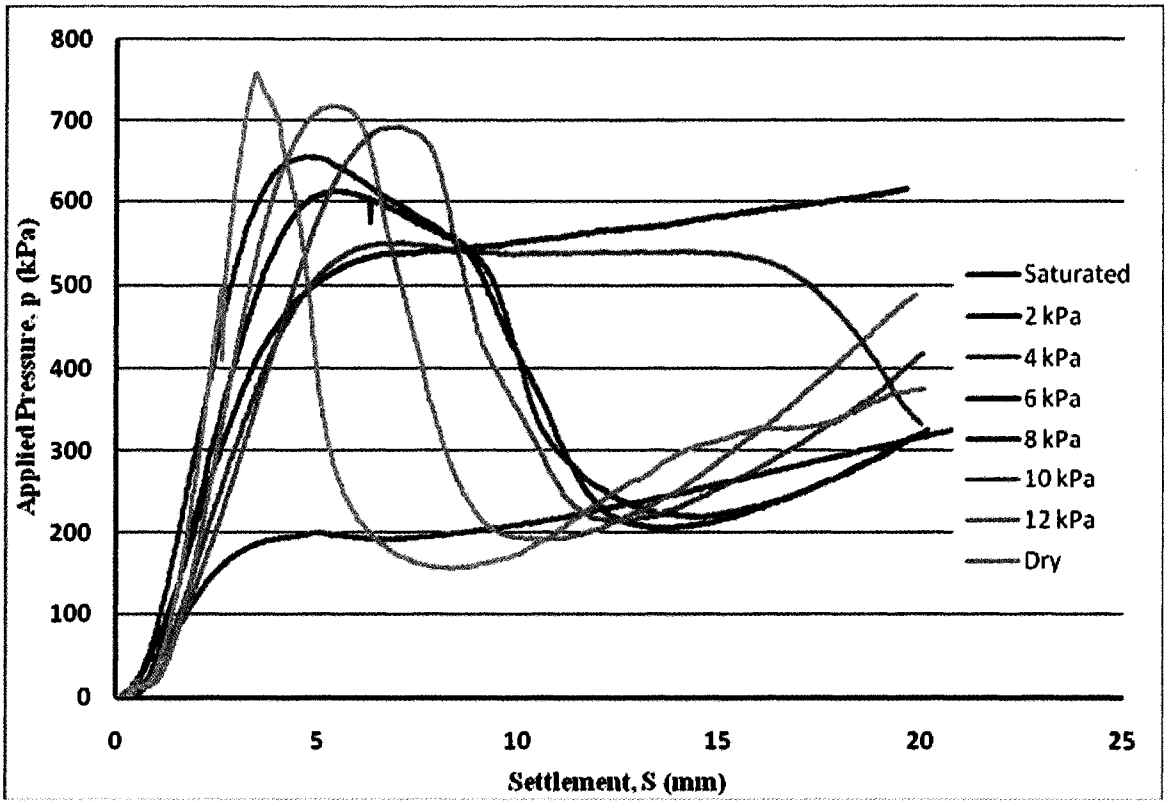

Figure A- 15 Bearing Capacity test of Unimin 7030 – Tall Soil Container Footing 37.5mm × 37.5mm

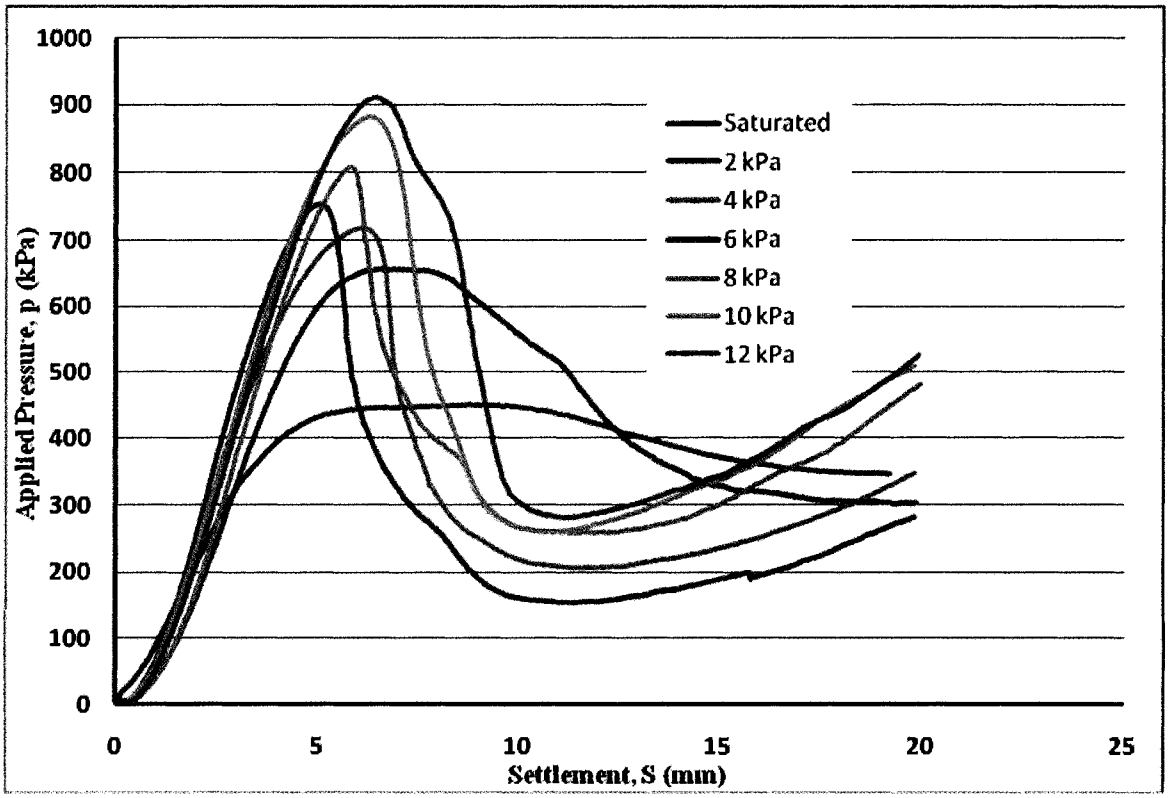

Figure A- 16 Bearing Capacity test of Unimin 7030 – Tall Soil Container Footing 50mm × 50mm